SUPPORTING INFORMATION

Metal-organic frameworks generated from oligomeric ligands with functionalized tethers

Hyunyong Kim and Seth M. Cohen*

Department of Chemistry and Biochemistry, University of California, San Diego, La Jolla, California, 92093, United States

Email: scohen@ucsd.edu

Table of Contents

A. Synthesis of oligomeric ligands

General information. Starting materials were purchased from commercially available sources such as Sigma-Aldrich, Thermo Scientific, and Combi-blocks, Inc., and used without further purification. Diethyl 2-hydroxyterephthalate (Bolton, O.; Kim, J. *J. Mater. Chem.* **2007**, *17*, 1981-1988) was synthesized by following reported procedures. Silica column chromatography was performed using a CombiFlash Rf+ automated system from TeledyneISCO (Lincoln, USA). ^{1}H and ^{13}C NMR spectra were collected by Bruker spectrometer operated at 300 MHz, or Jeol spectrometer operated at 400 MHz or 500 MHz. High resolution mass spectrometry (HRMS) and electrospray Ionisation Mass Spectrometry (ESI-MS) were performed using an Agilent 6230 accurate-mass time-of-flight mass spectrometer and a ThermoFinnigan LCQ-DECA mass spectrometer, respectively at the Molecular Mass Spectrometry Facility (MMSF) in the Department of Chemistry and Biochemistry at the University of California, San Diego. Infrared spectra were collected using a Bruker Alpha-P ATR FTIR and analyzed using Opus 6.5 software.

Synthesis of dimer ligands with pyridine tethers in different positions (L1-L5) and xylyl tether with alkyne group (L6)

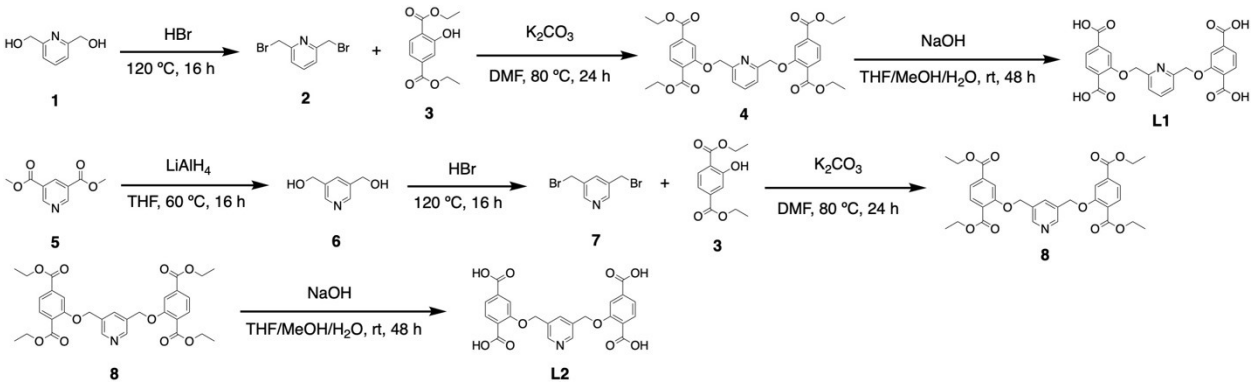

Figure S1. Synthesis of dimer with pyridine tether (**L1, L2**).

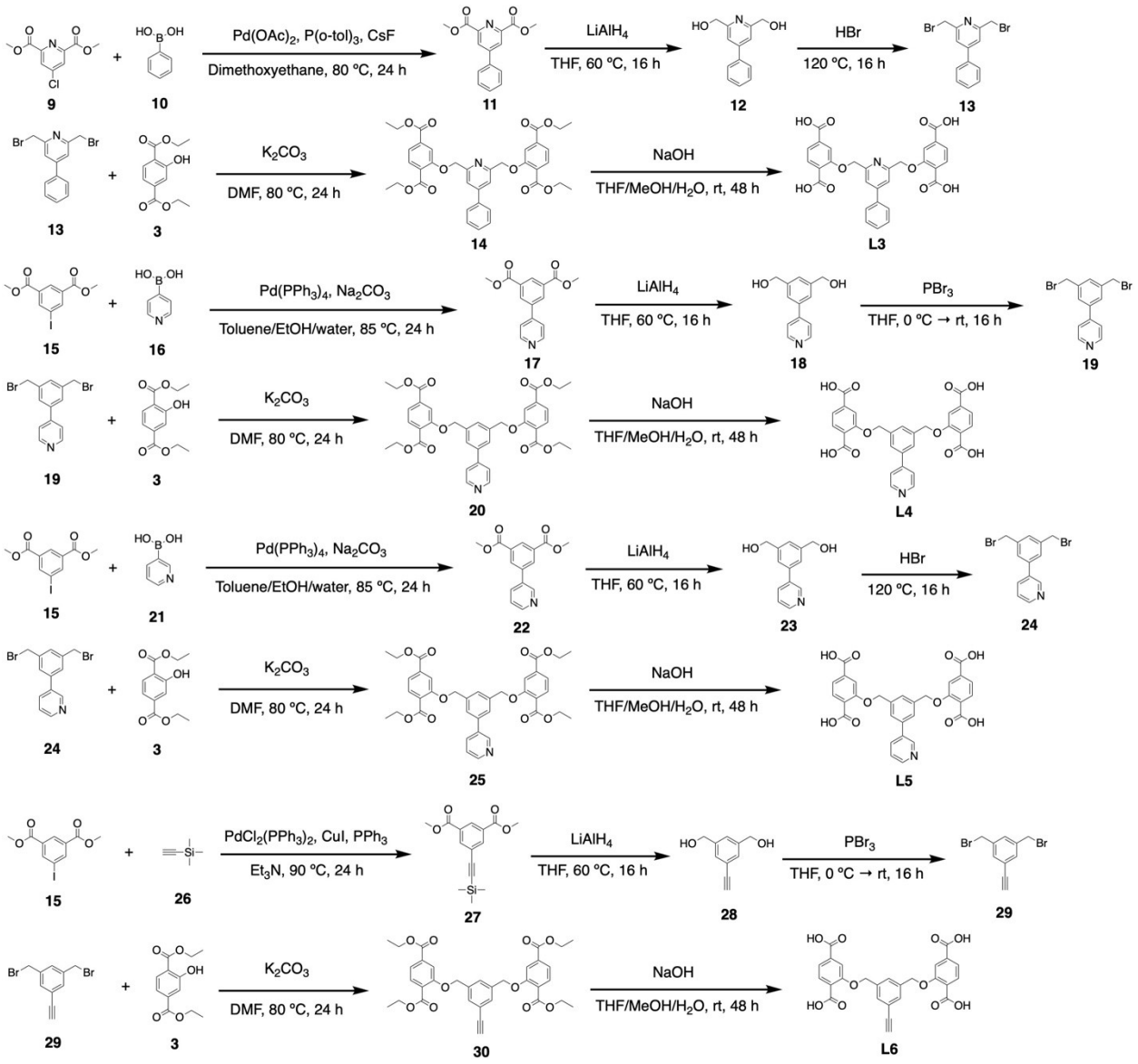

Figure S2. Synthesis of dimer linker with pyridine in different positions (**L3-L5**) and xylyl tether with terminal alkyne (**L6**).

2,6-bis(bromomethyl)pyridine (2)

Pyridine-2,6-diyldimethanol (**1**) (200 mg, 1.44 mmol) was cooled at 0 ºC by using ice bath. Hydrogen bromide (HBr, 48% in water, 6.2 mL, 55 mmol) was slowly added. The reaction mixture was gradually warmed up to room temperature and heated at 120 ºC for 16 h. The crude compound was cooled at 0 ºC. Saturated $NaHCO_3$ was slowly added until bubble ceased. The

resulting solid was washed with water, and dried under vacuum to obtain brown solid. Yield: 162 mg (43%). ^{1}H NMR (300 MHz, $CDCl_3$): δ 7.71 (t, J = 7.8 Hz, 1H), 7.38 (d, J = 7.7 Hz, 2H), 4.54 (s, 4H); ^{13}C NMR (125 MHz, $CDCl_3$): δ 156.87, 138.31, 122.98, 33.58; HRMS *m/z* calculated for $[C_7H_7Br_2N+H]^+$: 265.8998, found: 265.8994.

Tetraethyl 2,2'-((pyridine-2,6-diylbis(methylene))bis(oxy))diterephthalate (4)

2,6-bis(bromomethyl)pyridine (**2**) (130 mg, 491 μmol) was dissolved in 20 mL of DMF. To the solution, diethyl 2-hydroxyterephthalate (**3**) (257 mg, 1.08 mmol), and potassium carbonate (271 mg, 1.96 mmol) were added. The reaction mixture was stirred at 80 ºC for 24 h. The crude compound was extracted with ethyl acetate, washed with water, dried over $MgSO_4$, and further purified by silica column chromatography (hexane/ethyl acetate, R_f: 0.33, Hex:EA=2:1) and dried under vacuum to give a white solid. Yield: 231 mg (82%). ^{1}H NMR (500 MHz, $CDCl_3$): δ 7.89 (m, 3H), 7.75 (m, 4H), 7.71 (dd, J = 8.0, 1.5 Hz, 2H), 5.35 (s, 4H), 4.41 (dq, J = 14.2, 7.1 Hz, 8H), 1.41 (td, J = 7.1, 2.2 Hz, 12H); ^{13}C NMR (100 MHz, $CDCl_3$): δ 165.72, 165.66, 157.54, 156.06, 138.25, 135.03, 131.81, 124.66, 121.95, 120.23, 114.12, 71.07, 61.69, 61.46, 14.44; HRMS *m/z* calculated for $[C_{31}H_{33}NO_{10}+H]^+$: 580.2177, found: 580.2172.

2,2'-((pyridine-2,6-diylbis(methylene))bis(oxy))diterephthalic acid (L1)

Tetraethyl 2,2'-((pyridine-2,6-diylbis(methylene))bis(oxy))diterephthalate (**4**) (220 mg, 380 μmol) was dissolved in 20 mL of CH_2Cl_2, 10 mL of THF, and 10 mL of water. To the solution, sodium hydroxide (304 mg, 7.59 mmol) was added. The reaction mixture was stirred at room temperature for 48 h, dried under vacuum using a rotary evaporator, and acidified with 1 M HCl until the pH reached 1. The resulting precipitate was collected by filtration, washed with water, and dried under vacuum to obtain a white solid. Yield: 115 mg (65%). ^{1}H NMR (300 MHz, DMSO-d_6): δ 7.94 (t, J = 7.8 Hz, 1H), 7.77 (d, J = 7.9 Hz, 2H), 7.69 (s, 2H), 7.61 (d, J = 7.8 Hz, 4H), 5.35 (s, 4H); ^{13}C NMR (100 MHz, $CDCl_3$): δ 166.92, 166.52, 156.37, 156.10, 138.09, 134.69, 130.74, 125.97, 121.65, 120.16, 114.09, 70.47; HRMS *m/z* calculated for $[C_{23}H_{17}NO_{10}+H]^+$: 468.0925, found: 468.0924.

Pyridine-3,5-diyldimethanol (6)

Dimethyl pyridine-3,5-dicarboxylate (**5**) (1.0 g, 5.12 mmol) was dissolved into 70 mL of THF and cooled at 0 ºC by using ice bath. Lithium aluminum hydride (486 mg, 12.81 mmol) was slowly added. The reaction mixture was heated to 60 ºC for 16 h. The remaining lithium aluminum hydride was quenched by the slow addition of saturated aq. $NaHCO_3$ solution at 0 ºC. The crude compound was extracted with ethyl acetate, washed with water, and dried under $MgSO_4$ and vacuum. The crude compound was purified by silica column chromatography (CH_2Cl_2/MeOH, R_f: 0.35, CH_2Cl_2:MeOH=9:1) and dried under vacuum to give a pale yellow solid. Yield: 320 mg (45%). ^{1}H NMR (400 MHz, DMSO-d_6): δ 8.38 (m, 2H), 7.66 (m, 1H), 5.32 (t, J = 5.7 Hz, 2H), 4.52 (d, J = 5.7 Hz, 4H); ^{13}C NMR (100 MHz, DMSO-d_6): δ 146.59, 137.13, 132.68, 60.64; HRMS *m/z* calculated for $[C_7H_9NO_2+H]^+$: 140.0706, found: 140.0704.

3,5-bis(bromomethyl)pyridine (7)

Pyridine-3,5-diyldimethanol (**6**) (150 mg, 1.08 mmol) was cooled at 0 ºC by using ice bath. HBr (48% in water, 4.6 mL, 41 mmol) was slowly added. The reaction was warmed up to room temperature and heated at 120 ºC for 16 h with continuous stirring. After the reaction, the remaining HBr was quenched by the slow addition of saturated aq. $NaHCO_3$ solution at 0 ºC. The resulting brown solid was collected by filtration, washed with water, and dried under vacuum. Yield: 135 mg (47% yield). ^{1}H NMR (400 MHz, $CDCl_3$): δ 8.56 (d, J = 2.2 Hz, 2H), 7.78 (t, J = 2.2 Hz, 1H), 4.47 (s, 4H); ^{13}C NMR (125 MHz, $CDCl_3$): δ 149.76, 137.26, 133.94, 29.14; HRMS *m/z* calculated for $[C_7H_7Br_2N+H]^+$: 263.9018, found: 263.9017.

Tetraethyl 2,2'-((pyridine-3,5-diylbis(methylene))bis(oxy))diterephthalate (8)

3,5-bis(bromomethyl)pyridine (**7**) (130 mg, 491 µmol) was dissolved into 20 mL of DMF. Diethyl 2-hydroxyterephthalate (**3**) (257 mg, 1.08 mmol), and potassium carbonate (271 mg, 1.96 mmol) were added to the solution. The reaction mixture was stirred at 80 ºC for 24 h. The crude compound was extracted with ethyl acetate, washed with water, dried over $MgSO_4$, and further

purified by silica column chromatography (hexane/ethyl acetate, R_f: 0.32, Hex:EA=1:1) and dried under vacuum to give a white solid. Yield: 232 mg (82%). ^{1}H NMR (300 MHz, $CDCl_3$): δ 8.79 (s, 2H), 8.11 (s, 1H), 7.87 (d, J = 8.4 Hz, 2H), 7.72 (m, 4H), 5.29 (s, 4H), 4.39 (dq, J = 13.2, 7.1 Hz, 8H), 1.42 (t, J = 7.1 Hz, 6H), 1.33 (t, J = 7.1 Hz, 6H); ^{13}C NMR (100 MHz, $CDCl_3$): δ 165.78, 165.70, 157.34, 148.08, 134.87, 134.42, 132.24, 131.86, 125.33, 122.24, 114.39, 68.49, 61.76, 61.57, 14.43, 14.37; HRMS *m/z* calculated for $[C_{31}H_{33}NO_{10}+H]^+$: 580.2177, found: 580.2171.

2,2'-((pyridine-3,5-diylbis(methylene))bis(oxy))diterephthalic acid (L2)

Tetraethyl 2,2'-((pyridine-3,5-diylbis(methylene))bis(oxy))diterephthalate (**8**) (220 mg, 380 μmol) was dissolved in 15 mL of CH_2Cl_2, 10 mL of THF, 10 mL of MeOH, and 10 mL of water. To the solution, sodium hydroxide (455 mg, 11.4 mmol) was added. The reaction mixture was stirred at room temperature for 48 h, dried under vacuum using a rotary evaporator, and acidified with 1 M HCl until the pH reached 1. The resulting precipitate was collected by filtration, washed with water, and dried under vacuum to obtain a white solid. Yield: 127 mg (72%). ^{1}H NMR (300 MHz, DMSO-d_6): δ 8.75 (d, J = 2.0 Hz, 2H), 8.09 (d, J = 2.1 Hz, 1H), 7.75 (m, 4H), 7.62 (dd, J = 7.9, 1.4 Hz, 2H), 5.36 (s, 4H); ^{13}C NMR (125 MHz, DMSO-d_6): δ 166.88, 166.56, 156.51, 146.16, 135.68, 134.75, 133.22, 130.85, 125.95, 121.76, 114.16, 67.50; HRMS *m/z* calculated for $[C_{23}H_{17}NO_{10}+H]^+$: 468.0925, found: 468.0920.

Dimethyl 4-phenylpyridine-2,6-dicarboxylate (11)

Dimethyl 4-chloropyridine-2,6-dicarboxylate (**9**) (1.0 g, 4.36 mmol), phenylboronic acid (**10**) (637 mg, 5.23 mmol), tri(o-tolyl)phosphine (133 mg, 436 μmol), and cesium fluoride (1.65 g, 10.9 mmol) were dispersed into 30 mL of dimethoxyethane and degassed with nitrogen gas for 30 min. The reaction mixture was stirred at 80 ºC for 24 h. The crude compound was extracted with ethyl acetate, purified by silica column chromatography (hexane/ethyl acetate, R_f: 0.23, Hex:EA=2:1), and dried under vacuum to give a white solid. Yield: 420 mg (36%). ^{1}H NMR (300 MHz, $CDCl_3$): δ 8.56 (s, 2H), 7.77 (dd, J = 7.6, 2.0 Hz, 2H), 7.54 (m, 3H), 4.06 (s, 6H); ^{13}C NMR (100 MHz, $CDCl_3$): δ 165.42, 151.33, 148.95, 136.29, 130.33, 129.59, 127.31, 125.88, 53.46; HRMS *m/z* calculated for $[C_{15}H_{13}NO_4+H]^+$: 272.0917, found: 272.0918.

(4-phenylpyridine-2,6-diyl)dimethanol (12)

Dimethyl 4-phenylpyridine-2,6-dicarboxylate (**11**) (400 mg, 4.36 mmol) was dissolved into 15 mL of THF and cooled at 0 ºC by using ice bath. Lithium aluminum hydride (280 mg, 7.37 mmol) was slowly added. The reaction mixture was heated to 60 ºC for 16 h. The remaining lithium aluminum hydride was quenched by the slow addition of saturated aq. $NaHCO_3$ solution at 0 ºC. The crude compound was extracted with ethyl acetate, washed with water, and dried under $MgSO_4$ and vacuum. The crude compound was purified by silica column chromatography (CH_2Cl_2/methanol, R_f: 0.36, CH_2Cl_2:MeOH=9:1) and dried under vacuum to give a pale yellow solid. Yield: 122 mg (38%). ^{1}H NMR (500 MHz, DMSO-d_6): δ 7.75 (d, J = 7.4 Hz, 2H), 7.60 (s, 2H), 7.54 (t, J = 7.5 Hz, 2H), 7.48 (t, J = 7.3 Hz, 1H), 5.47 (t, J = 6.0 Hz, 2H), 4.59 (d, J = 5.9 Hz, 4H); ^{13}C NMR (100 MHz, DMSO-d_6): δ 161.83, 148.18, 138.08, 129.32, 129.15, 126.74, 115.68, 64.22; HRMS *m/z* calculated for $[C_{13}H_{13}NO_2+H]^+$: 216.1019, found: 216.1022.

2,6-bis(bromomethyl)-4-phenylpyridine (13)

(4-phenylpyridine-2,6-diyl)dimethanol (**12**) (110 mg, 511 µmol) was cooled at 0 ºC by using ice bath. HBr (48% in water, 2.3 mL, 20 mmol) was slowly added. The reaction mixture was warmed up to room temperature and heated at 120 ºC for 16 h with continuous stirring. After 16 h, the remaining HBr was quenched by the slow addition of saturated aq. $NaHCO_3$ solution at 0 ºC. The resulting brown solid was collected by filtration, washed with water, and dried under vacuum. Yield: 120 mg (69% yield). ^{1}H NMR (500 MHz, $CDCl_3$): δ 7.64 (m, 2H), 7.59 (s, 2H), 7.49 (m, 3H), 4.61 (s, 4H); ^{13}C NMR (125 MHz, $CDCl_3$): δ 157.41, 151.06, 137.52, 129.66, 129.37, 127.22, 121.11, 33.72; HRMS *m/z* calculated for $[C_{13}H_{11}Br_2N+H]^+$: 339.9331, found: 339.9326.

Tetraethyl 2,2'-(((4-phenylpyridine-2,6-diyl)bis(methylene))bis(oxy))diterephthalate (14)

2,6-bis(bromomethyl)-4-phenylpyridine (**13**) (120 mg, 352 µmol) was dissolved into 20 mL of DMF. Diethyl 2-hydroxyterephthalate (**3**) (184 mg, 774 µmol), and potassium carbonate (195 mg, 1.41 mmol) were added to the solution. The reaction mixture was stirred at 80 ºC for 24 h. The

crude compound was extracted with ethyl acetate, washed with water, dried over $MgSO_4$, and further purified by silica column chromatography (hexane/ethyl acetate, R_f: 0.35, Hex:EA=2:1) and dried under vacuum to give a white solid. Yield: 183 mg (79%). ^{1}H NMR (500 MHz, $CDCl_3$): δ 8.03 (s, 2H), 7.88 (d, J = 8.0 Hz, 2H), 7.79 (m, 4H), 7.71 (dd, J = 7.9, 1.4 Hz, 2H), 7.49 (m, 3H), 5.41 (s, 4H), 4.40 (q, J = 7.1 Hz, 8H), 1.41 (t, J = 7.1 Hz, 6H), 1.32 (t, J = 7.1 Hz, 6H); ^{13}C NMR (100 MHz, $CDCl_3$): δ 165.83, 165.67, 157.48, 156.64, 138.27, 134.99, 131.71, 129.41, 129.19, 127.32, 124.97, 122.04, 118.21, 114.28, 71.16, 61.70, 61.47, 14.44, 14.39; HRMS *m/z* calculated for $[C_{37}H_{37}NO_{10}+H]^+$: 656.2490, found: 656.2491.

2,2'-(((4-phenylpyridine-2,6-diyl)bis(methylene))bis(oxy))diterephthalic acid (L3)

Tetraethyl 2,2'-(((4-phenylpyridine-2,6-diyl)bis(methylene))bis(oxy))diterephthalate (**14**) (170 mg, 259 μmol) was dissolved in 10 mL of CH_2Cl_2, 10 mL of THF, 5 mL of MeOH, and 5 mL of water. To the solution, sodium hydroxide (311 mg, 7.78 mmol) was added. The reaction mixture was stirred at room temperature for 48 h, dried under vacuum using a rotary evaporator, and acidified with 1 M HCl until the pH reached 1. The resulting precipitate was collected by filtration, washed with water, and dried under vacuum to obtain a white solid. Yield: 135 mg (96%). ^{1}H NMR (500 MHz, DMSO-d_6): δ 8.07 (s, 2H), 7.82 (dd, J = 7.6, 3.3 Hz, 4H), 7.76 (s, 2H), 7.62 (d, J = 7.9 Hz, 2H), 7.55 (dt, J = 15.2, 6.8 Hz, 3H), 5.41 (s, 4H); ^{13}C NMR (100 MHz, DMSO-d_6): δ 167.01, 166.57, 157.06, 156.62, 148.77, 137.14, 134.93, 131.12, 129.65, 129.52, 126.72, 125.57, 121.64, 117.36, 114.12, 70.34; HRMS *m/z* calculated for $[C_{29}H_{21}NO_{10}+H]^+$: 544.1238, found: 544.1236.

Dimethyl 5-(pyridin-4-yl)isophthalate (17)

Dimethyl 5-iodoisophthalate (**15**) (3.2 g, 10 mmol), pyridin-4-ylboronic acid (**16**) (1.6 g, 13 mmol), and sodium carbonate (3.7 g, 35 mmol) were dispersed in a mixture of 125 mL of toluene, 30 mL of ethanol, and 10 mL of water and degassed with nitrogen gas for 30 min. To the reaction mixture, tetrakis(triphenylphosphine)palladium (578 mg, 500 μmol) was added and stirred at 85 ºC for 24 h. The crude compound was extracted with ethyl acetate, purified by silica column chromatography (hexane/ethyl acetate, R_f: 0.33, Hex:EA=1:1), and dried under vacuum to give a

white solid. Yield: 1.1 g (40%). ^{1}H NMR (300 MHz, $CDCl_3$): δ 8.75 (t, J = 1.6 Hz, 3H), 8.51 (d, J = 1.6 Hz, 2H), 7.60 (d, J = 4.9 Hz, 2H), 4.00 (s, 6H); ^{13}C NMR (100 MHz, $CDCl_3$): δ 165.94, 150.49, 146.59, 139.04, 132.30, 131.80, 131.15, 121.85, 52.79; HRMS *m/z* calculated for $[C_{15}H_{13}NO_4+H]^+$: 272.0917, found: 272.0919.

(5-(pyridin-4-yl)-1,3-phenylene)dimethanol (18)

Dimethyl 5-(pyridin-4-yl)isophthalate (**17**) (480 mg, 1.8 mmol) was dissolved into 18 mL of THF and cooled at 0 ºC by using ice bath. Lithium aluminum hydride (336 mg, 8.9 mmol) was slowly added. The reaction mixture was heated to 60 ºC for 16 h. The remaining lithium aluminum hydride was quenched by the slow addition of saturated aq. $NaHCO_3$ solution at 0 ºC. The crude compound was extracted with ethyl acetate, washed with water, and dried under $MgSO_4$ and vacuum. The crude compound was purified by silica column chromatography (CH_2Cl_2/methanol, R_f: 0.24, CH_2Cl_2:MeOH=9:1) and dried under vacuum to give a pale yellow solid. Yield: 234 mg (61%). ^{1}H NMR (500 MHz, DMSO-d_6): δ 8.62 (m, 2H), 7.67 (m, 2H), 7.59 (d, J = 1.5 Hz, 2H), 7.39 (m, 1H), 5.31 (t, J = 5.8 Hz, 2H), 4.58 (d, J = 5.4 Hz, 4H); ^{13}C NMR (100 MHz, DMSO-d_6): δ 150.30, 147.34, 143.53, 136.77, 125.45, 123.16, 121.22, 62.79; HRMS *m/z* calculated for $[C_{13}H_{13}NO_2+H]^+$: 216.1019, found: 216.1022.

4-(3,5-bis(bromomethyl)phenyl)pyridine (19)

(5-(Pyridin-4-yl)-1,3-phenylene)dimethanol (**18**) (230 mg, 1.1 mmol) was dissolved in 20 mL of THF. Phosphorous tribromide (PBr_3, 500 µL, 5.3 mmol) was slowly added at 0 ºC. The reaction mixture was stirred at room temperature for 16 h. The remaining PBr_3 was quenched by slow addition of saturated sodium bicarbonate at 0 ºC. The crude compound was extracted with ethyl acetate and isolated by silica column chromatography (hexane/ethyl acetate, R_f: 0.39, Hex:EA=1:1) and dried under vacuum to give a white solid. Yield: 199 mg (55%). ^{1}H NMR (500 MHz, $CDCl_3$): δ 8.69 (d, J = 6.0 Hz, 2H), 7.59 (d, J = 1.6 Hz, 2H), 7.51 (ddd, J = 6.2, 4.0, 1.7 Hz, 3H), 4.54 (s, 4H); ^{13}C NMR (100 MHz, $CDCl_3$): δ 146.84, 140.12, 131.33, 128.02, 122.84, 32.02; HRMS *m/z* calculated for $[C_{13}H_{11}Br_2\ N+H]^+$: 339.9331, found: 339.9331.

Tetraethyl 2,2'-(((5-(pyridin-4-yl)-1,3-phenylene)bis(methylene))bis(oxy))diterephthalate (20)

4-(3,5-Bis(bromomethyl)phenyl)pyridine (**19**) (180 mg, 528 μmol) was dissolved into 20 mL of DMF. Diethyl 2-hydroxyterephthalate (**3**) (277 mg, 1.16 mmol), and potassium carbonate (292 mg, 2.11 mmol) were added to the solution. The reaction mixture was stirred at 80 ºC for 24 h. The crude compound was extracted with ethyl acetate, washed with water, dried over $MgSO_4$, and further purified by silica column chromatography (hexane/ethyl acetate, R_f: 0.24, Hex:EA=1:1) and dried under vacuum to give a white solid. Yield: 244 mg (71%). ^{1}H NMR (300 MHz, $CDCl_3$): δ 8.72 (d, J = 6.0 Hz, 2H), 7.89 (m, 4H), 7.73 (m, 7H), 5.35 (s, 4H), 4.41 (dq, J = 12.0, 7.1 Hz, 8H), 1.43 (t, J = 7.1 Hz, 6H), 1.33 (t, J = 7.1 Hz, 6H); ^{13}C NMR (100 MHz, $CDCl_3$): δ 165.81, 165.77, 157.60, 150.02, 148.35, 138.80, 137.96, 134.80, 131.67, 126.32, 125.52, 125.27, 121.94, 114.44, 70.43, 61.72, 61.45, 14.42, 14.34; HRMS *m/z* calculated for $[C_{37}H_{37}NO_{10}+H]^+$: 656.2490, found: 656.2494.

2,2'-(((5-(pyridin-4-yl)-1,3-phenylene)bis(methylene))bis(oxy))diterephthalic acid (L4)

Tetraethyl 2,2'-(((5-(pyridin-4-yl)-1,3-phenylene)bis(methylene))bis(oxy))diterephthalate (**20**) (230 mg, 351 μmol) was dissolved in 20 mL of CH_2Cl_2, 10 mL of THF, and 10 mL of water. To the solution, sodium hydroxide (281 mg, 7.02 mmol) was added. The reaction mixture was stirred at room temperature for 48 h, dried under vacuum using a rotary evaporator, and acidified with 1 M HCl until the pH reached 1. The resulting precipitate was collected by filtration, washed with water, and dried under vacuum to obtain a white solid. Yield: 186 mg (98%). ^{1}H NMR (500 MHz, DMSO-d_6): δ 8.68 (m, 2H), 8.04 (d, J = 1.5 Hz, 2H), 7.74 (m, 7H), 7.61 (dd, J = 7.9, 1.4 Hz, 2H), 5.37 (s, 4H); ^{13}C NMR (125 MHz, DMSO-d_6): δ 167.12, 166.63, 156.74, 150.31, 146.89, 138.16, 137.31, 134.72, 130.84, 126.43, 125.94, 124.82, 121.50, 121.17, 114.09, 69.49; HRMS *m/z* calculated for $[C_{29}H_{21}NO_{10}+H]^+$: 544.1238, found: 544.1233.

Dimethyl 5-(pyridin-3-yl)isophthalate (22)

Dimethyl 5-iodoisophthalate (**15**) (3.2 g, 10 mmol), pyridin-3-ylboronic acid (**21**) (1.6 g, 13 mmol), and sodium carbonate (3.7 g, 35 mmol) were dispersed in a mixture of 125 mL of toluene, 30 mL of ethanol, and 10 mL of water and degassed with nitrogen gas for 30 min. To the reaction mixture, tetrakis(triphenylphosphine)palladium (578 mg, 500 μmol) was added and stirred at 85 ºC for 24 h. The crude compound was extracted with ethyl acetate, purified by silica column chromatography (hexane/ethyl acetate, R_f: 0.21, Hex:EA=2:1), and dried under vacuum to give a white solid. Yield: 1.2 g (41%). ^{1}H NMR (400 MHz, $CDCl_3$): δ 8.92 (d, J = 2.3 Hz, 1H), 8.72 (s, 1H), 8.67 (dd, J = 4.9, 1.7 Hz, 1H), 8.46 (d, J = 1.7 Hz, 2H), 7.97 (dt, J = 7.9, 2.1 Hz, 1H), 7.44 (dd, J = 8.0, 4.8 Hz, 1H), 3.99 (s, 6H); ^{13}C NMR (100 MHz, $CDCl_3$): δ 166.07, 149.40, 148.23, 138.72, 134.93, 134.83, 132.41, 131.70, 130.28, 123.96, 52.75; HRMS *m/z* calculated for $[C_{15}H_{13}NO_4+H]^+$: 272.0917, found: 272.0917.

(5-(pyridin-3-yl)-1,3-phenylene)dimethanol (23)

Dimethyl 5-(pyridin-3-yl)isophthalate (**22**) (500 mg, 1.8 mmol) was dissolved into 18 mL of THF and cooled at 0 ºC by using ice bath. Lithium aluminum hydride (350 mg, 9.2 mmol) was slowly added. The reaction mixture was heated to 60 ºC for 16 h. The remaining lithium aluminum hydride was quenched by the slow addition of saturated aq. $NaHCO_3$ solution at 0 ºC. The crude compound was extracted with ethyl acetate, washed with water, and dried under $MgSO_4$ and vacuum. The crude compound was purified by silica column chromatography (CH_2Cl_2/MeOH, R_f: 0.32, CH_2Cl_2:MeOH=9:1) and dried under vacuum to give a pale yellow solid. Yield: 320 mg (81%). ^{1}H NMR (500 MHz, DMSO-d_6): δ 8.86 (m, 1H), 8.56 (dd, J = 4.8, 1.6 Hz, 1H), 8.04 (m, 1H), 7.51 (m, 2H), 7.48 (m, 1H), 7.35 (s, 1H), 5.27 (t, J = 5.4 Hz, 2H), 4.57 (d, J = 5.3 Hz, 4H); ^{13}C NMR (100 MHz, DMSO-d_6): δ 148.45, 147.60, 143.43, 136.66, 135.90, 134.09, 124.39, 123.95, 123.29, 62.86; HRMS *m/z* calculated for $[C_{13}H_{13}NO_2+H]^+$: 216.1019, found: 216.1020.

3-(3,5-bis(bromomethyl)phenyl)pyridine (24)

(5-(pyridin-3-yl)-1,3-phenylene)dimethanol (**23**) (310 mg, 1.4 mmol) was cooled at 0 ºC by using ice bath. HBr (48% in water, 6.2 mL, 55 mmol) was slowly added. The reaction mixture was warmed up to room temperature and heated at 120 ºC for 16 h with continuous stirring. After 16

h, the remaining HBr was quenched by the slow addition of saturated aq. $NaHCO_3$ solution at 0 ºC. The resulting brown solid was collected by filtration, washed with water, and dried under vacuum. Yield: 412 mg (84% yield). ^{1}H NMR (300 MHz, $CDCl_3$): δ 8.87 (m, 1H), 8.66 (m, 1H), 7.92 (d, J = 7.6 Hz, 1H), 7.56 (d, J = 1.6 Hz, 2H), 7.49 (s, 1H), 7.43 (dd, J = 7.9, 4.8 Hz, 1H), 4.56 (s, 4H); ^{13}C NMR (100 MHz, $CDCl_3$): δ 149.05, 148.23, 139.55, 139.26, 135.68, 134.77, 129.36, 127.99, 123.85, 32.56; HRMS *m/z* calculated for $[C_{13}H_{11}Br_2N+H]^+$: 339.9331, found: 339.9326.

Tetraethyl 2,2'-(((5-(pyridin-3-yl)-1,3-phenylene)bis(methylene))bis(oxy))diterephthalate (25)

3-(3,5-bis(bromomethyl)phenyl)pyridine (**24**) (150 mg, 440 μmol) was dissolved into 20 mL of DMF. Diethyl 2-hydroxyterephthalate (**3**) (262 mg, 1.10 mmol), and potassium carbonate (304 mg, 2.20 mmol) were added to the solution. The reaction mixture was stirred at 80 ºC for 24 h. The crude compound was extracted with ethyl acetate, washed with water, dried over $MgSO_4$, and further purified by silica column chromatography (hexane/ethyl acetate, R_f: 0.28, Hex:EA=1:1) and dried under vacuum to give a white solid. Yield: 193 mg (67%). ^{1}H NMR (500 MHz, $CDCl_3$): δ 8.93 (s, 1H), 8.62 (d, J = 4.4 Hz, 1H), 8.01 (d, J = 7.3 Hz, 1H), 7.85 (d, J = 7.9 Hz, 2H), 7.80 (s, 2H), 7.74 (d, J = 1.4 Hz, 2H), 7.69 (dd, J = 7.9, 1.4 Hz, 2H), 7.65 (s, 1H), 7.43 (s, 1H), 5.32 (s, 4H), 4.38 (dq, J = 21.3, 7.1 Hz, 8H), 1.40 (t, J = 7.1 Hz, 6H), 1.29 (t, J = 7.1 Hz, 6H); ^{13}C NMR (100 MHz, $CDCl_3$): 165.86, 165.79, 157.63, 148.49, 148.09, 138.50, 137.89, 134.99, 134.78, 131.66, 125.64, 125.47, 125.30, 123.87, 121.90, 114.47, 70.54, 61.70, 61.46, 14.42, 14.33; HRMS *m/z* calculated for $[C_{37}H_{37}NO_{10}+H]^+$: 656.2490, found: 656.2484.

2,2'-(((5-(pyridin-3-yl)-1,3-phenylene)bis(methylene))bis(oxy))diterephthalic acid (L5)

Tetraethyl 2,2'-(((5-(pyridin-3-yl)-1,3-phenylene)bis(methylene))bis(oxy))diterephthalate (**25**) (193 mg, 294 μmol) was dissolved in 10 mL of CH_2Cl_2, 10 mL of THF, 10 mL of MeOH, and 10 mL of water. To the solution, sodium hydroxide (353 mg, 8.83 mmol) was added. The reaction mixture was stirred at room temperature for 48 h, dried under vacuum using a rotary evaporator, and acidified with 1 M HCl until the pH reached 1. The resulting precipitate was collected by

filtration, washed with water, and dried under vacuum to obtain a white solid. Yield: 155 mg (97%). ^{1}H NMR (500 MHz, DMSO-d_6): δ 8.97 (s, 1H), 8.64 (d, J = 5.0 Hz, 1H), 8.17 (s, 1H), 7.97 (s, 2H), 7.76 (m, 4H), 7.69 (s, 1H), 7.61 (d, J = 7.7 Hz, 3H), 5.37 (s, 4H); ^{13}C NMR (125 MHz, DMSO-d_6): δ 167.09, 166.62, 156.73, 146.13, 138.13, 136.66, 135.93, 134.69, 130.76, 126.00, 125.72, 125.03, 124.77, 121.50, 114.09, 69.57; HRMS *m/z* calculated for $[C_{29}H_{21}NO_{10}+H]^+$: 544.1238, found: 544.1241.

Dimethyl 5-((trimethylsilyl)ethynyl)isophthalate (27)

Dimethyl 5-iodoisophthalate (**15**) (2.00 g, 6.25 mmol), triphenylphosphine (328 mg, 1.25 mmol), bis(triphenylphosphine)palladium(II) dichloride (439 mg, 625 μmol), and copper(I) iodide (238 mg, 1.25 mmol) were dispersed into 37 mL of triethylamine and degassed by three freeze pump thaw cycles. Trimethylsilylacetylene (**26**) (1.00 mL, 7.50 mmol) was slowly added. The reaction mixture was stirred at 90 ºC for 24 h. The remaining catalyst was removed by passing through a pad of Celite. The filtrate was dried under vacuum using a rotary evaporator and purified by silica column chromatography (hexane/ethyl acetate, R_f: 0.36, Hex:EA=9:1) and dried under vacuum to give a white solid. Yield: 1.75 g (96%). ^{1}H NMR (400 MHz, $CDCl_3$): δ 8.60 (t, J = 1.6 Hz, 1H), 8.29 (t, J = 1.5 Hz, 2H), 3.95 (s, 6H), 0.26 (s, 9H); ^{13}C NMR (100 MHz, $CDCl_3$): δ 165.71, 137.01, 130.94, 130.41, 124.34, 102.83, 96.86, 52.67, -0.08; HRMS *m/z* calculated for $[C_{15}H_{18}O_4Si+H]^+$: 291.1047, found: 291.1046.

(5-ethynyl-1,3-phenylene)dimethanol (28)

Dimethyl 5-((trimethylsilyl)ethynyl)isophthalate (**27**) (1.70 g, 5.85 mmol) was dissolved in 60 mL of THF. To the mixture, lithium aluminum hydride (1.11 g, 29.3 mmol) was slowly added. The reaction mixture was stirred at 60 ºC for 24 h. After 24 h, saturated aqueous sodium bicarbonate solution was slowly added at 0 ºC until bubble ceased. The crude compound was extracted with ethyl acetate, dried over $MgSO_4$, and isolated by silica column chromatography (hexane/ethyl acetate, R_f: 0.28, Hex:EA=2:3) and dried under vacuum to give a white solid. Yield: 808 mg (85%). ^{1}H NMR (300 MHz, DMSO-d_6): δ 7.30 (s, 1H), 7.27 (s, 2H), 5.26 (t, J = 5.4 Hz, 2H), 4.47 (d, J = 5.0 Hz, 4H), 4.11 (s, 1H); ^{13}C NMR (100 MHz, DMSO-d_6): δ 143.03, 127.88, 125.10,

121.17, 83.86, 80.14, 62.39; MS (EI) *m/z* calculated for $[C_{10}H_{10}O_2]^+$: 162.07, found: 162.05.

1,3-bis(bromomethyl)-5-ethynylbenzene (29)

(5-Ethynyl-1,3-phenylene)dimethanol (**28**) (800 mg, 4.93 mmol) was dissolved in 40 mL of THF. PBr_3 (2.3 mL, 24.7 mmol) was slowly added at 0 ºC. The reaction mixture was stirred at room temperature for 16 h. The remaining PBr_3 was quenched by slow addition of saturated sodium bicarbonate at 0 ºC. The crude compound was extracted with ethyl acetate and isolated by silica column chromatography using hexane as eluent (hexane/ethyl acetate, R_f: 0.29, Hex:EA=100:0) and dried under vacuum to give a white solid. Yield: 1.11 g (78%). ^{1}H NMR (300 MHz, $CDCl_3$): δ 7.45 (d, J = 1.7 Hz, 2H), 7.40 (t, J = 1.8 Hz, 1H), 4.43 (s, 4H), 3.11 (s, 1H); ^{13}C NMR (100 MHz, $CDCl_3$): δ 138.84, 132.66, 130.12, 123.44, 82.44, 78.42, 32.05; MS (EI) *m/z* calculated for $[C_{10}H_8Br_2]^+$: 285.90, found: 285.89.

Tetraethyl 2,2'-(((5-ethynyl-1,3-phenylene)bis(methylene))bis(oxy))diterephthalate (30)

1,3-Bis(bromomethyl)-5-ethynylbenzene (**29**) (1.00 g, 3.47 mmol), diethyl 2-hydroxyterephthalate (**3**) (1.82 g, 7.64 mmol), and potassium carbonate (1.92 g, 13.9 mmol) were dispersed into 40 mL of DMF. The reaction mixture was stirred at 80 ºC for 24 h. The crude compound was extracted with ethyl acetate, washed with water, dried under vacuum using rotatory evaporator, and purified by silica column chromatography (hexane/ethyl acetate, R_f: 0.42, Hex:EA=2:1) and dried under vacuum to give a white solid. Yield: 1.93 g (92%). ^{1}H NMR (500 MHz, $CDCl_3$): δ 7.85 (d, J = 8.3 Hz, 2H), 7.69 (dd, J = 5.8, 1.5 Hz, 4H), 7.66 (s, 2H), 7.59 (s, 1H), 5.21 (s, 4H), 4.40 (qd, J = 7.2, 3.9 Hz, 8H), 3.10 (s, 1H), 1.41 (t, J = 7.2 Hz, 6H), 1.36 (t, J = 7.2 Hz, 6H); ^{13}C NMR (100 MHz, $CDCl_3$): δ 166.14, 165.78, 157.45, 137.18, 134.77, 131.78, 130.38, 126.01, 125.32, 122.95, 121.93, 114.34, 83.21, 77.91, 70.17, 61.69, 61.59, 14.42, 14.39; HRMS *m/z* calculated for $[C_{34}H_{34}O_{10}+H]^+$: 603.2225, found: 603.2217.

2,2'-(((5-ethynyl-1,3-phenylene)bis(methylene))bis(oxy))diterephthalic acid (L6)

2,2'-(((5-Ethynyl-1,3-phenylene)bis(methylene))bis(oxy))diterephthalic acid (**30**) (1.85 g, 3.07

mmol) was dissolved in 50 mL of THF, 50 mL of water, and 25 mL of MeOH. To the solution, sodium hydroxide (6.14 g, 154 mmol) was added. The reaction mixture was stirred at room temperature for 48 h, dried under vacuum using a rotary evaporator, and acidified with 1 M HCl until the pH reached 1. The resulting precipitate was collected by filtration, washed with water, and dried under vacuum to obtain a white solid. Yield: 1.45 g (96%). ^{1}H NMR (400 MHz, DMSO-d_6): δ 7.73 (d, J = 7.9 Hz, 2H), 7.67 (s, 3H), 7.61 (m, 4H), 5.28 (s, 4H), 4.25 (s, 1H); ^{13}C NMR (100 MHz, DMSO-d_6): δ 167.13, 166.65, 156.51, 137.73, 134.56, 130.59, 129.43, 126.28, 126.08, 122.01, 121.57, 114.00, 83.42, 81.12, 69.10; HRMS *m/z* calculated for $[C_{26}H_{18}O_{10}\text{-}H]^-$: 489.0827, found: 489.0831.

Synthesis of monomer with pyridine derivatives

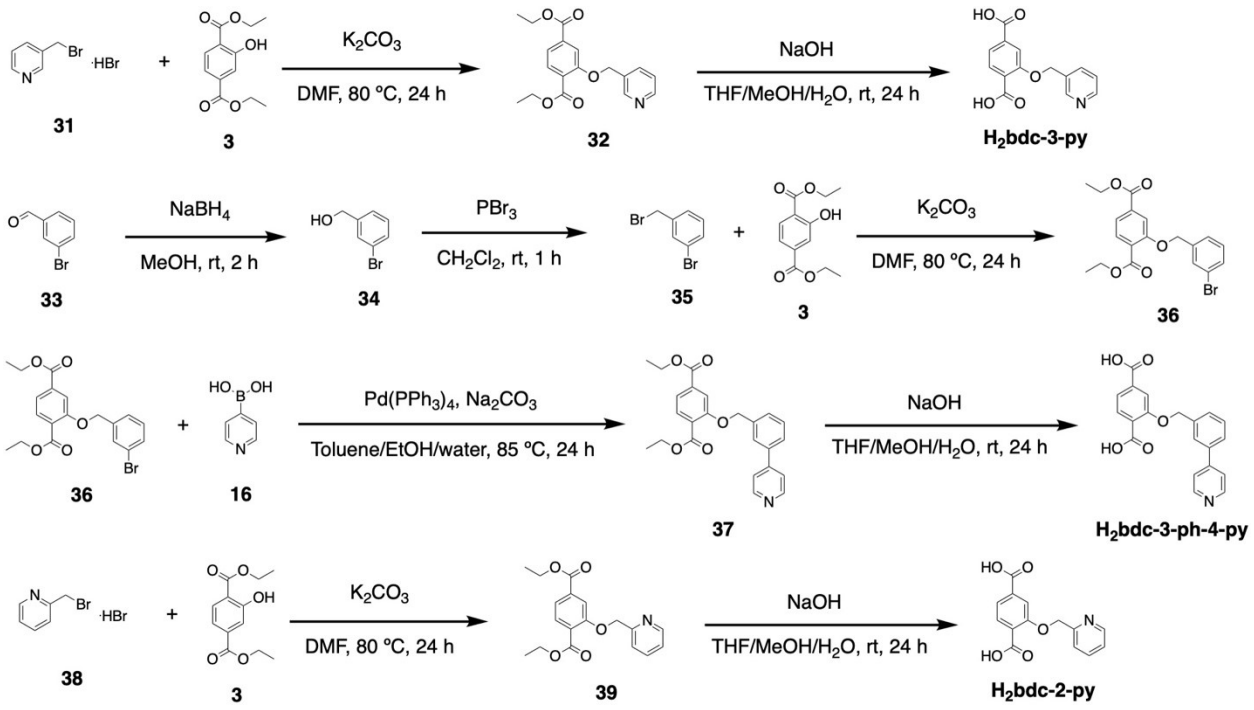

Figure S3. Synthesis of monomer linkers with pyridine tethers (**H_2bdc-3-py**, **H_2bdc-3-ph-4-py**, **H_2bdc-2-py**).

Diethyl 2-(pyridin-3-ylmethoxy)terephthalate (32)

3-(Bromomethyl)pyridine hydrobromide (**31**) (350 mg, 1.38 mmol) was dissolved into 20 mL of DMF. Diethyl 2-hydroxyterephthalate (**3**) (396 mg, 1.66 mmol), and potassium carbonate (1.91 g, 13.8 mmol) were added to the solution. The reaction mixture was stirred at 80 ºC for 24 h. The crude compound was extracted with ethyl acetate, washed with water, dried over $MgSO_4$, and further purified by silica column chromatography (hexane/ethyl acetate, R_f: 0.20, Hex:EA=2:1) and dried under vacuum to give a white solid. Yield: 395 mg (87%). ^{1}H NMR (500 MHz, $CDCl_3$): δ 8.79 (s, 1H), 8.62 (d, J = 4.9 Hz, 1H), 8.03 (d, J = 7.9 Hz, 1H), 7.87 (dd, J = 8.3, 0.7 Hz, 1H), 7.71 (m, 2H), 7.45 (dd, J = 8.0, 5.0 Hz, 1H), 5.26 (s, 2H), 4.40 (dq, J = 14.2, 7.1 Hz, 4H), 1.43 (t, J = 7.1 Hz, 3H), 1.36 (t, J = 7.1 Hz, 3H); ^{13}C NMR (125 MHz, $CDCl_3$): δ 165.85, 165.72, 157.39, 149.42, 148.56, 135.41, 134.85, 132.18, 131.79, 125.30, 123.76, 122.12, 114.34, 68.51, 61.75, 61.54, 14.43, 14.38; HRMS *m/z* calculated for $[C_{18}H_{19}NO_5+H]^+$: 330.1336, found: 330.1338.

2-(pyridin-3-ylmethoxy)terephthalic acid (H_2bdc-3-py)

Diethyl 2-(pyridine-3-ylmethoxy)terephthalate (**32**) (380 mg, 1.15 mmol) was dissolved in 10 mL of THF, 5 mL of MeOH, and 10 mL of water. To the solution, sodium hydroxide (923 mg, 23.1 mmol) was added. The reaction mixture was stirred at room temperature for 24 h, dried under vacuum using a rotary evaporator, and acidified with 1 M HCl until the pH reached 1. The resulting precipitate was collected by filtration, washed with water, and dried under vacuum to obtain a white solid. Yield: 289 mg (92%). ^{1}H NMR (500 MHz, DMSO-d_6): δ 8.73 (s, 1H), 8.54 (dd, J = 4.8, 1.7 Hz, 1H), 7.91 (d, J = 7.7 Hz, 1H), 7.73 (m, 2H), 7.60 (dd, J = 7.9, 1.4 Hz, 1H), 7.44 (dd, J = 7.9, 4.8 Hz, 1H), 5.32 (s, 2H); ^{13}C NMR (125 MHz, DMSO-d_6): δ 167.01, 166.60, 156.44, 149.06, 148.52, 135.09, 134.59, 132.48, 130.67, 126.18, 123.62, 121.61, 114.03, 67.61; HRMS *m/z* calculated for $[C_{14}H_{11}NO_5+H]^+$: 274.0710, found: 274.0711.

3-bromobenzyl alcohol (34)

3-Bromobenzaldehyde (**33**) (2.0 g, 10.8 mmol) was dissolved into 50 mL of methanol and cooled at 0 ºC by using ice bath. Sodium borohydride (490 mg, 13.0 mmol) was slowly added. The

reaction mixture was stirred at room temperature for 2 h. The remaining sodium borohydride was quenched by the slow addition of saturated aq. $NaHCO_3$ solution at 0 ºC. The desired compound was extracted with ethyl acetate, washed with water, and dried under $MgSO_4$ and vacuum to give a colorless liquid. Yield: 1.82 g (90%). ^{1}H NMR (300 MHz, DMSO-d_6): δ 7.50 (s, 1H), 7.42 (dt, J = 6.3, 2.4 Hz, 1H), 7.30 (m, 2H), 5.31 (t, J = 5.7 Hz, 1H), 4.49 (d, J = 5.5 Hz, 2H); ^{13}C NMR (100 MHz, DMSO-d_6): δ 145.54, 130.32, 129.43, 129.01, 125.31, 121.56, 62.08; MS (EI) *m/z* calculated for $[C_7H_7BrO]^+$: 185.97, found: 185.96.

1-bromo-3-(bromomethyl)benzene (35)

3-Bromobenzyl alcohol (**34**) (1.8 g, 9.62 mmol) was dissolved into 50 mL of CH_2Cl_2 and cooled at 0 ºC by using ice bath. PBr_3 (1.2 mL, 12.5 mmol) was slowly added. The reaction mixture was stirred at room temperature for 1 h. The remaining phosphorous tribromide was quenched by the slow addition of saturated aq. $NaHCO_3$ solution at 0 ºC. The crude compound was extracted with ethyl acetate, washed with water, dried over $MgSO_4$, and further purified by silica column chromatography (hexane/ethyl acetate, R_f: 0.58, Hex:EA=100:0) and dried under vacuum to give a colorless liquid. Yield: 2.1 g (85%). ^{1}H NMR (300 MHz, $CDCl_3$): δ 7.55 (t, J = 1.9 Hz, 1H), 7.43 (dt, J = 7.8, 1.5 Hz, 1H), 7.32 (m, 1H), 7.22 (t, J = 7.8 Hz, 1H), 4.43 (s, 2H); ^{13}C NMR (100 MHz, DMSO-d_6): δ 140.03, 132.20, 131.66, 130.48, 127.78, 122.72, 32.15; MS (EI) *m/z* calculated for $[C_7H_6Br_2]^+$: 247.88, found: 247.79.

Diethyl 2-((3-bromobenzyl)oxy)terephthalate (36)

1-Bromo-3-(bromomethyl)benzene (**35**) (700 mg, 2.80 mmol) was dissolved into 30 mL of DMF. Diethyl 2-hydroxyterephthalate (**3**) (800 mg, 3.36 mmol), and potassium carbonate (1.94 g, 14.0 mmol) were added to the solution. The reaction mixture was stirred at 80 ºC for 24 h. The crude compound was extracted with ethyl acetate, washed with water, dried over $MgSO_4$, and further purified by silica column chromatography (hexane/ethyl acetate, R_f: 0.33, Hex:EA=9:1) and dried under vacuum to give a white solid. Yield: 965 mg (85%). ^{1}H NMR (300 MHz, $CDCl_3$): δ 7.85 (d, J = 8.4 Hz, 1H), 7.69 (m, 3H), 7.45 (t, J = 8.1 Hz, 2H), 7.26 (d, J = 15.8 Hz, 1H), 5.18 (s, 2H), 4.40 (qd, J = 7.1, 2.5 Hz, 4H), 1.40 (dt, J = 10.5, 7.1 Hz, 6H); ^{13}C NMR (100 MHz, $CDCl_3$): δ

166.13, 165.78, 157.38, 138.71, 134.75, 131.77, 131.18, 130.26, 130.15, 125.64, 125.27, 122.80, 121.91, 114.26, 69.87, 61.70, 61.61, 14.43; HRMS *m/z* calculated for $[C_{19}H_{19}BrO_5+H]^+$: 407.0489, found: 407.0487.

Diethyl 2-((3-(pyridin-4-yl)benzyl)oxy)terephthalate (37)

Diethyl 2-((3-bromobenzyl)oxy)terephthalate (**36**) (500 mg, 1.23 mmol), pyridin-4-ylboronic acid (**16**) (196 mg, 1.60 mmol), sodium carbonate (455 mg, 4.30 mmol) were dispersed in a mixture of 20 mL of toluene, 5 mL of ethanol, and 5 mL of water and degassed with nitrogen gas for 30 min. To the reaction mixture, tetrakis(triphenylphosphine)palladium (142 mg, 120 μmol) was added and stirred at 85 ºC for 24 h. The crude compound was extracted with ethyl acetate, purified by silica column chromatography (hexane/ethyl acetate, R_f: 0.35, Hex:EA=1:1), and dried under vacuum to give a white solid. Yield: 245 mg (49%). ^{1}H NMR (300 MHz, $CDCl_3$): δ 8.69 (s, 2H), 7.87 (m, 2H), 7.60 (m, 7H), 5.31 (s, 2H), 4.39 (dq, J = 8.7, 7.1 Hz, 4H), 1.37 (dt, J = 24.3, 7.1 Hz, 6H); ^{13}C NMR (100 MHz, $CDCl_3$): δ 165.90, 165.81, 157.61, 149.98, 148.62, 138.40, 137.58, 134.76, 131.65, 129.54, 127.98, 126.73, 125.93, 125.24, 121.84, 114.40, 70.48, 61.71, 61.47, 14.42, 14.35; HRMS *m/z* calculated for $[C_{24}H_{23}NO_5+H]^+$: 406.1649, found: 406.1648.

2-(pyridin-3-ylmethoxy)terephthalic acid (H_2bdc-3-ph-4-py)

Diethyl 2-((3-(pyridin-4-yl)benzyl)oxy)terephthalate (**37**) (210 mg, 518 μmol) was dissolved in 10 mL of THF, 5 mL of MeOH, and 10 mL of water. To the solution, sodium hydroxide (923 mg, 23.1 mmol) was added. The reaction mixture was stirred at room temperature for 24 h, dried under vacuum using a rotary evaporator, and acidified with 1 M HCl until the pH reached 1. The resulting precipitate was collected by filtration, washed with water, and dried under vacuum to obtain a white solid. Yield: 172 mg (95%). ^{1}H NMR (300 MHz, DMSO-d_6): δ 8.68 (d, J = 5.1 Hz, 2H), 8.05 (s, 1H), 7.76 (m, 5H), 7.59 (q, J = 6.8 Hz, 3H), 5.37 (s, 2H); ^{13}C NMR (100 MHz, DMSO-d_6): δ 167.18, 166.65, 156.62, 149.66, 147.67, 138.06, 136.99, 134.64, 130.78, 129.43, 128.11, 126.31, 126.05, 125.61, 121.48, 114.04, 69.38; HRMS *m/z* calculated for $[C_{20}H_{15}NO_5+H]^+$: 350.1023, found: 350.1025.

Diethyl 2-(pyridin-2-ylmethoxy)terephthalate (39)

2-(Bromomethyl)pyridine hydrobromide (**38**) (350 mg, 1.38 mmol) was dissolved into 20 mL of DMF. Diethyl 2-hydroxyterephthalate (**3**) (396 mg, 1.66 mmol), and potassium carbonate (1.91 g, 13.8 mmol) were added to the solution. The reaction mixture was stirred at 80 ºC for 24 h. The crude compound was extracted with ethyl acetate, washed with water, dried over $MgSO_4$, and further purified by silica column chromatography (hexane/ethyl acetate, R_f: 0.26, Hex:EA=2:1) and dried under vacuum to give a white solid. Yield: 380 mg (83%). ^{1}H NMR (300 MHz, $CDCl_3$): δ 8.60 (m, 1H), 7.88 (d, J = 8.0 Hz, 1H), 7.78 (m, 2H), 7.73 (d, J = 1.5 Hz, 1H), 7.69 (dd, J = 8.0, 1.5 Hz, 1H), 7.23 (t, J = 2.8 Hz, 1H), 5.35 (s, 2H), 4.40 (p, J = 7.2 Hz, 4H), 1.40 (td, J = 7.1, 2.2 Hz, 6H); ^{13}C NMR (100 MHz, $CDCl_3$): δ 165.76, 165.69, 157.57, 156.69, 149.09, 137.26, 135.01, 131.77, 124.67, 122.84, 121.90, 121.31, 114.21, 71.21, 61.69, 61.45, 14.42; HRMS *m/z* calculated for $[C_{18}H_{19}NO_5+H]^+$: 330.1336, found: 330.1335.

2-(pyridin-2-ylmethoxy)terephthalic acid (H_2bdc-2-py)

Diethyl 2-(pyridin-2-ylmethoxy)terephthalate (**39**) (370 mg, 1.12 mmol) was dissolved in 10 mL of THF, 5 mL of MeOH, and 10 mL of water. To the solution, sodium hydroxide (890 mg, 22.5 mmol) was added. The reaction mixture was stirred at room temperature for 24 h, dried under vacuum using a rotary evaporator, and acidified with 1 M HCl until the pH reached 1. The resulting precipitate was collected by filtration, washed with water, and dried under vacuum to obtain a white solid. Yield: 250 mg (81%). ^{1}H NMR (500 MHz, DMSO-d_6): δ 8.65 (s, 1H), 8.01 (s, 1H), 7.75 (dd, J = 18.0, 7.4 Hz, 2H), 7.66 (s, 1H), 7.61 (d, J = 7.9 Hz, 1H), 7.48 (s, 1H), 5.40 (s, 2H); ^{13}C NMR (100 MHz, DMSO-d_6): δ 166.76, 166.46, 156.17, 153.98, 145.64, 141.83, 134.84, 131.05, 126.00, 124.67, 123.17, 122.12, 114.39, 68.52; HRMS *m/z* calculated for $[C_{14}H_{11}NO_5+H]^+$: 274.0710, found: 274.0709.

B. Synthesis and characterization of oligoMOFs

OligoIRMOF-1-L1. $Zn(NO_3)_2 \cdot 6H_2O$ (98 mg, 330 μmol) and **L1** (20 mg, 43 μmol) were dissolved in 2.6 mL of DMF in 1.5 dram vial and placed in an oven. The temperature was raised from room temperature to 100 °C at 0.5 °C/min, held for 72 h. The vial was removed and allowed to cool to room temperature. The mother liquor was decanted and the oligoMOF was washed with fresh DMF three times and rinsed with CH_2Cl_2 three times. Prior to analysis, oligoMOF samples were activated under vacuum at room temperature for 16 h. Yield: 24 mg (58% w.r.t. **L1**, molecular formula: $Zn_4O(\mathbf{L1})_{1.5}$).

OligoIRMOF-1-L3. $Zn(NO_3)_2 \cdot 6H_2O$ (84 mg, 284 μmol) and **L3** (20 mg, 37 μmol) were dissolved in 2.6 mL of DMF in 1.5 dram vial and placed in an oven. The temperature was raised from room temperature to 100 °C at 0.5 °C/min, held for 72 h. The vial was removed and allowed to cool to room temperature. The mother liquor was decanted and the oligoMOF was washed with fresh DMF three times and rinsed with CH_2Cl_2 three times. Prior to analysis, oligoMOF samples were activated under vacuum at room temperature for 16 h. Yield: 19 mg (47% w.r.t. **L3**, molecular formula: $Zn_4O(\mathbf{L3})_{1.5}$).

OligoIRMOF-1-L6. $Zn(NO_3)_2 \cdot 6H_2O$ (93 mg, 314 μmol) and **L6** (20 mg, 41 μmol) were dissolved in 2.5 mL of DMF in 1.5 dram vial and placed in an oven. The temperature was raised from room temperature to 100 °C at 0.5 °C/min, held for 72 h. The vial was removed and allowed to cool to room temperature. The mother liquor was decanted and the oligoMOF was washed with fresh DMF three times and rinsed with CH_2Cl_2 three times. Prior to analysis, oligoMOF samples were activated under vacuum at room temperature for 16 h. Yield: 26 mg (63% w.r.t. **L6**, molecular formula: $Zn_4O(\mathbf{L6})_{1.5}$).

Zn(H_2bdc-3-py). $Zn(NO_3)_2 \cdot 6H_2O$ (41 mg, 139 μmol) and **H_2bdc-3-py** (10 mg, 37 μmol) were dissolved in 1 mL of DEF in 1.5 dram vial and placed in an oven. The temperature was raised from room temperature to 100 °C at 0.5 °C/min, held for 72 h. The vial was removed and allowed

to cool to room temperature. The mother liquor was decanted and the oligoMOF was washed with fresh DMF three times and rinsed with CH_2Cl_2 three times. Prior to analysis, oligoMOF samples were activated under vacuum at room temperature for 16 h. Yield: 9 mg (72% w.r.t. (**H_2bdc-3-py**), molecular formula: Zn(**H_2bdc-3-py**)).

Nitrogen adsorption isotherm analysis

Around 20-50 mg of dried oligoMOF was transferred to a preweighed sample tube and degassed at 50 °C on a Micromeritics ASAP 2020 Adsorption analyzer for 18 h and the sample tube was then reweighed to determine the sample mass. Nitrogen adsorption was then performed at 77 K on the same instrument. BET surface areas were determined from sorption isotherms using the BETSI program (Fairen-Jimenez, D. et al. *Adv. Mater.* **2022**, *34*, 2201502).

Powder X-Ray Diffraction (PXRD)

Dried oligoMOF powder (10 mg) was mounted on a silicon sample holder. PXRD data were collected at ambient temperature on a Bruker D8 Advance diffractometer using LynxEye detector at 40 kV, 40 mA for Cu Kα (λ = 1.5418 Å), with a scan speed of 0.5 sec/step, a step size of 0.02° in 2θ, and a 2θ range of 4-40°.

Scanning Electron Microscopy (SEM) images of oligoMOFs

MOF samples were dispersed in CH_2Cl_2 (~1 mg/mL) and placed them onto silicon wafers using a thin glass capillary. The silicon wafers were mounted on an aluminum sample holder disk with carbon tape and coated using an Ir-sputter coating for 60 sec. A FEI Quanta FEG 250 SEM instrument was used for acquiring images using an accelerating voltage of 5 kV under vacuum at a working distance at 10 mm.

^{1}H NMR spectrum of digested oligoMOFs

Around 3 mg of activated samples were digested in the mixture of 600 µL of DMSO-d_6 and 40 µL of 35 % DCl in D_2O. The resulting solutions were analyzed by ^{1}H NMR.

Synthesis of IRMOF-1 from L1 linker

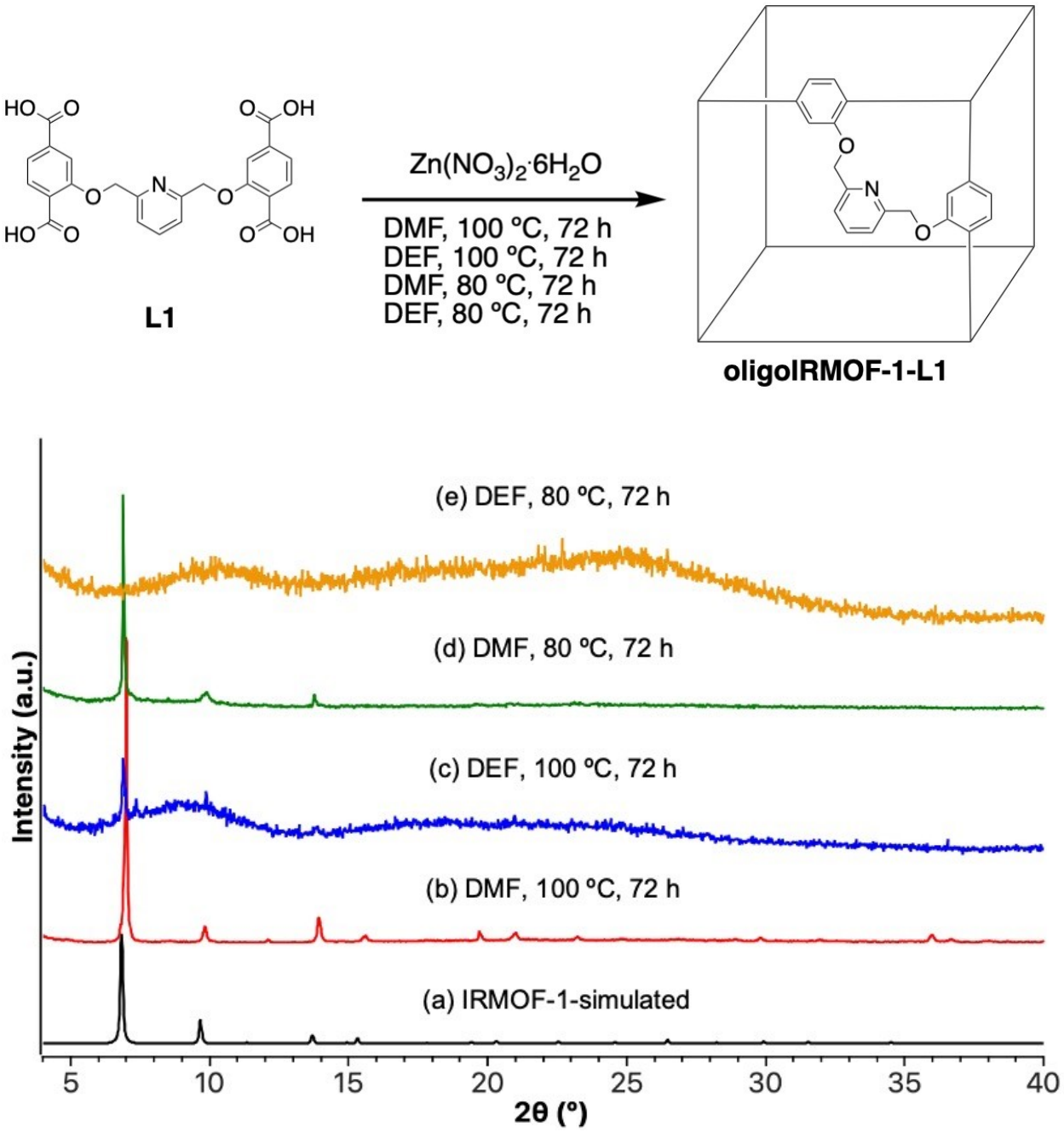

Figure S4. *Top:* Schematic representation of the synthesis of oligoIRMOF-1-L1. *Bottom:* PXRD patterns of (a) simulated IRMOF-1 and oligoIRMOF-1-L1 prepared under different reaction conditions: (b) DMF, 100 ºC 72 h, (c) DEF, 100 ºC 72 h, (d) DMF, 80 ºC 72 h, (e) DEF, 80 ºC 72 h.

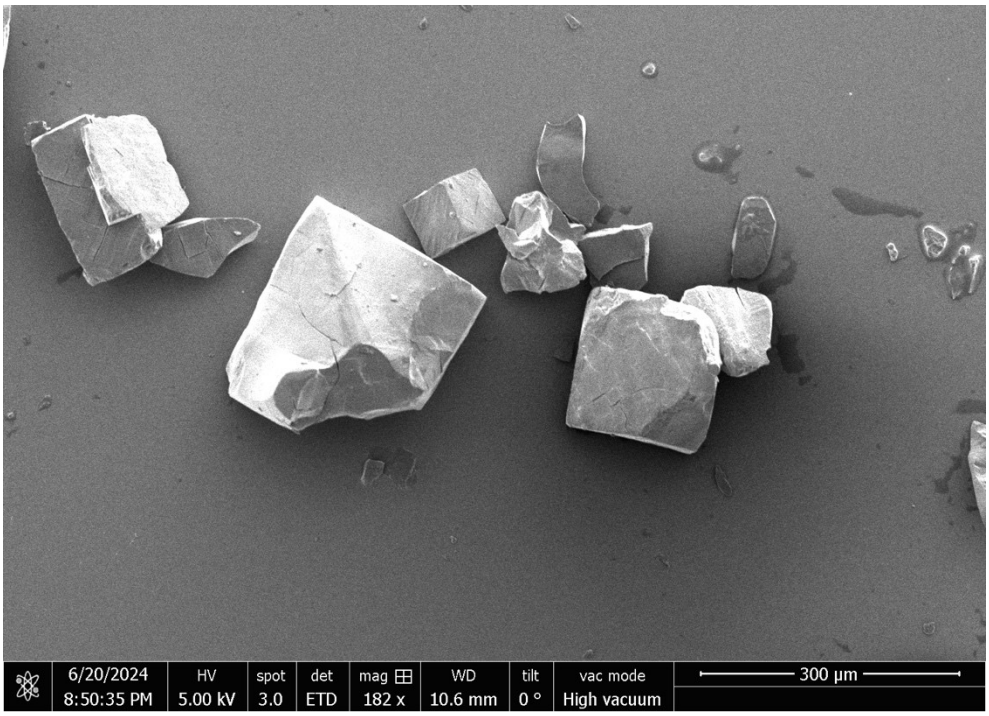

Figure S5. SEM image of oligoIRMOF-1-L1.

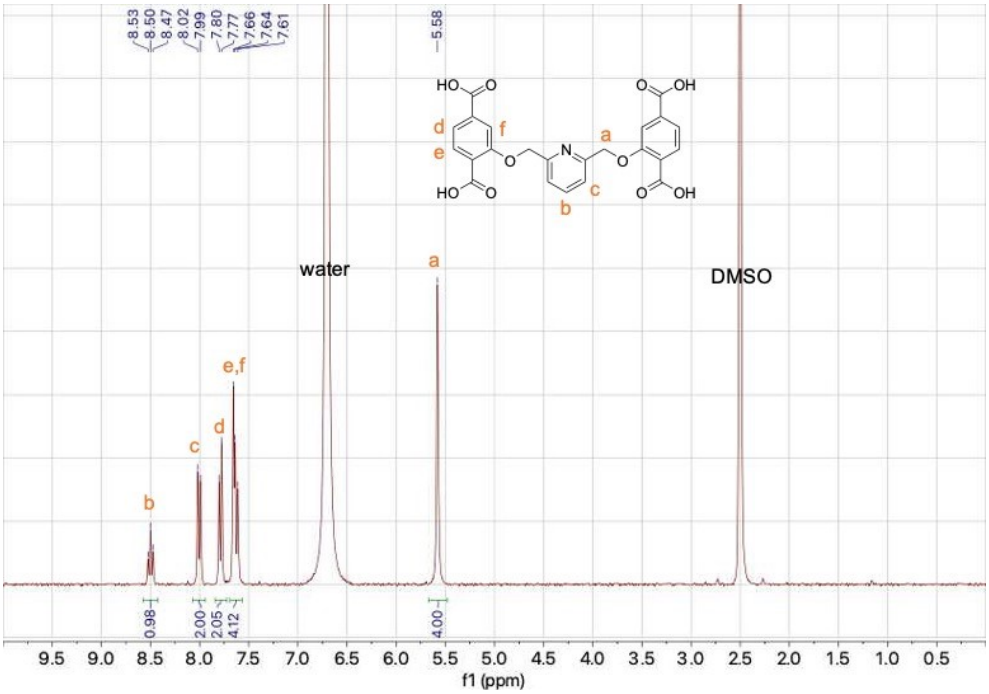

Figure S6. ^{1}H NMR spectrum of digested oligoIRMOF-1-L1.

Synthetic trials for the formation of IRMOF-1 from L2 linker

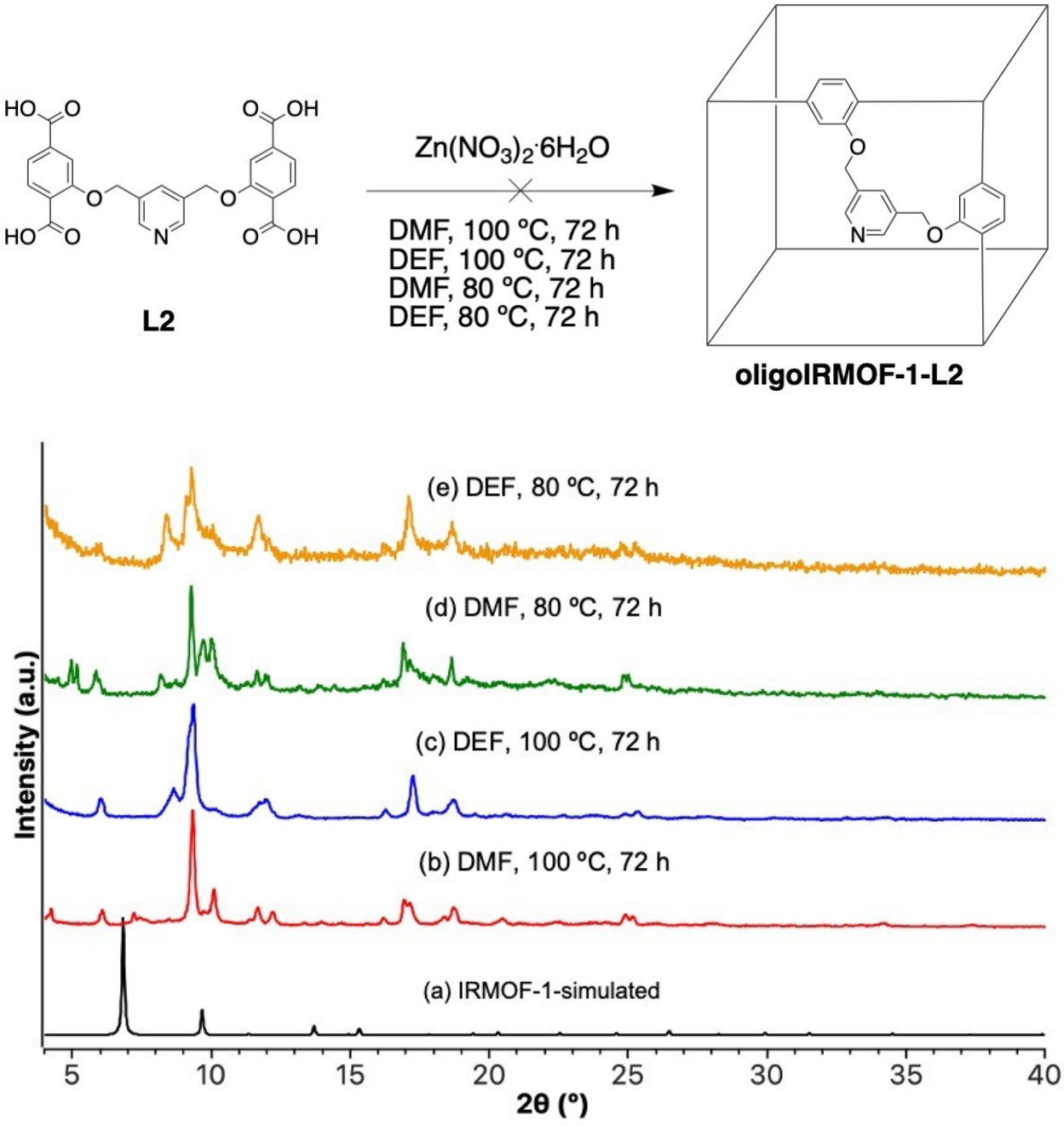

Figure S7. *Top:* Schematic representation of the synthetic trials for oligoIRMOF-1-L2. *Bottom:* PXRD patterns of (a) simulated IRMOF-1, and oligoIRMOF-1-L2 prepared under different reaction conditions: (b) DMF, 100 ºC 72 h, (c) DEF, 100 ºC 72 h, (d) DMF, 80 ºC 72 h, (e) DEF, 80 ºC 72 h.

Synthesis of oligoIRMOF-1-L3 from L3 linker

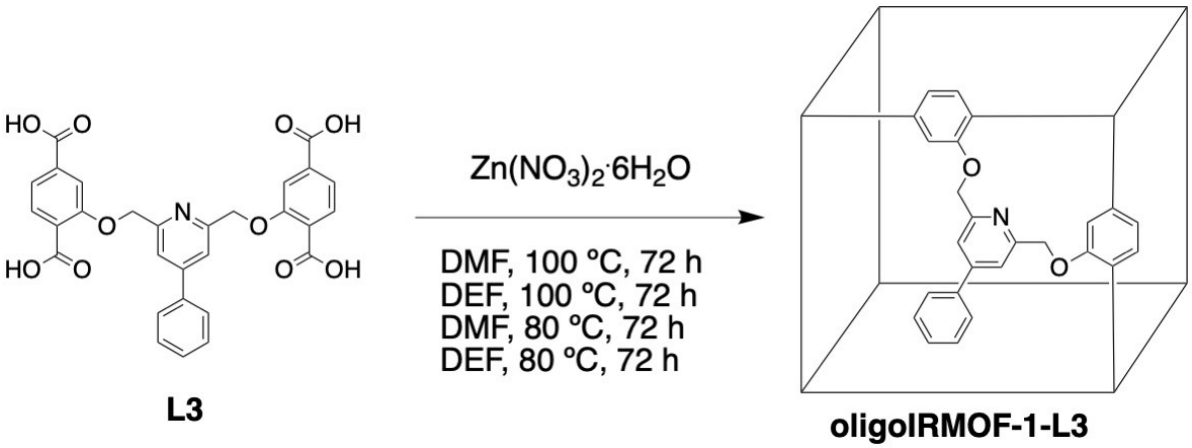

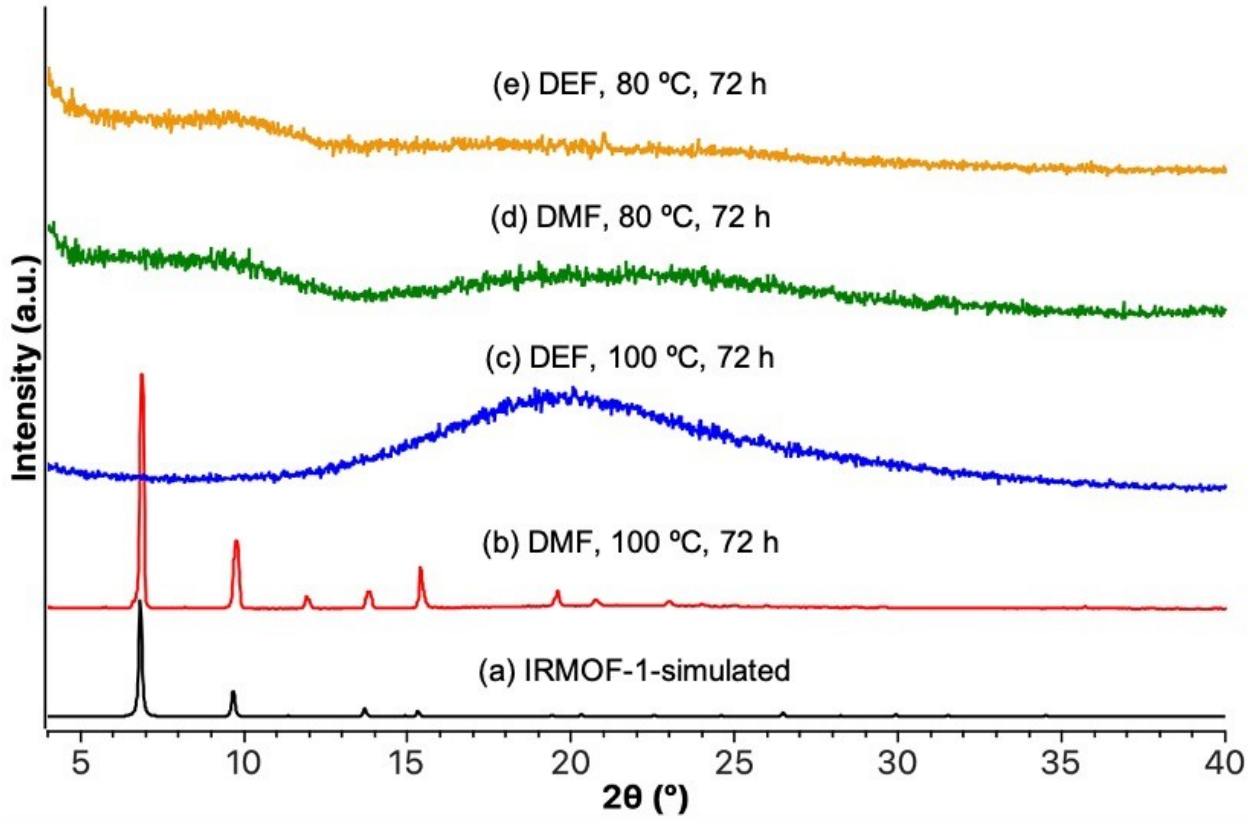

Figure S8. *Top:* Schematic representation of the synthesis of oligoIRMOF-1-L3. *Bottom:* PXRD patterns of (a) simulated IRMOF-1 and oligoIRMOF-1-L3 prepared under different reaction conditions: (b) DMF, 100 ºC 72 h, (c) DEF, 100 ºC 72 h, (d) DMF, 80 ºC 72 h, (e) DEF, 80 ºC 72 h.

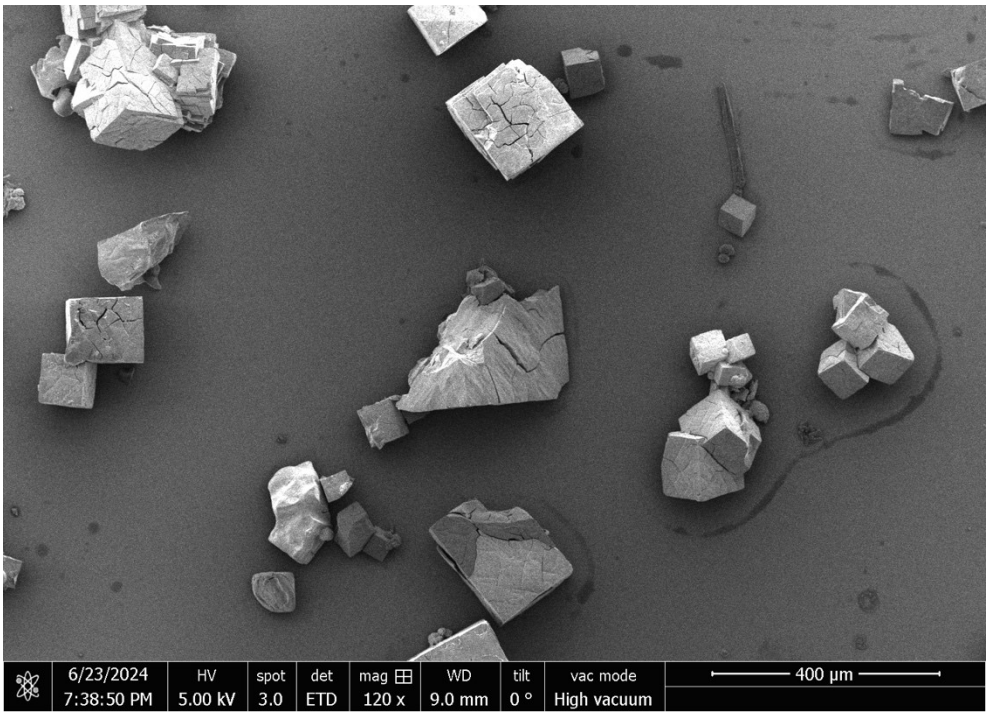

Figure S9. SEM image of oligoIRMOF-1-L3.

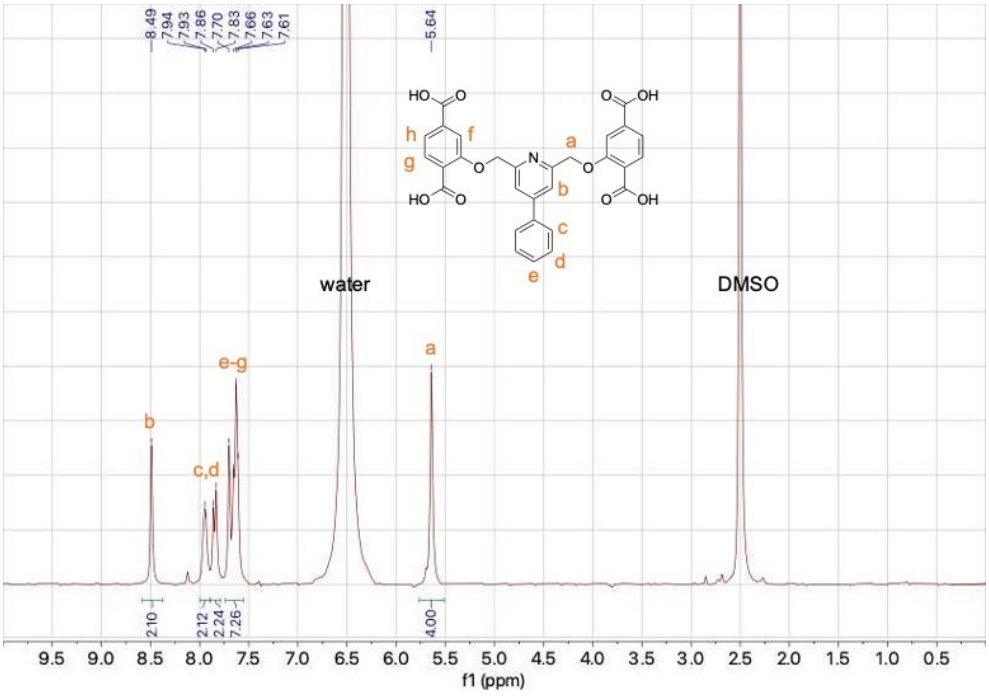

Figure S10. ^{1}H NMR spectrum of digested oligoIRMOF-1-L3.

Synthetic trials for the formation of IRMOF-1 from L4 linker

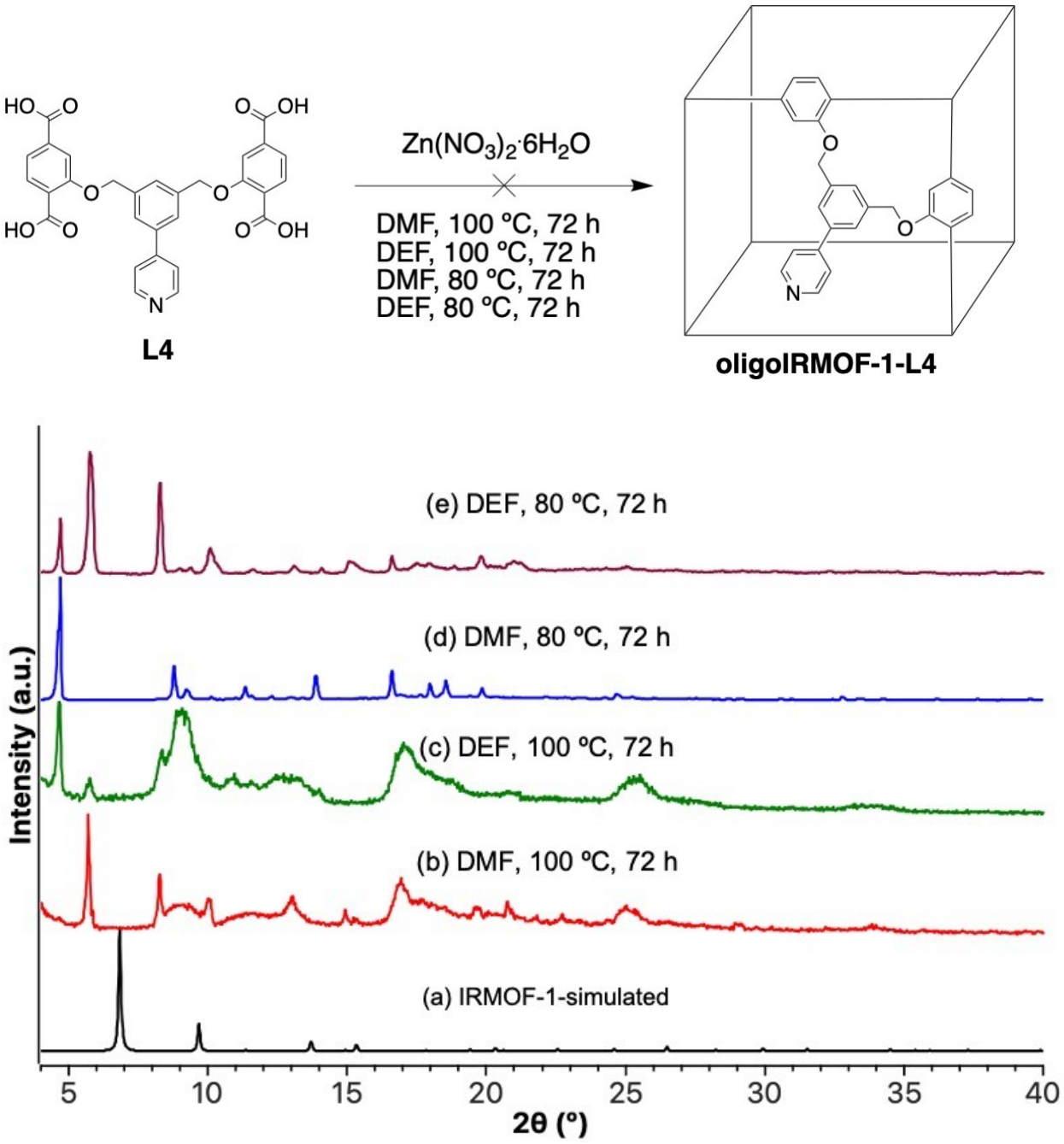

Figure S11. *Top:* Schematic representation of the synthesis of oligoIRMOF-1-L4. *Bottom:* PXRD patterns of (a) simulated IRMOF-1, and oligoIRMOF-1-L4 prepared under different reaction conditions: (b) DMF, 100 ºC 72 h, (c) DEF, 100 ºC 72 h, (d) DMF, 80 ºC 72 h, (e) DEF, 80 ºC 72 h.

Synthetic trials for the formation of IRMOF-1 from L5 linker

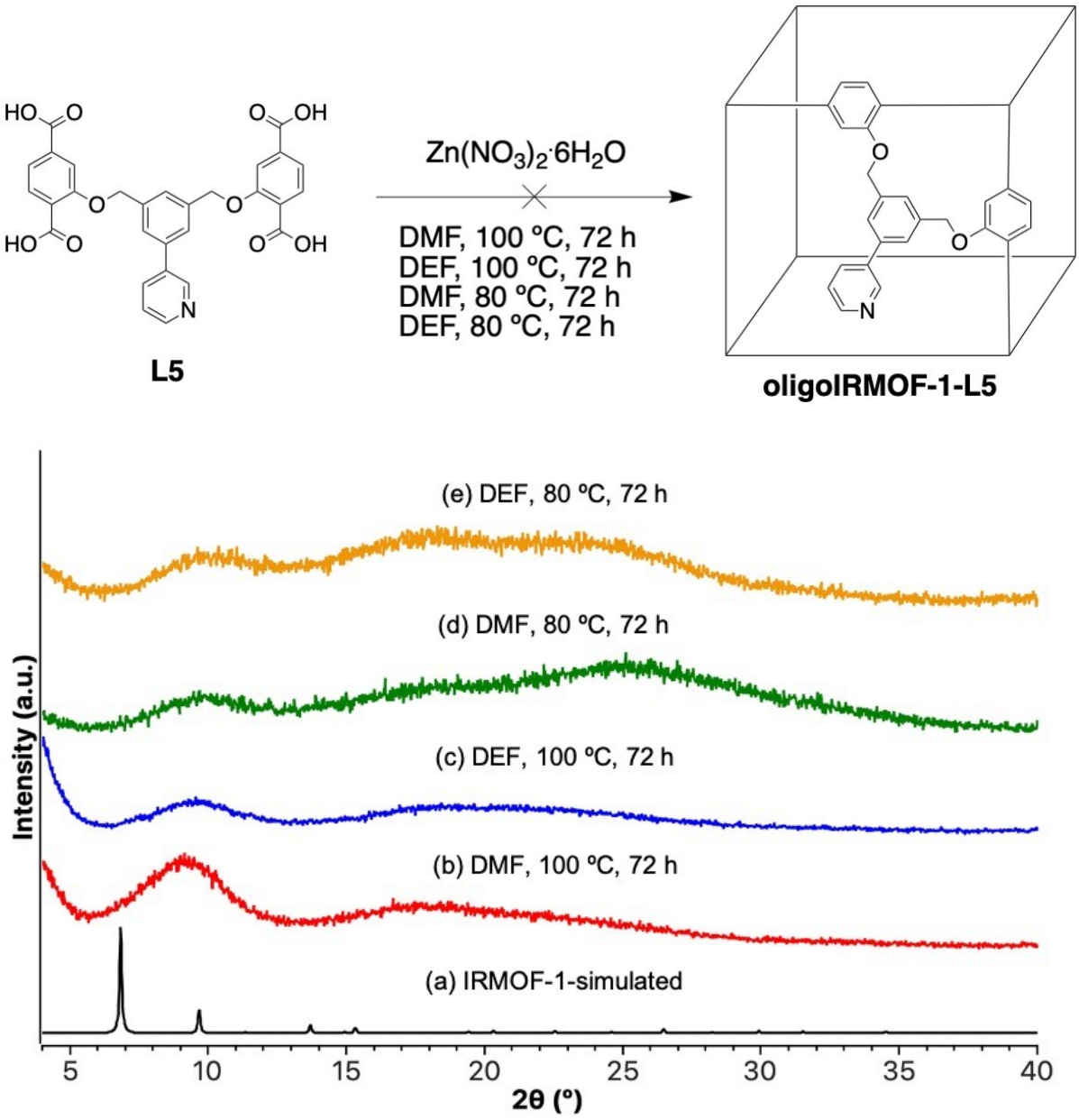

Figure S12. *Top:* Schematic representation of the synthesis of oligoIRMOF-1-L5. *Bottom:* PXRD patterns of (a) simulated IRMOF-1 and oligoIRMOF-1-L5 prepared under different reaction conditions: (b) DMF, 100 ºC 72 h, (c) DEF, 100 ºC 72 h, (d) DMF, 80 ºC 72 h, (e) DEF, 80 ºC 72 h.

Synthesis of Zn(H_2bdc-3-py) from H_2bdc-3-py linker

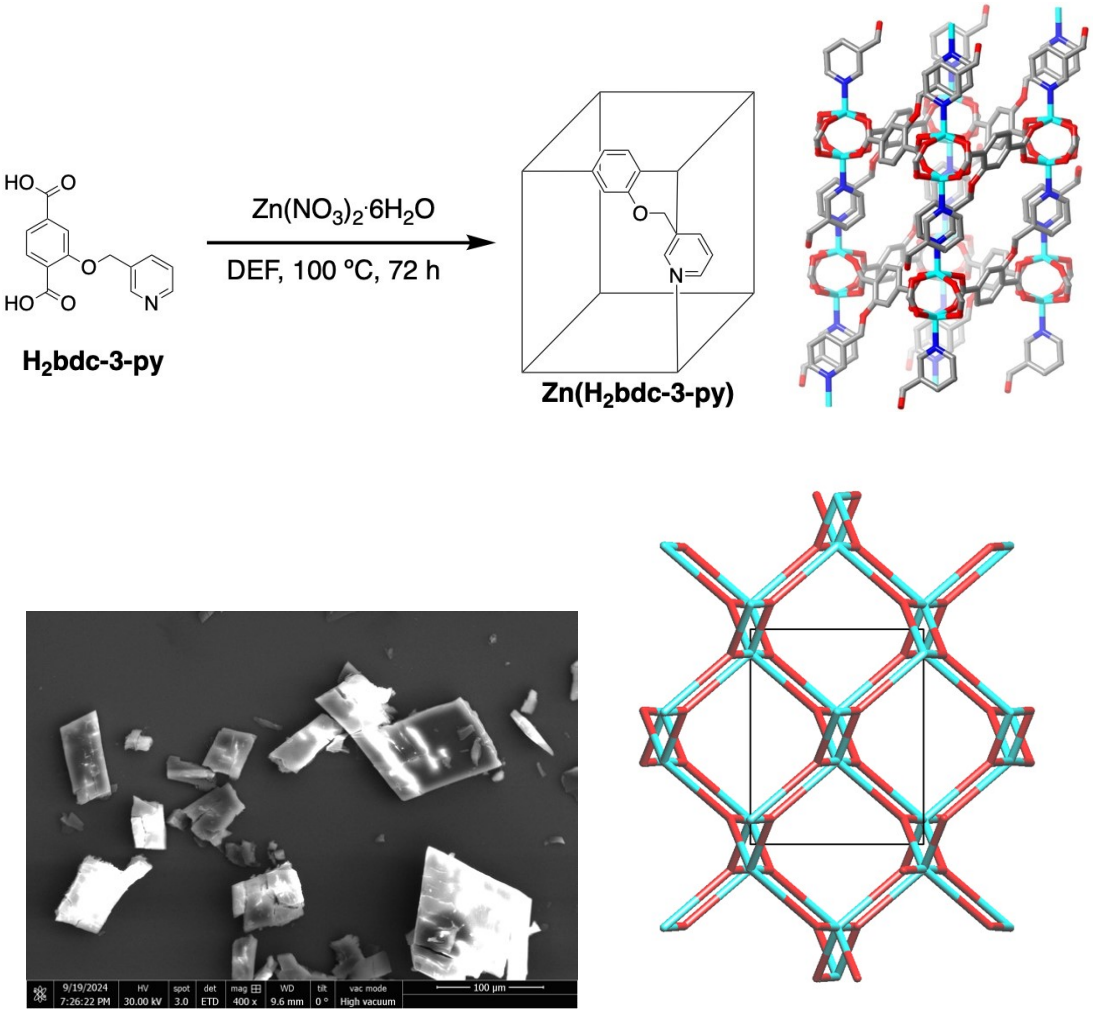

Figure S13. *Top Left:* Schematic representation of the preparation of Zn(H_2bdc-3-py). *Top Right*: crystal structure of Zn(H_2bdc-3-py). Color scheme: C=gray, O=red, N=blue, Zn=cyan. *Bottom Left*: SEM image of Zn(H_2bdc-3-py). *Bottom Right*: Topological diagram of Zn(H_2bdc-3-py). Color scheme: Zn node=cyan, Ligand node=red.

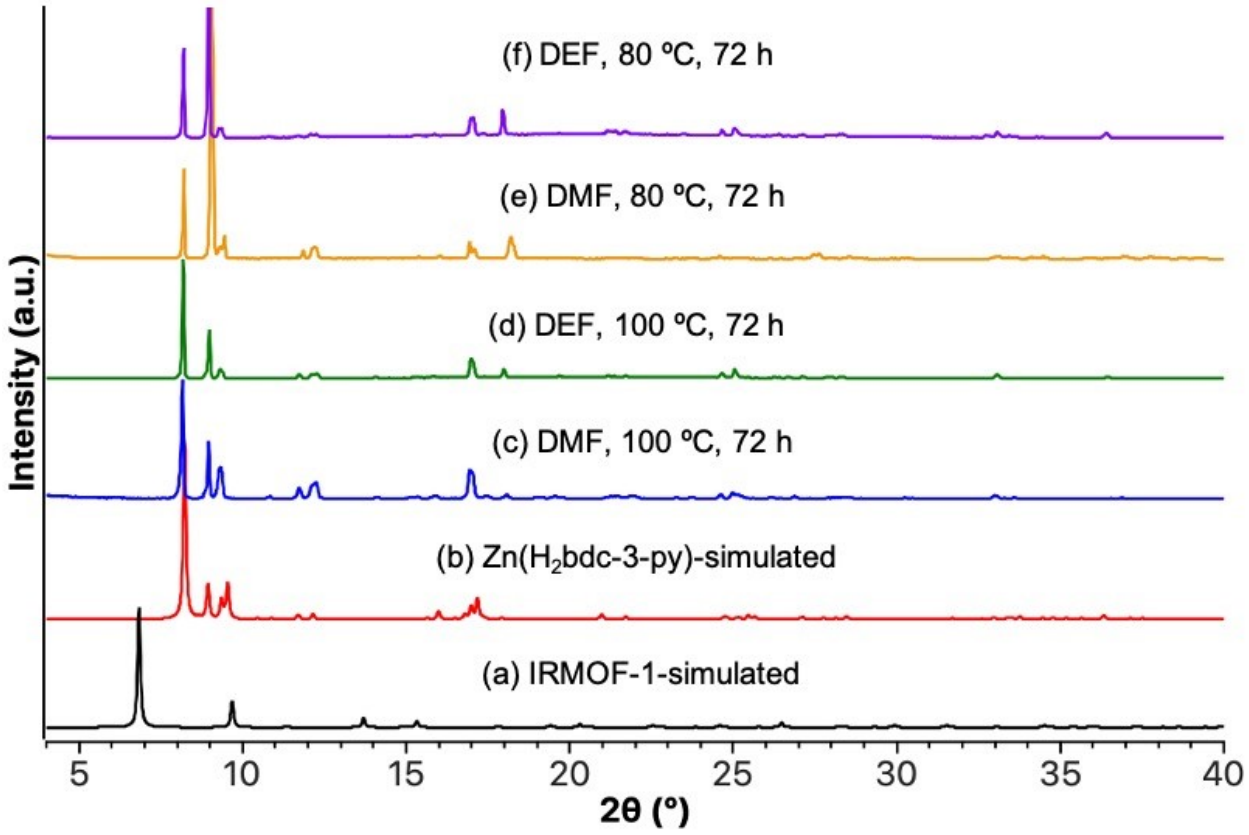

Figure S14. PXRD patterns of (a) simulated IRMOF-1, (b) simulated Zn(H_2bdc-3-py), and Zn(H_2bdc-3-py) prepared under different reaction conditions: (c) DMF, 100 ºC 72 h, (d) DEF, 100 ºC 72 h, (e) DMF, 80 ºC 72 h, (f) DEF, 80 ºC 72 h.

Synthetic trials for the formation of IRMOF-1 from H_2bdc-3-ph-4-py

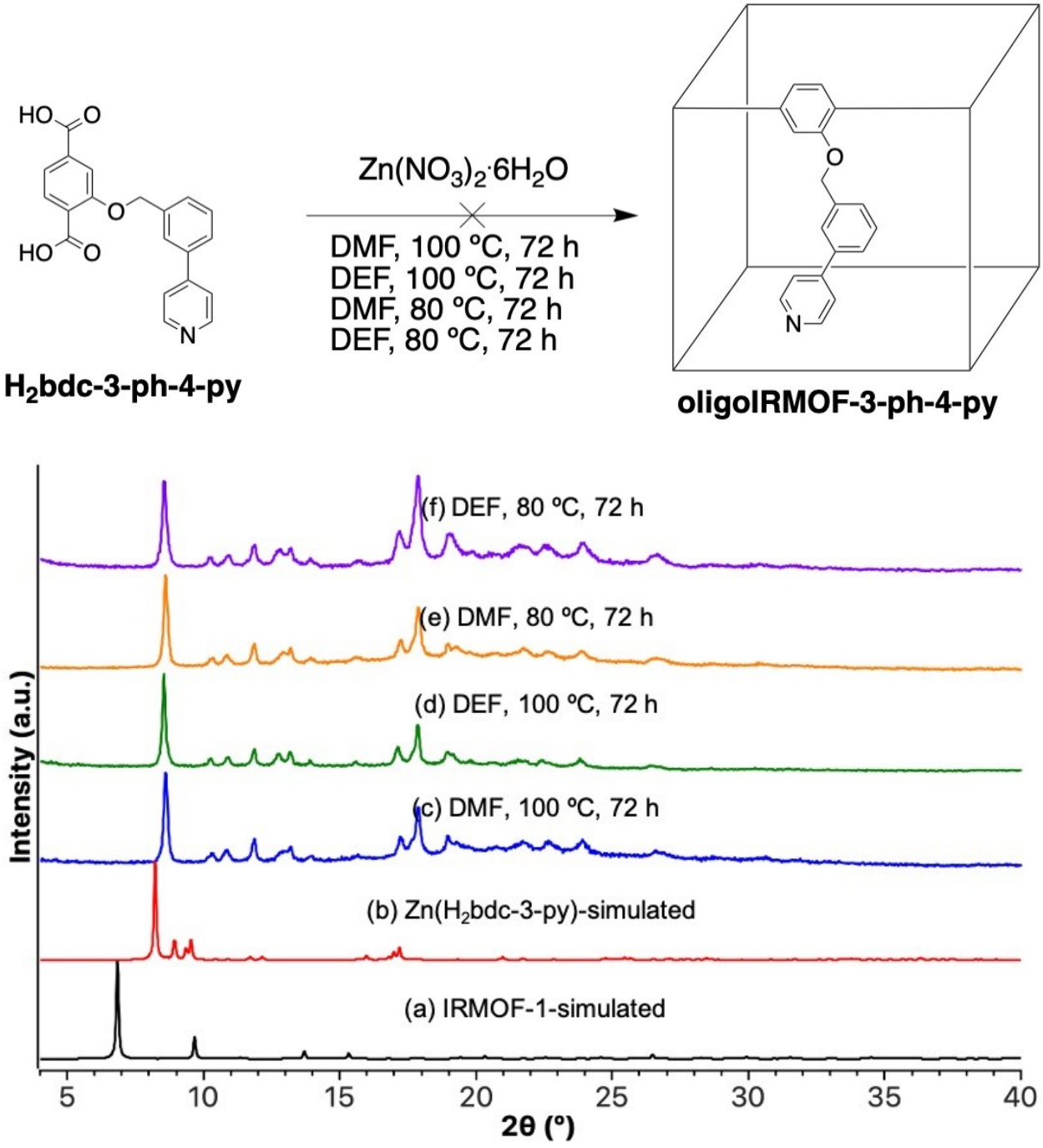

Figure S15. *Top:* Schematic representation of the synthesis of oligoIRMOF-3-ph-4-py. *Bottom:* PXRD patterns of (a) simulated IRMOF-1, (b) simulated Zn(H_2bdc-3-py), and oligoIRMOF-2,6-ph-4-py prepared under different reaction conditions: (c) DMF, 100 ºC 72 h, (d) DEF, 100 ºC 72 h, (e) DMF, 80 ºC 72 h, (f) DEF, 80 ºC 72 h.

Synthetic trials for the formation of IRMOF-1 from H_2bdc-2-py

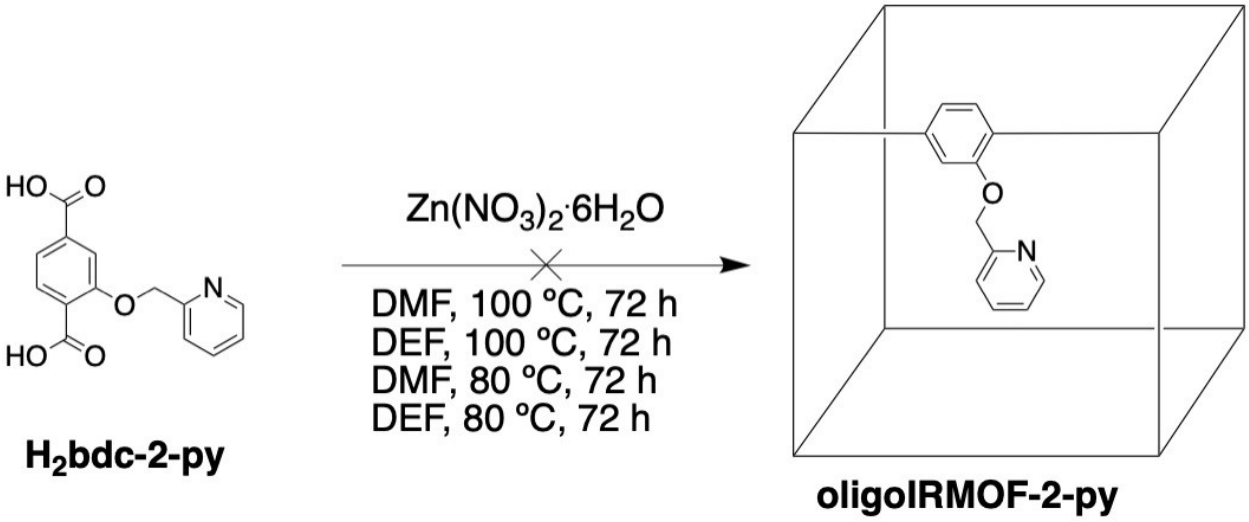

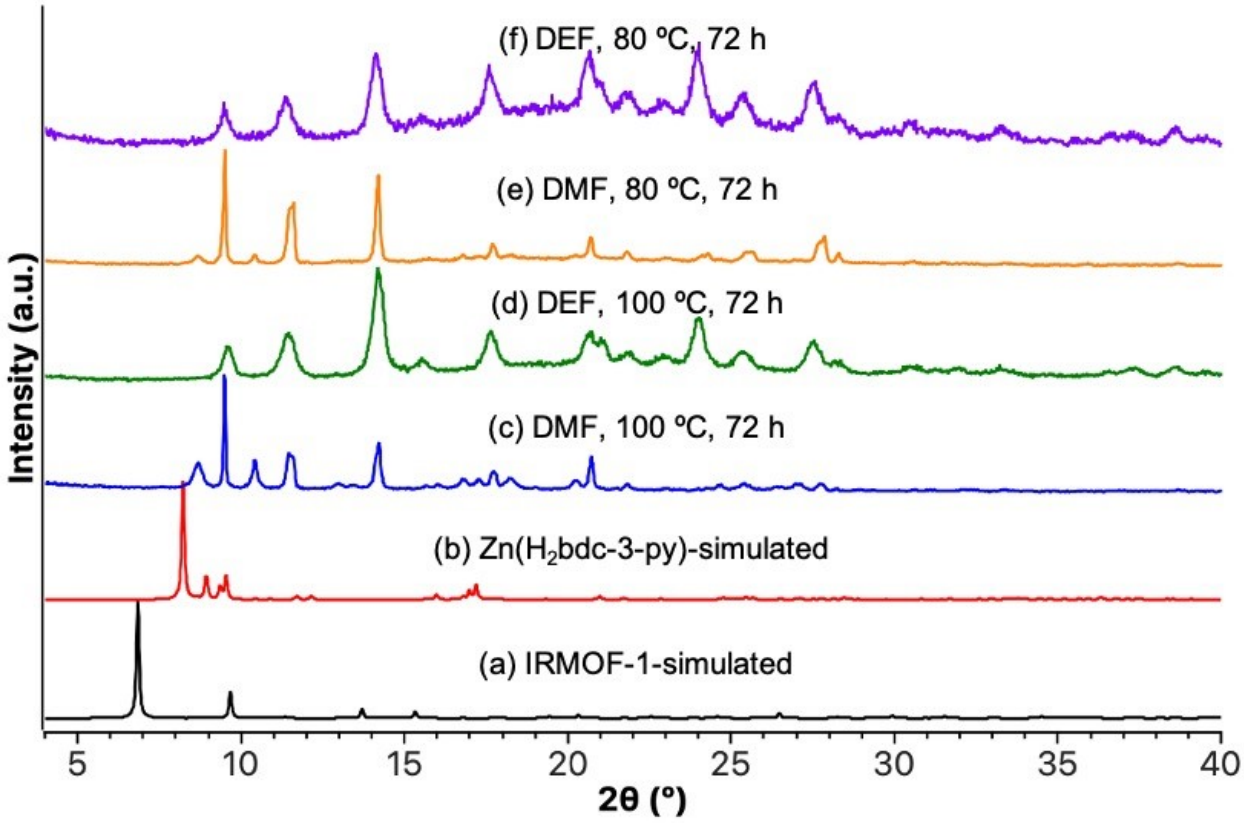

Figure S16. *Top:* Schematic representation of the synthesis of oligoIRMOF-2-py. *Bottom:* PXRD patterns of (a) simulated IRMOF-1, (b) simulated Zn(H_2bdc-3-py), and oligoIRMOF-2-py prepared under different reaction conditions: (c) DMF, 100 ºC 72 h, (d) DEF, 100 ºC 72 h, (e) DMF, 80 ºC 72 h, (f) DEF, 80 ºC 72 h.

SEM image and nitrogen adsorption of oligoIRMOF-1-L6

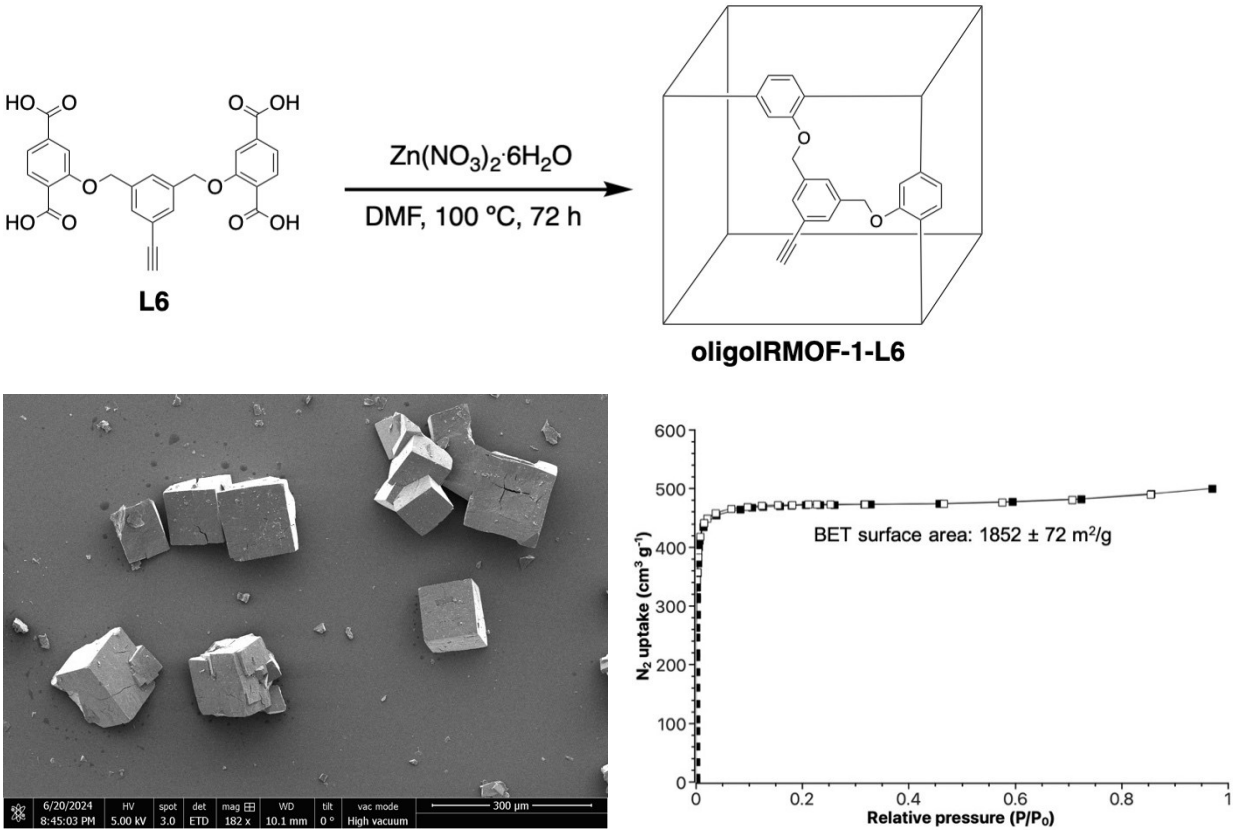

Figure S17. *Top:* Schematic representation of the synthesis of oligoIRMOF-1-L6. *Bottom Left*: SEM image of oligoIRMOF-1-L6. *Bottom Right:* Nitrogen isotherm of oligoIRMOF-1-L6. The filled and unfilled squares correspond to adsorption and desorption, respectively.

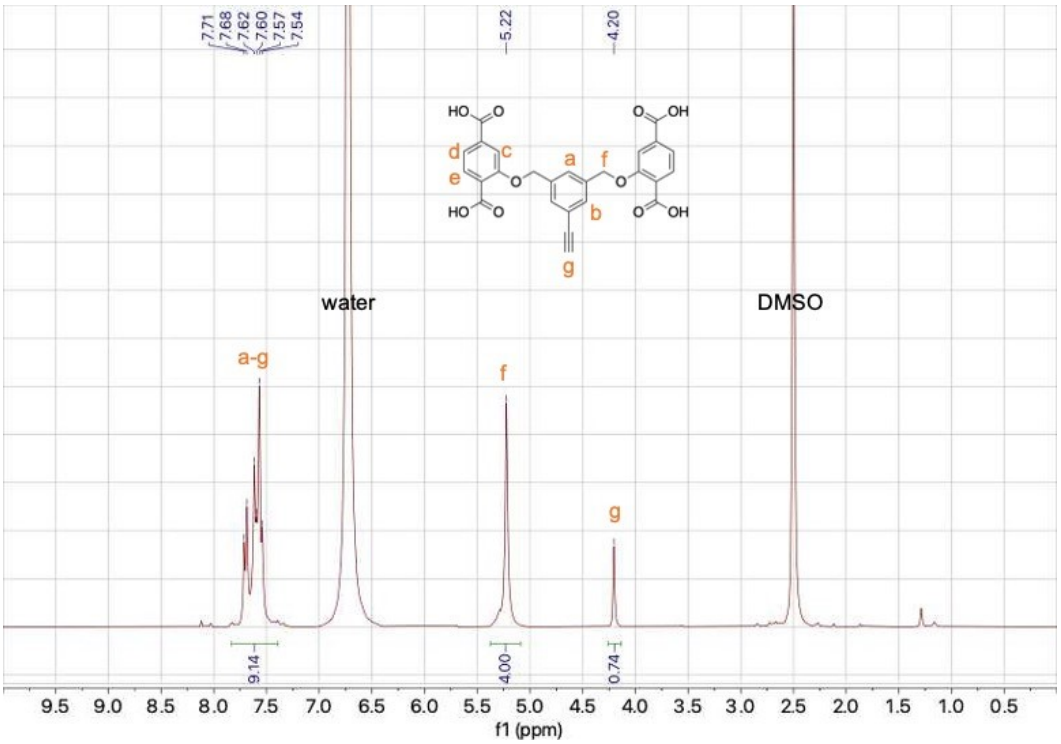

Figure S18. ^{1}H NMR spectrum of digested oligoIRMOF-1-L6.

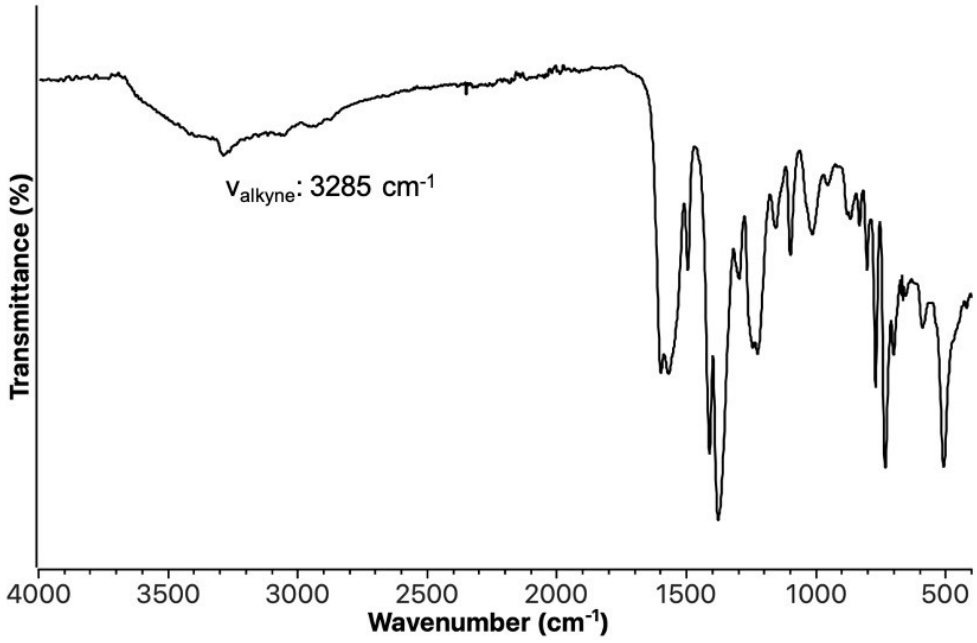

Figure S19. FTIR spectrum of oligoIRMOF-1-L6.

Crystal structure of oligoIRMOF-1-L6 and modeled structure of L6

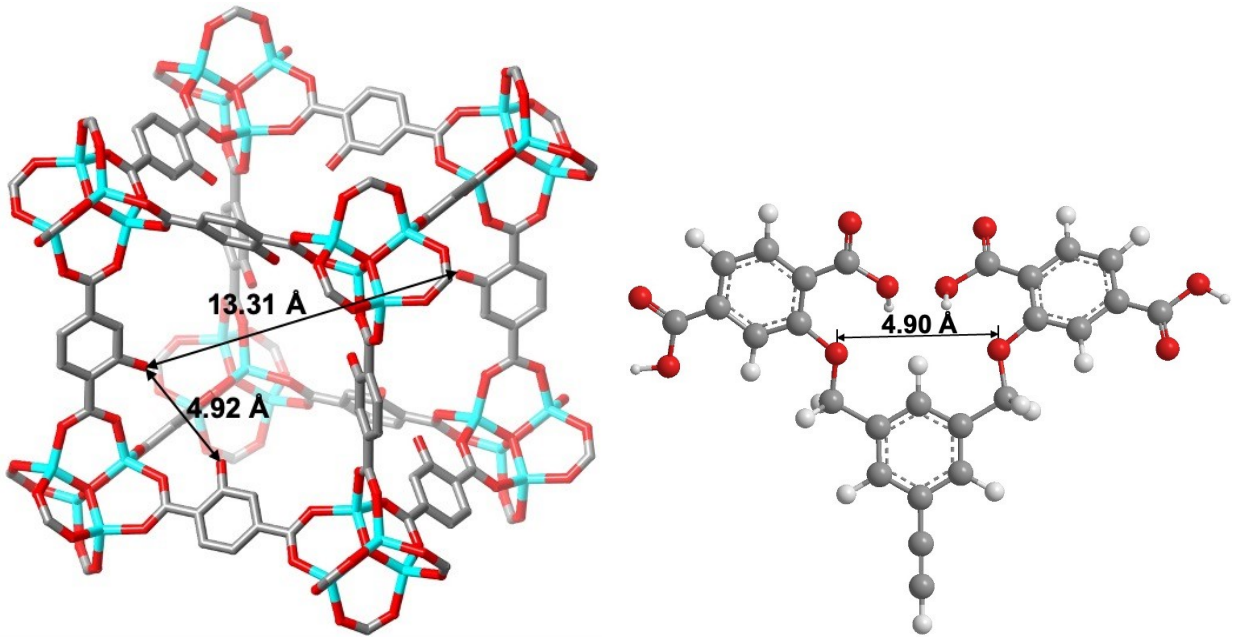

Figure S20. *Left*: Crystal structure of oligoIRMOF-1-L6, displaying distances between oxygen atoms from perpendicular linkers (4.92 Å) and parallel linkers (13.31 Å). Color scheme: carbon (gray), oxygen (red), zinc (cyan). *Right*: Geometrically optimized structure of **L6** showing the distances between oxygen atoms (4.90 Å).

Postsynthetic modification of oligoIRMOF-1-L6 with benzyl azide (oligoIRMOF-1-benzyltriazole)

DEF (1 mL) was added to oligoIRMOF-1-L6 (10 mg, 9.9 μmol). Benzyl azide (26 mg, 200 μmol, dissolved in 500 μL of DEF) was added. 22 μL of the supernatant of the solution of CuBr (20 mg of CuBr in 100 μL of DEF) was added to the reaction mixture. The vial was placed into preheated oven at 80 °C for 6 h, 12 h, 24 h, or 48 h. The mother liquor was decanted and the resulting MOF crystals were washed with fresh DMF three times, rinsed with CH_2Cl_2 three times, and dried under vacuum at room temperature for 16 h. For the determination of conversion, the MOF crystals were digested in a mixture of 600 μL of DMSO-d_6 and 40 μL of 35 % DCl in D_2O. The resulting solutions were analyzed by ^1H NMR.

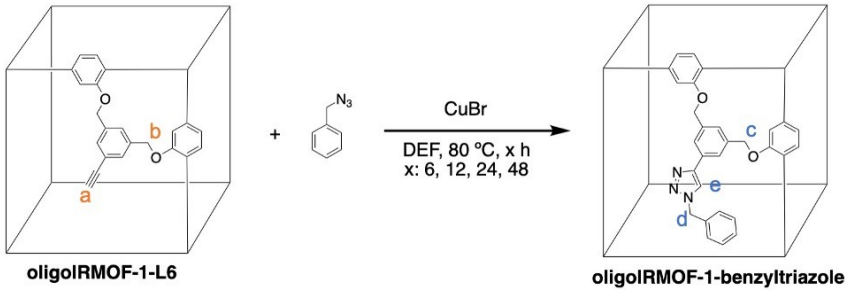

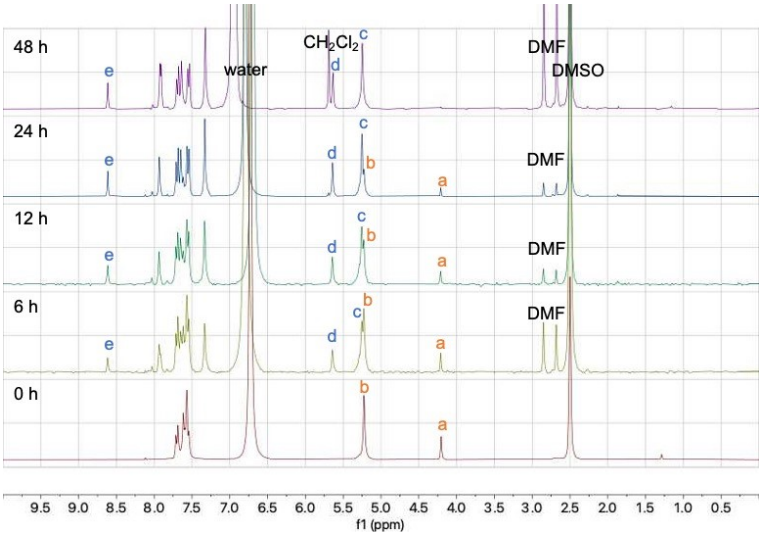

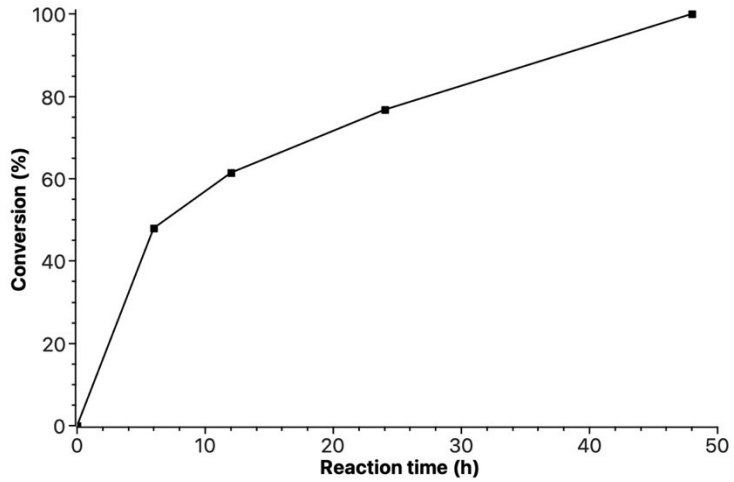

Figure S21. *Top*: Schematic representation of PSM of oligoIRMOF-1-L6 with benzyl azide. *Middle*: ^{1}H NMR spectrum of digested oligoIRMOF-1-L6 after PSM reaction in different reaction times (0 h, 6 h, 12 h, 24 h, 48 h). *Bottom*: Conversion rate of the PSM of oligoIRMOF-1-L6 with benzyl azide under different reaction times (0 h, 6 h, 12 h, 24 h, 48 h).

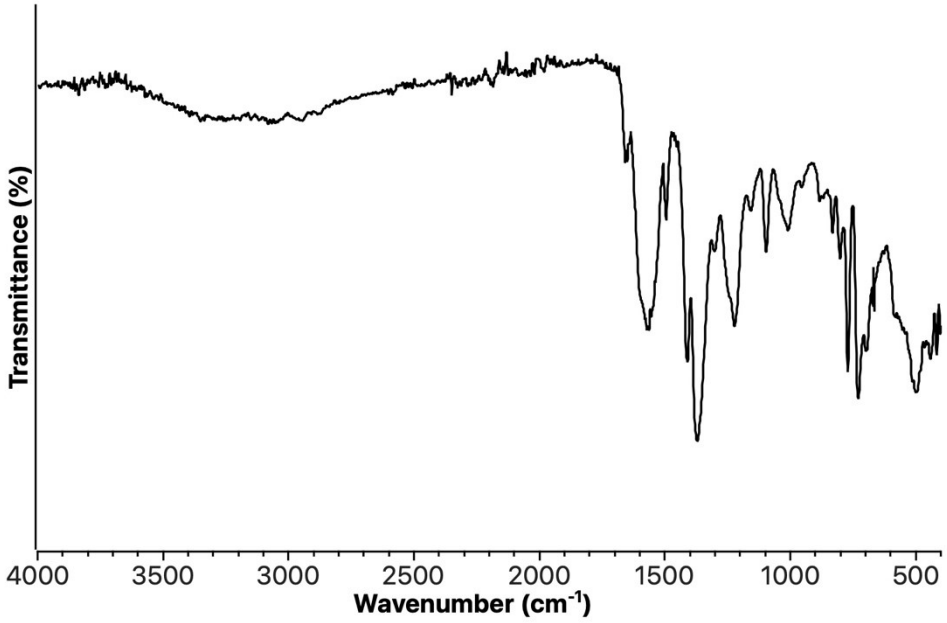

Figure S22. FTIR spectrum of oligoIRMOF-1-benzyltriazole.

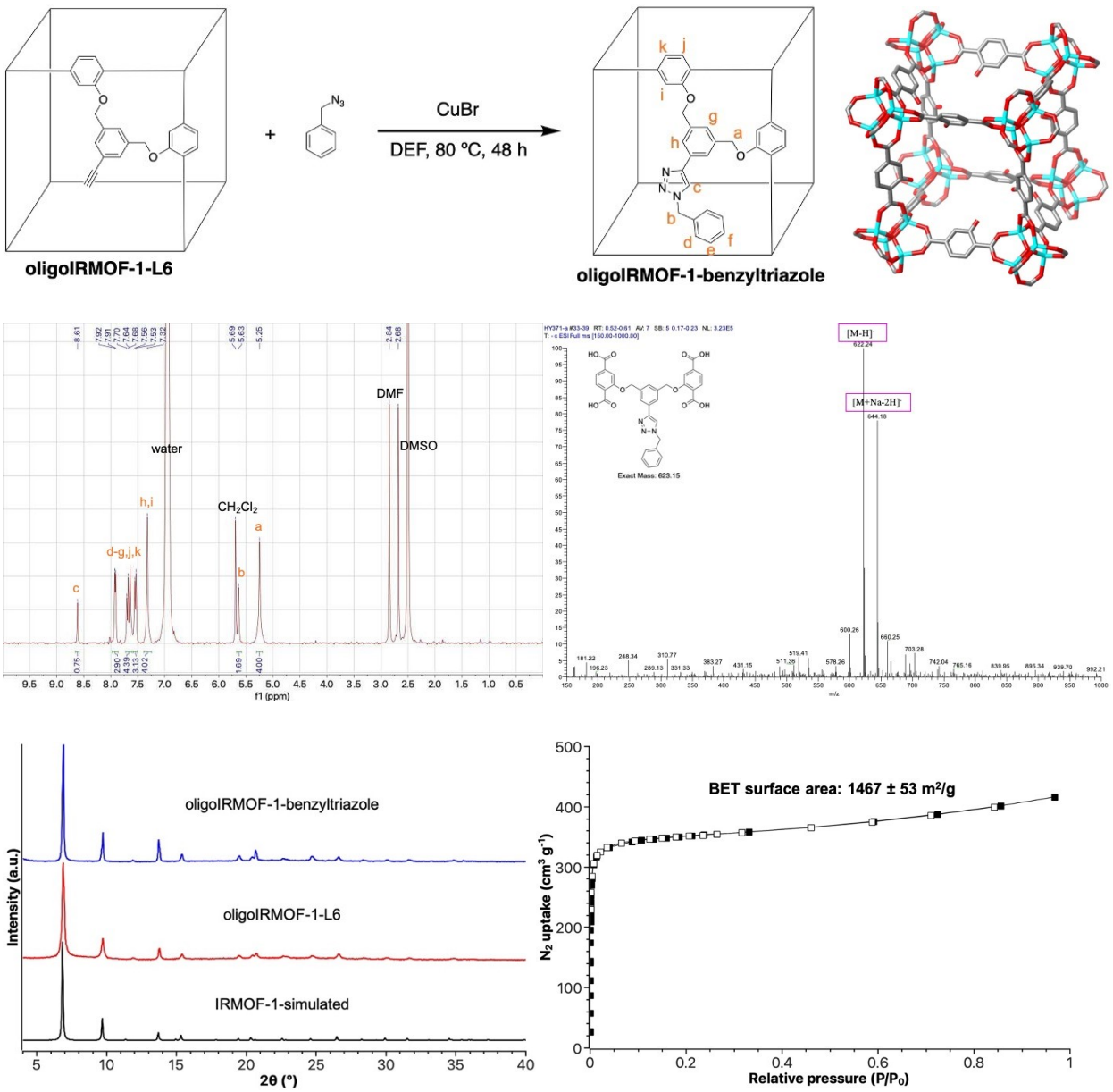

Figure S23. *Top Left:* PSM of oligoIRMOF-1-L6 with benzyl azide. *Top Right*: Crystal structure of oligoIRMOF-1-benzyltriazole. Color scheme: C=gray, O=red, Zn=cyan. *Middle Left:* ^{1}H NMR spectrum of digested solution of oligoIRMOF-1-L6 after PSM reaction at 80 ºC for 48 h. *Middle Right*: ESI-MS spectrum of oligoIRMOF-1-benzyltriazole. *Bottom Left*: PXRD patterns of simulated IRMOF-1 (black), oligoIRMOF-1-L6 (red), and oligoIRMOF-1-benzyltriazole (blue). *Bottom Right*: Nitrogen adsorption of oligoIRMOF-1-benzyltriazole. The filled and unfilled squares correspond to adsorption and desorption, respectively.

Postsynthetic modification of oligoIRMOF-1-L6 with 2-(azidomethyl)pyridine (oligoIRMOF-1-pyridinetriazole)

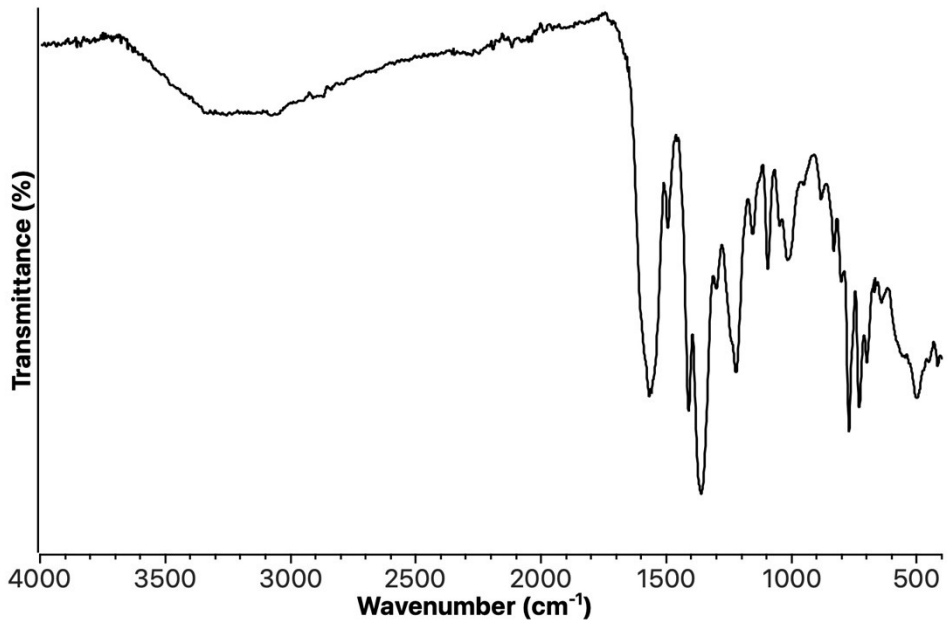

Figure S24. FTIR spectrum of oligoIRMOF-1-pyridinetriazole.

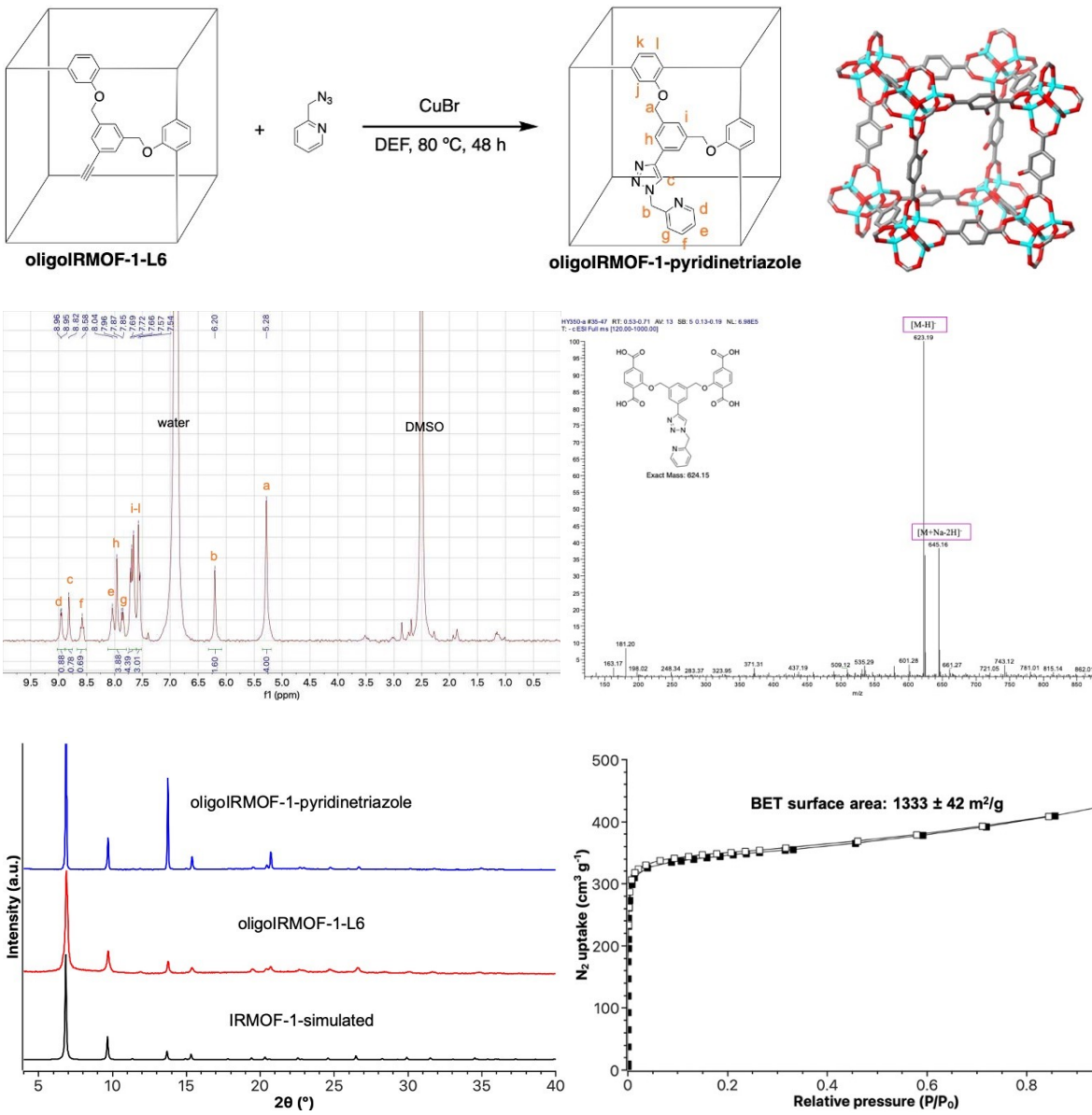

Figure S25. *Top Left:* PSM of oligoIRMOF-1-L6 with 2-(azidomethyl)pyridine. *Top Right*: Crystal structure of oligoIRMOF-1-pyridinetriazole. Color scheme: C=gray, O=red, Zn=cyan. *Middle Left:* ^{1}H NMR spectrum of digested solution of oligoIRMOF-1-L6 after PSM reaction at 80 ºC for 48 h. *Middle Right*: ESI-MS spectrum of oligoIRMOF-1-pyridinetriazole. *Bottom Left*: PXRD patterns of simulated IRMOF-1 (black), oligoIRMOF-1-L6 (red), oligoIRMOF-1-pyridinetriazole (blue). *Bottom Right*: Nitrogen adsorption of oligoIRMOF-1-pyridinetriazole. The filled and unfilled squares correspond to adsorption and desorption, respectively.

Postsynthetic modification of oligoIRMOF-1-L6 with 4-(azidomethyl)-1,1'-biphenyl (oligoIRMOF-1-biphenyltriazole)

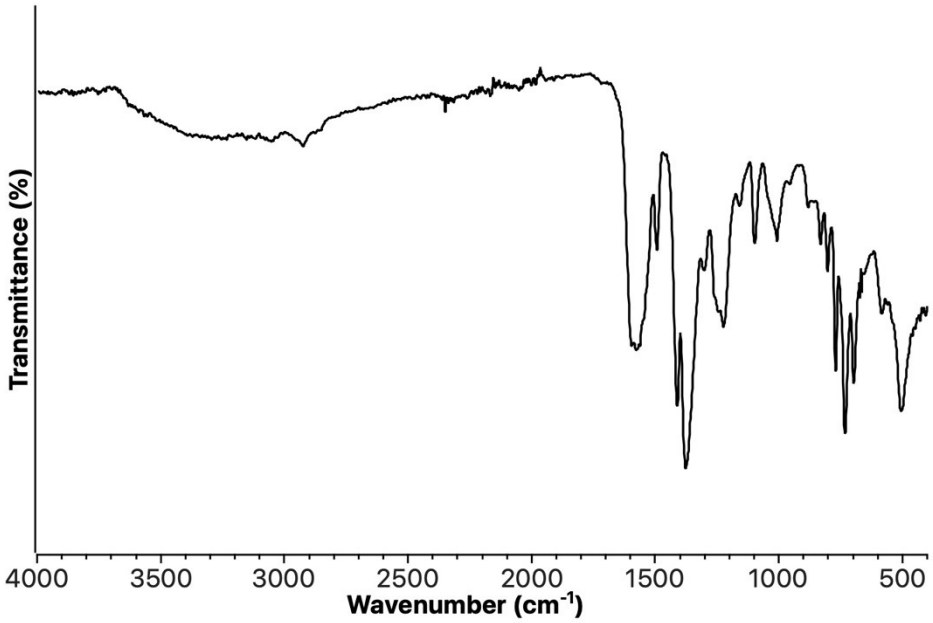

Figure S26. FTIR spectrum of oligoIRMOF-1-biphenyltriazole.

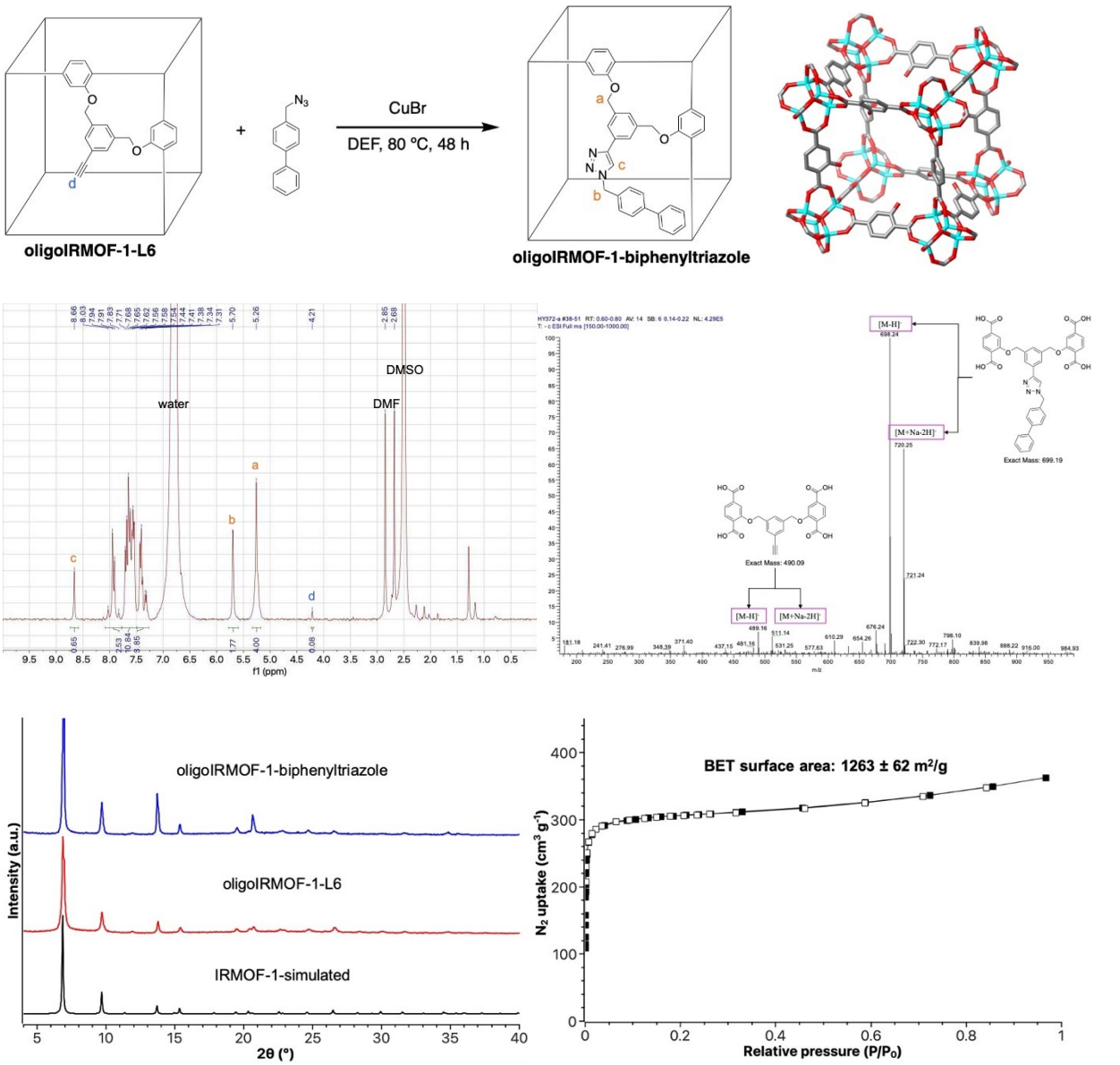

Figure S27. *Top Left:* PSM of oligoIRMOF-1-L6 with 4-(azidomethyl)-1,1'-biphenyl. *Top Right*: Crystal structure of oligoIRMOF-1-biphenyltriazole. Color scheme: C=gray, O=red, Zn=cyan. *Middle Left:* ^{1}H NMR spectrum of digested solution of oligoIRMOF-1-L6 after PSM reaction. *Middle Right*: ESI-MS spectrum of oligoIRMOF-1-biphenyltriazole. *Bottom Left*: PXRD patterns of simulated IRMOF-1 (black), oligoIRMOF-1-L6 (red), oligoIRMOF-1-biphenyltriazole (blue). *Bottom Right*: Nitrogen adsorption of oligoIRMOF-1-biphenyltriazole. The filled and unfilled squares correspond to adsorption and desorption, respectively.

Postsynthetic modification of oligoIRMOF-1-L6 with *ortho*-diazido xylene (oligoIRMOF-1-triazole$_2$-*o*-xylyl)

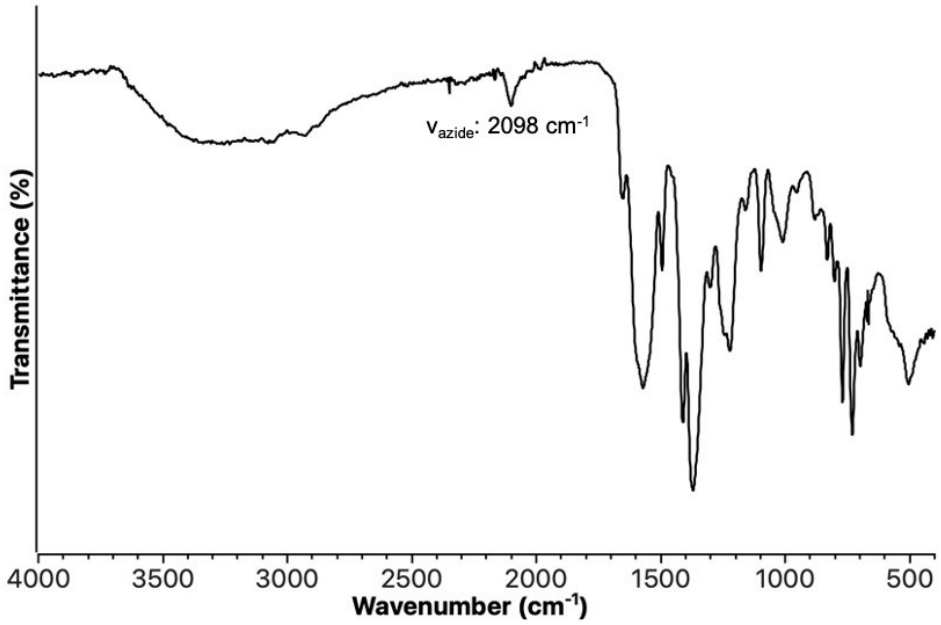

Figure S28. FTIR spectrum of oligoIRMOF-1-triazole$_2$-*o*-xylyl.

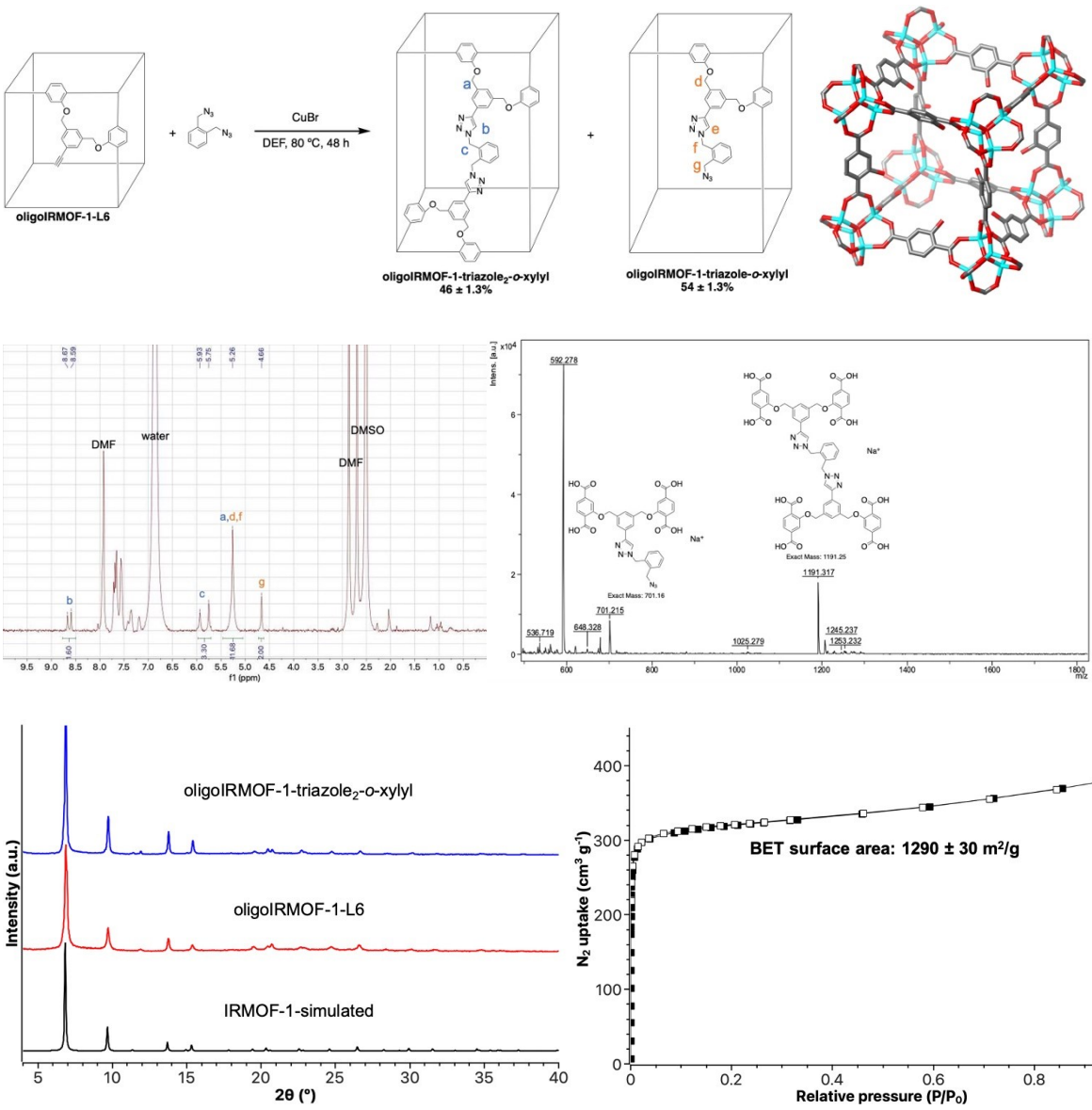

Figure S29. *Top Left:* PSM of oligoIRMOF-1-L6 with *ortho*-diazido xylene. *Top Right*: Crystal structure of oligoIRMOF-1-triazole$_2$-*o*-xylyl. Color scheme: C=gray, O=red, Zn=cyan. *Middle Left:* ^{1}H NMR spectrum of digested solution of oligoIRMOF-1-L6 after PSM reaction. *Middle Right*: ESI-MS spectrum of oligoIRMOF-1-triazole$_2$-*o*-xylyl. *Bottom Left*: PXRD patterns of simulated IRMOF-1 (black), oligoIRMOF-1-L6 (red), oligoIRMOF-1-triazole$_2$-*o*-xylyl (blue). *Bottom Right*: Nitrogen adsorption of oligoIRMOF-1-triazole$_2$-*o*-xylyl. The filled and unfilled squares correspond to adsorption and desorption, respectively.

Postsynthetic modification of oligoIRMOF-1-L6 with *meta*-diazido xylene (oligoIRMOF-1-triazole$_2$-*m*-xylyl)

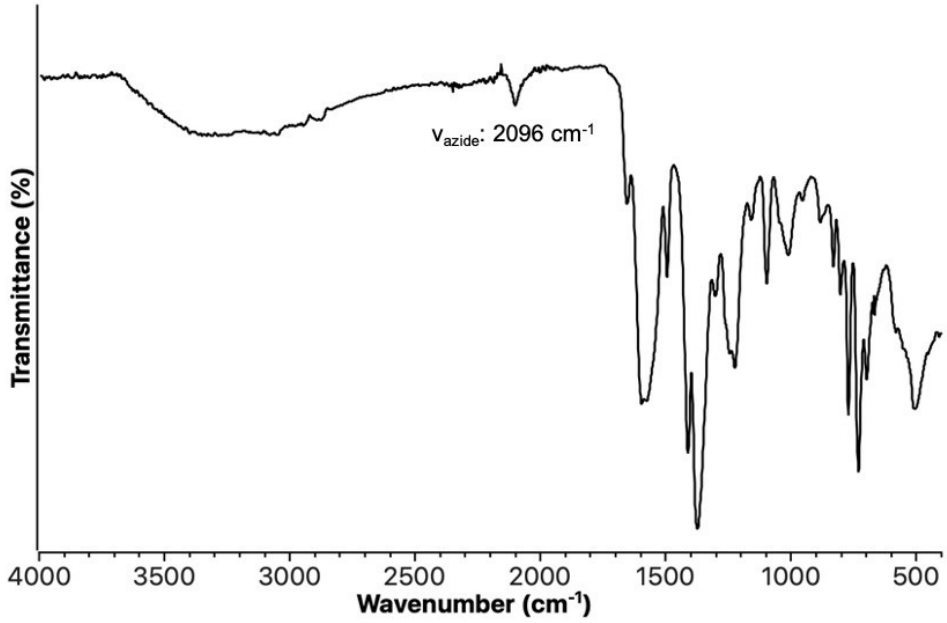

Figure S30. FTIR spectrum of oligoIRMOF-1-triazole$_2$-*m*-xylyl.

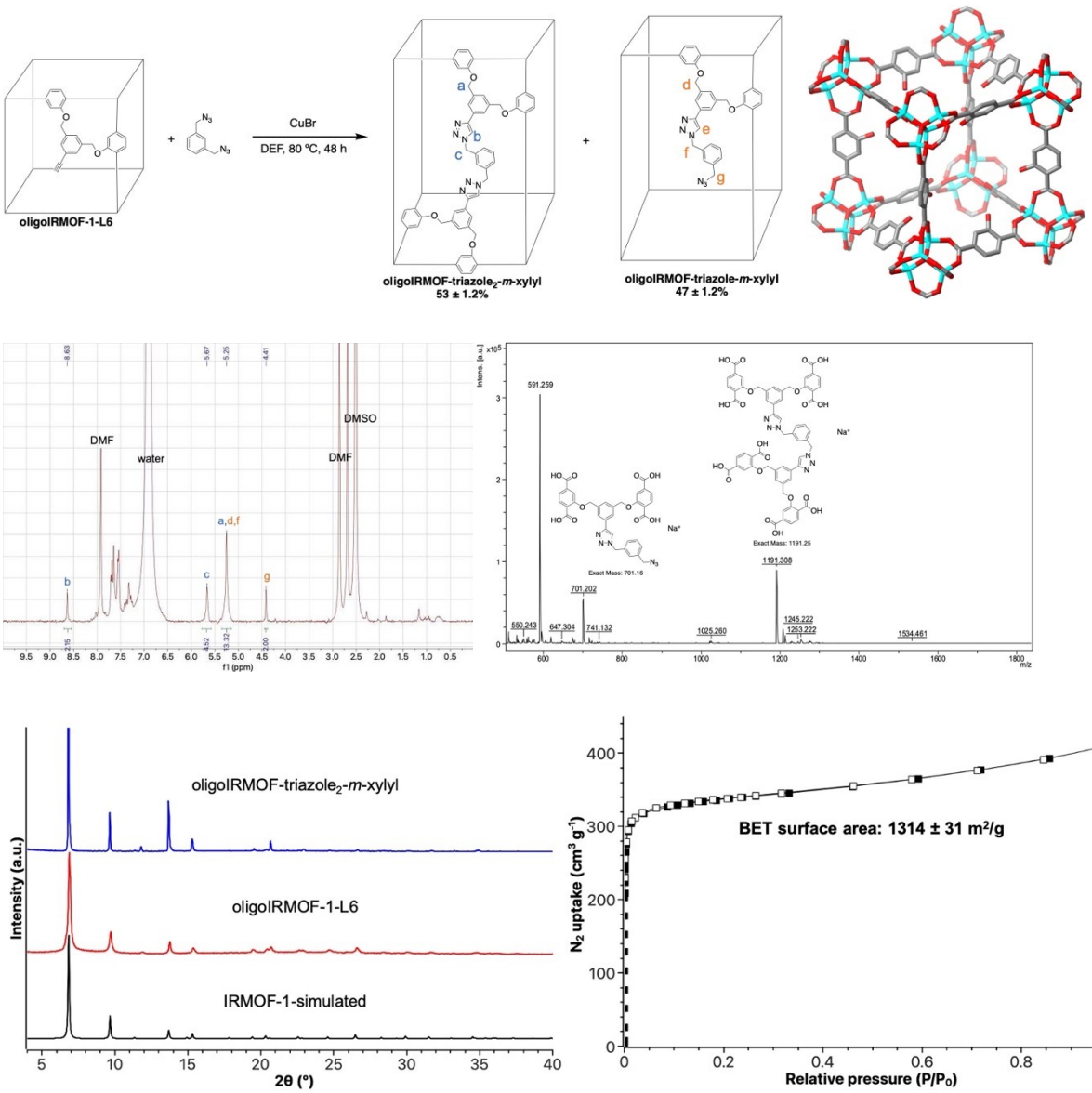

Figure S31. *Top Left:* PSM of oligoIRMOF-1-L6 with *meta*-diazido xylene. *Top Right*: Crystal structure of oligoIRMOF-1-triazole$_2$-*m*-xylyl. Color scheme: C=gray, O=red, Zn=cyan. *Middle Left:* ^{1}H NMR spectrum of digested solution of oligoIRMOF-1-L6 after PSM reaction. *Middle Right*: ESI-MS spectrum of oligoIRMOF-1-triazole$_2$-*m*-xylyl. *Bottom Left*: PXRD patterns of simulated IRMOF-1 (black), oligoIRMOF-1-L6 (red), oligoIRMOF-1-triazole$_2$-*m*-xylyl (blue). *Bottom Right*: Nitrogen adsorption of oligoIRMOF-1-triazole$_2$-*m*-xylyl. The filled and unfilled squares correspond to adsorption and desorption, respectively.

Postsynthetic modification of oligoIRMOF-1-L6 with *para*-diazido xylene (oligoIRMOF-1-triazole$_2$-*p*-xylyl)

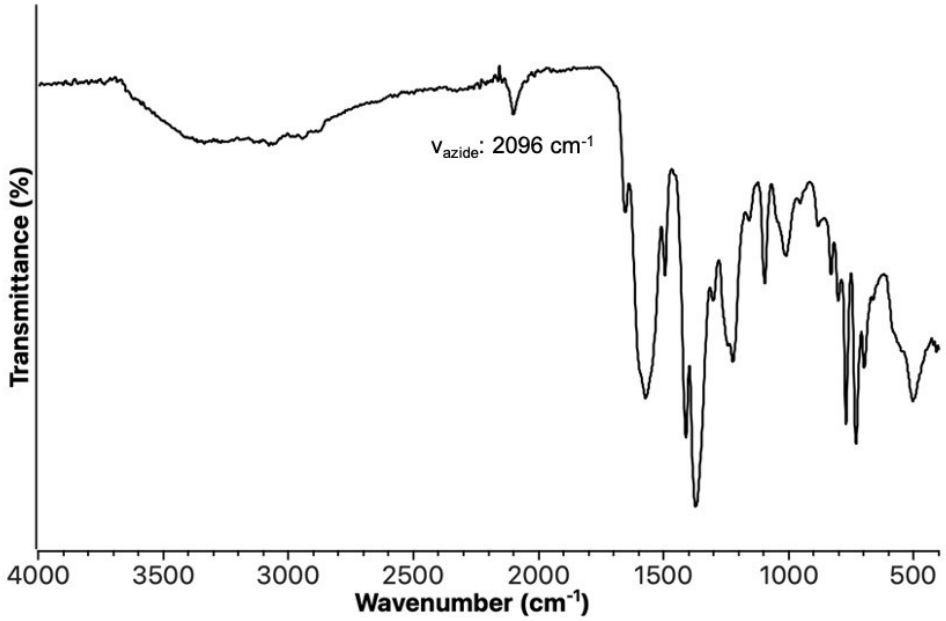

Figure S32. FTIR spectrum of oligoIRMOF-1-triazole$_2$-*p*-xylyl.

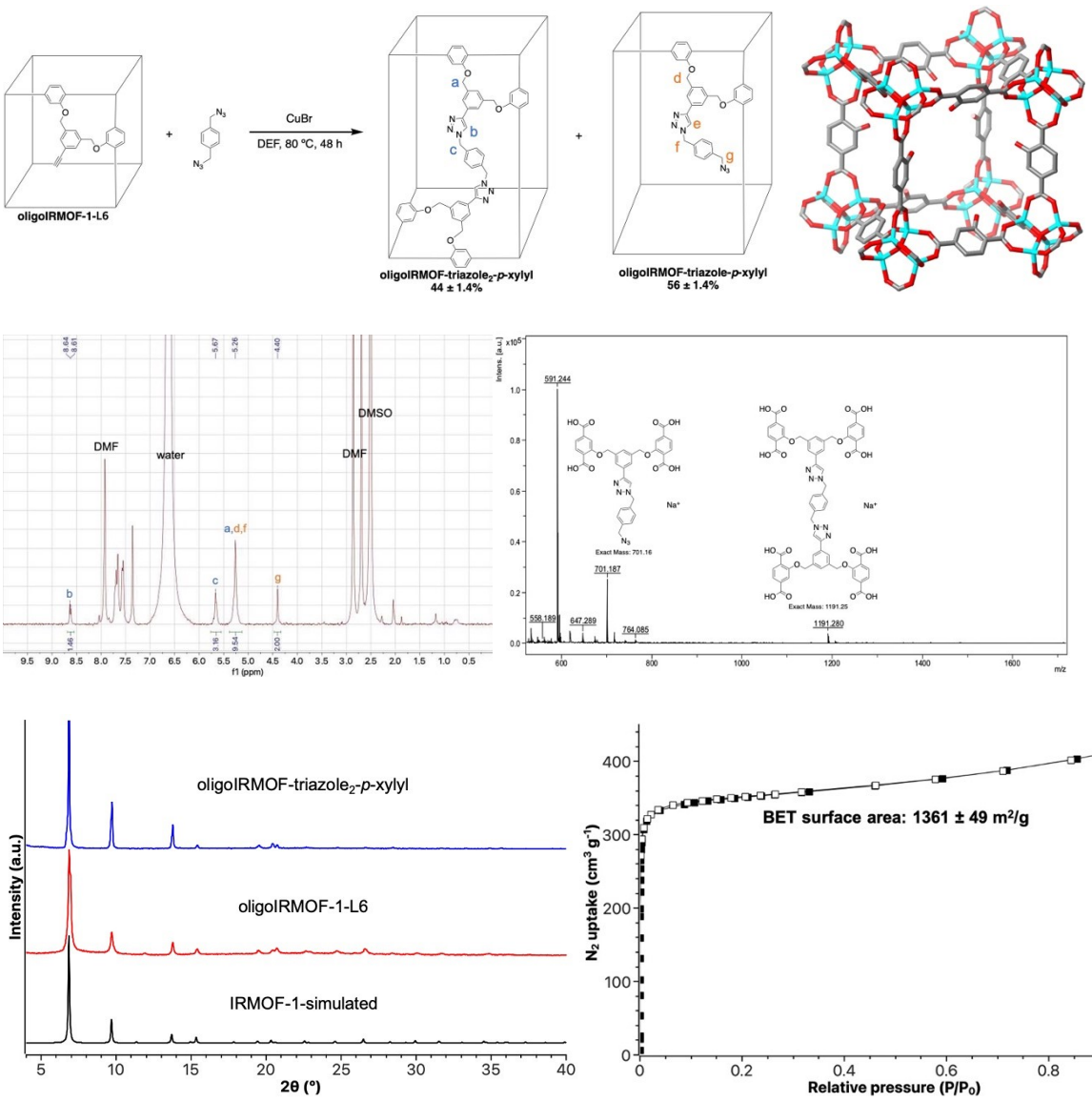

Figure S33. *Top Left:* PSM of oligoIRMOF-1-L6 with *para*-diazido xylene. *Top Right*: Crystal structure of oligoIRMOF-1-triazole$_2$-*p*-xylyl. Color scheme: C=gray, O=red, Zn=cyan. *Middle Left:* ^{1}H NMR spectrum of digested solution of oligoIRMOF-1-L6 after PSM reaction. *Middle Right*: ESI-MS spectrum of oligoIRMOF-1-triazole$_2$-*p*-xylyl. *Bottom Left*: PXRD patterns of simulated IRMOF-1 (black), oligoIRMOF-1-L6 (red), oligoIRMOF-1-triazole$_2$-*p*-xylyl (blue). *Bottom Right*: Nitrogen adsorption of oligoIRMOF-1-triazole$_2$-*p*-xylyl. The filled and unfilled squares correspond to adsorption and desorption, respectively.

SEM images of oligoMOFs after PSM reactions

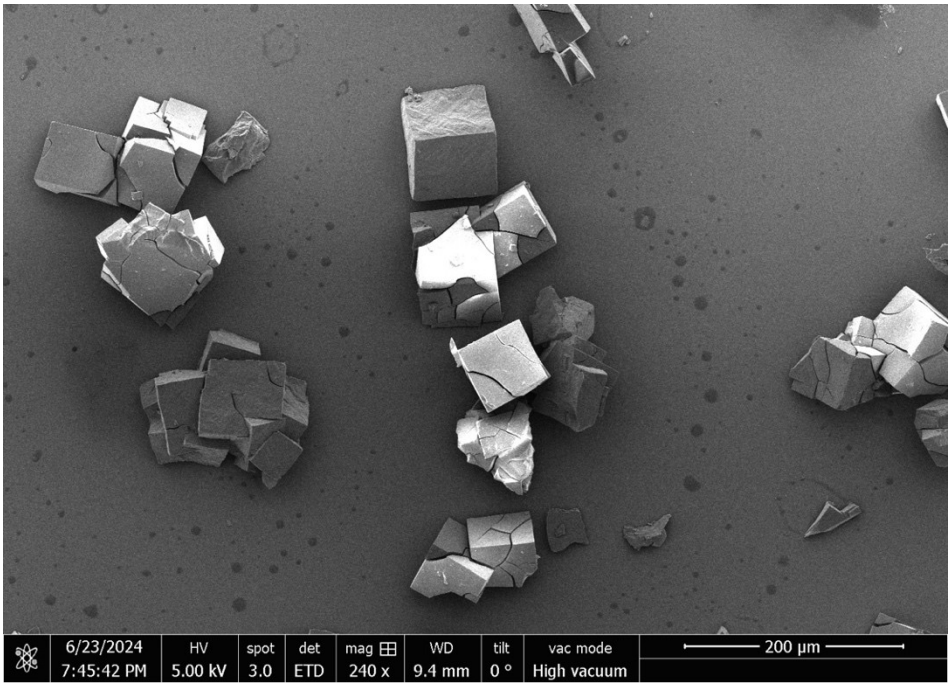

Figure S34. SEM image of oligoIRMOF-1-benzyltriazole.

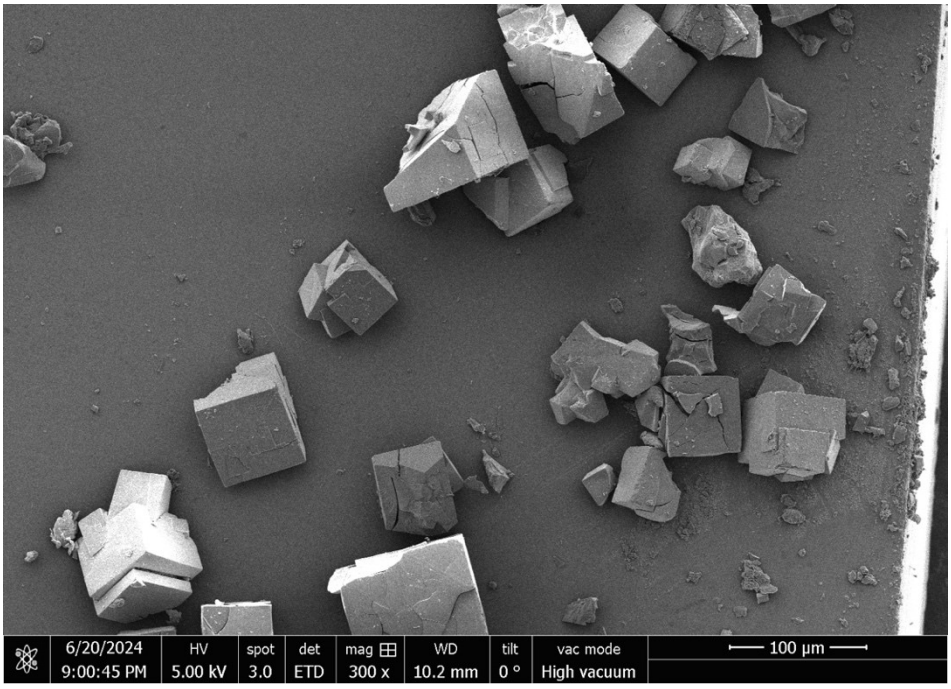

Figure S35. SEM image of oligoIRMOF-1-pyridinetriazole.

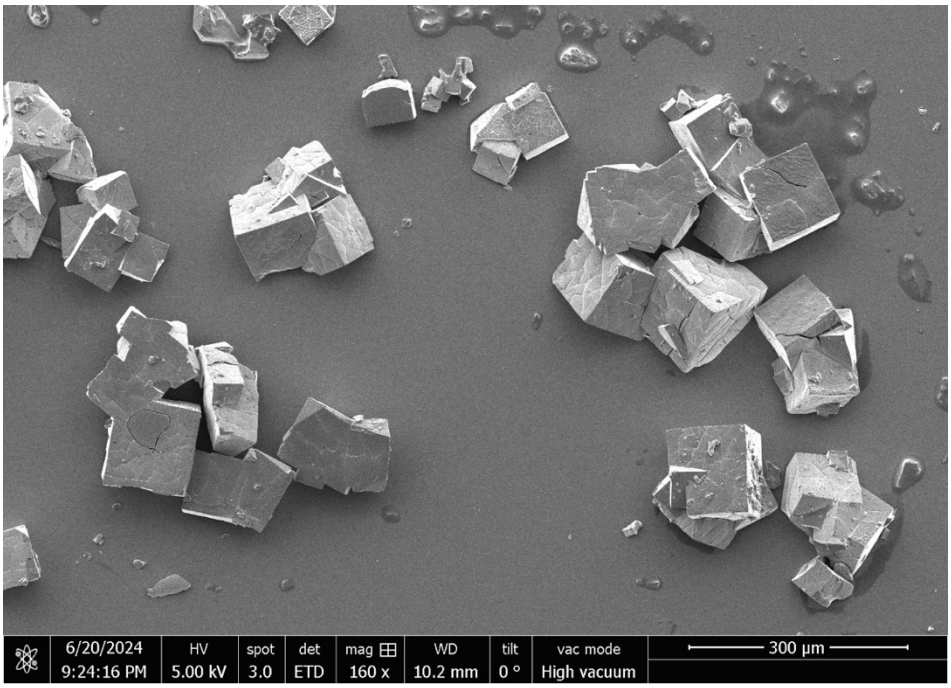

Figure S36. SEM image of oligoIRMOF-1-biphenyltriazole.

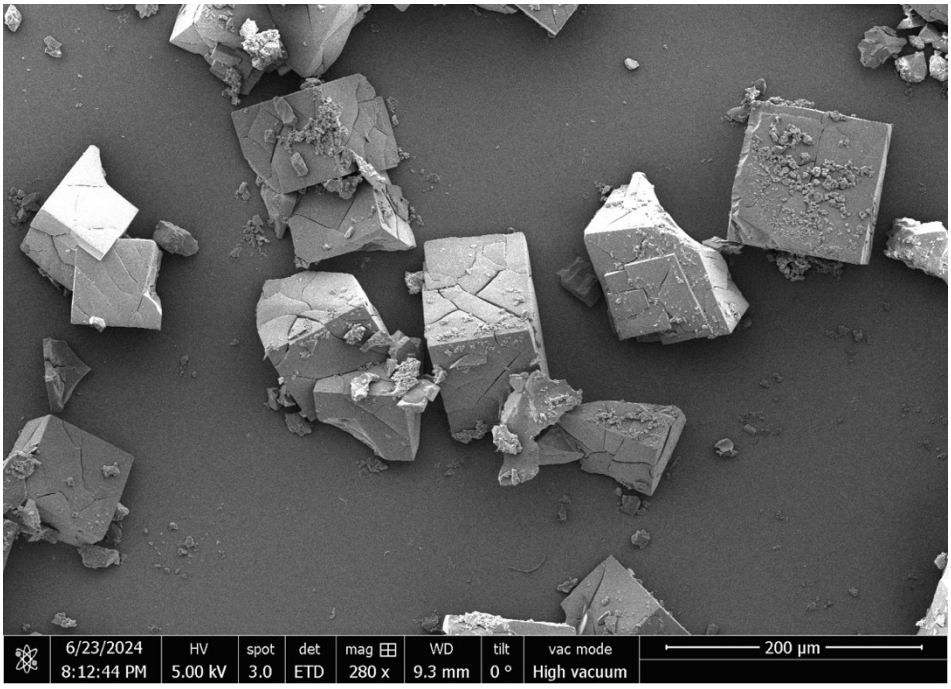

Figure S37. SEM image of oligoIRMOF-1-triazole$_2$-*o*-xylyl.

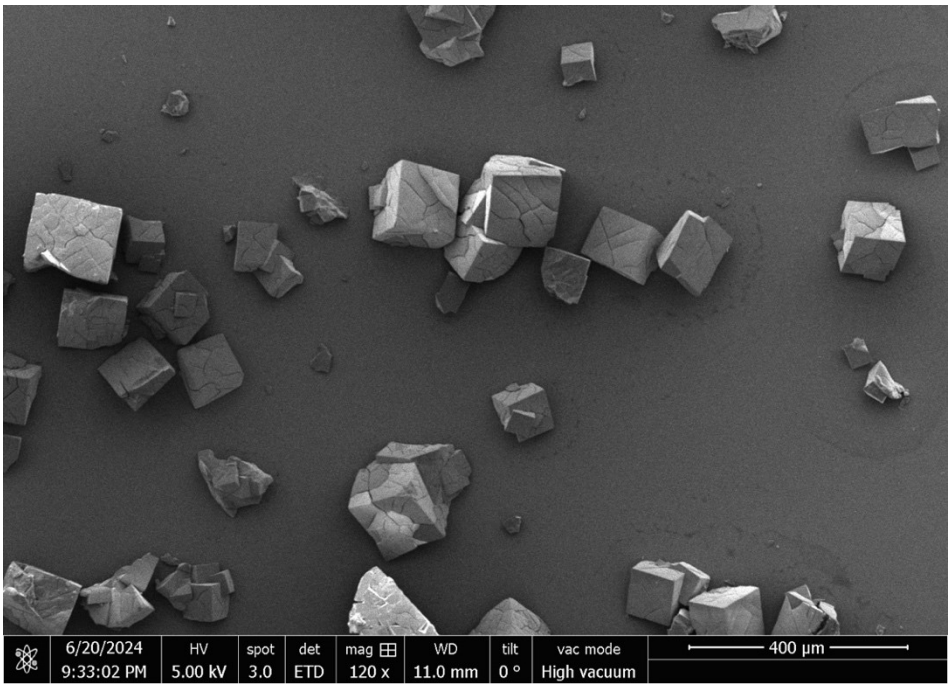

Figure S38. SEM image of oligoIRMOF-1-triazole$_2$-*m*-xylyl.

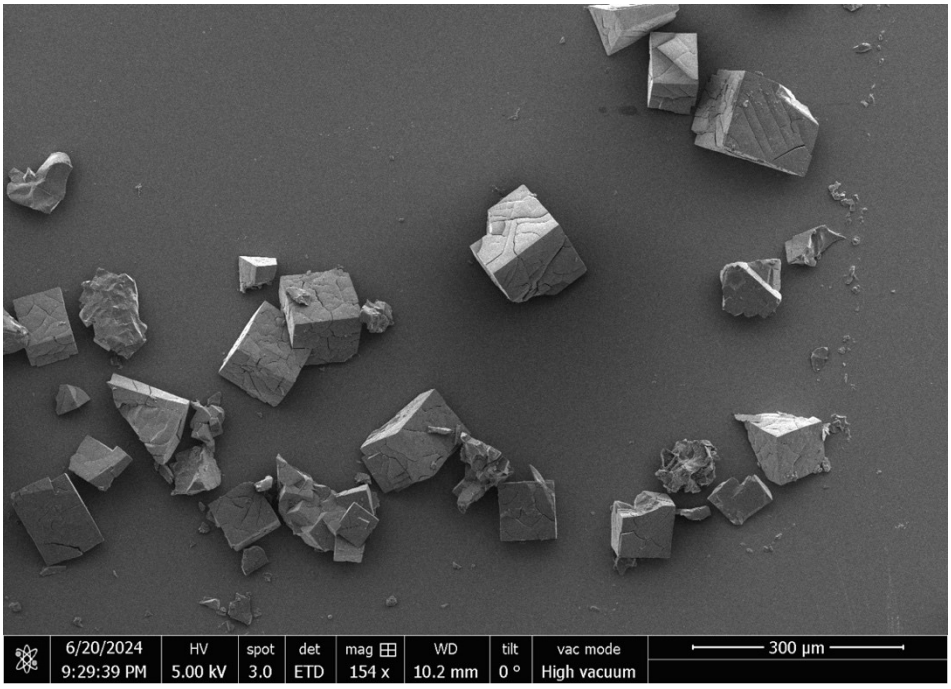

Figure S39. SEM image of oligoIRMOF-1-triazole$_2$-*p*-xylyl.

C. Inductively coupled plasma mass spectrometry (ICP-MS) analysis

Dried oligoMOF samples were digested in a mixture of nitric acid (70%, 700 μL) and hydrogen peroxide (30%, 300 μL). The resulting clear solutions were diluted to a volume of 10 mL with deionized water. An aliquot of the solution (1 mL) was further diluted to 10 mL with deionized water. The diluted solutions were analyzed using a Thermo iCAP RQ ICP-MS instrument to determine the zinc content in the digested samples.

To calculate the copper content in the digested sample solutions, the following equation was utilized:

$$Copper\ content\ in\ sample\ (mass\ \%) = \frac{Copper\ concentration\ from\ ICP\ MS\ (\mu g/L)}{Sample\ concentration\ (\mu g/L)} \times 100$$

Table S1. Observed copper concentration determined by ICP-MS from digested, diluted oligoMOF samples, and calculated copper content.

MOF	Sample amount (mg)	Copper concentration measured by ICP-MS (μg/L)	Copper content (%)
oligoIRMOF-1-L6	10.51	134	0.127
oligoIRMOF-1-L6 with copper(I) bromide	4.12	92.7	0.225
oligoIRMOF-1-benzyltriazole	4.37	93.3	0.213
oligoIRMOF-1-pyridinetriazole	3.94	91.1	0.231
oligoIRMOF-1-biphenyltriazole	6.07	123	0.202

D. Stability Studies of oligoMOFs (ambient air and thermal stability)

OligoMOF samples were activated under vacuum at room temperature for 16 h to remove residual solvents, exposed to ambient air for 1 week, and characterized by PXRD.

Thermal stability of oligoMOFs was evaluated by thermalgravimetric analysis (TGA); ~5 mg of dried oligoMOFs were placed in a ceramic crucible. Samples were analyzed on a TA Instruments Discovery SDT 650 using a temperature range of 30-600 °C, scanning at 10 °C/min under a nitrogen atmosphere (75 cm^3/min flow rate).

Stabiliy of oligoMOFs with functionalized tethers (oligoIRMOF-1-L1, oligoIRMOF-1-L3, oligoIRMOF-1-L6) exposed to air for 7 days.

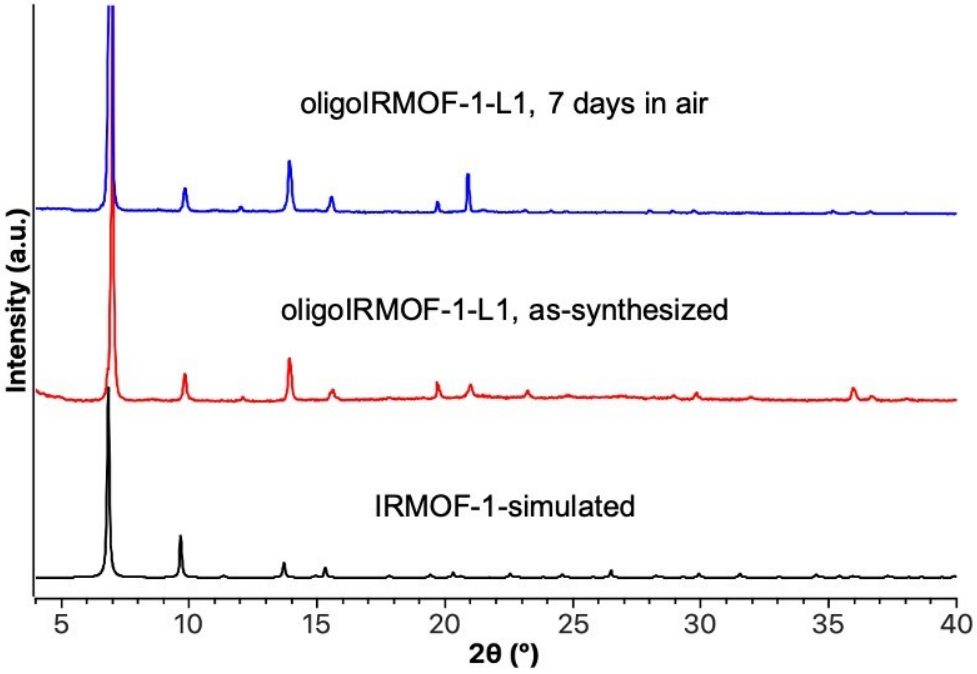

Figure S40. PXRD patterns of simulated IRMOF-1 (black), as-synthesized oligoIRMOF-1-L1 (red), and oligoIRMOF-1-L1 exposed to air for 7 days.

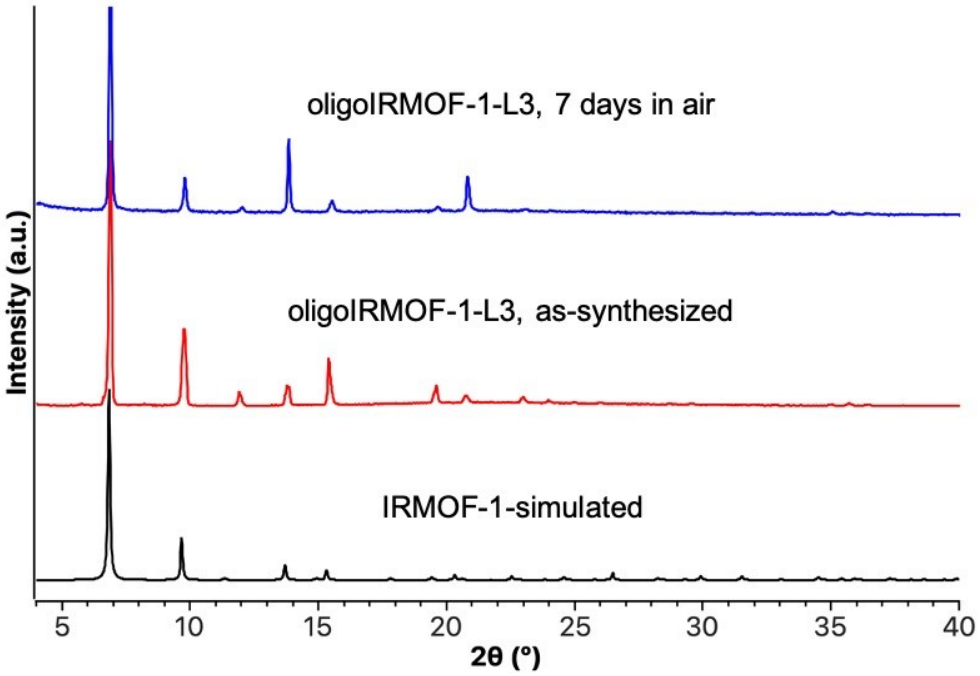

Figure S41. PXRD patterns of simulated IRMOF-1 (black), as-synthesized oligoIRMOF-1-L3 (red), and oligoIRMOF-1-L3 exposed to air for 7 days.

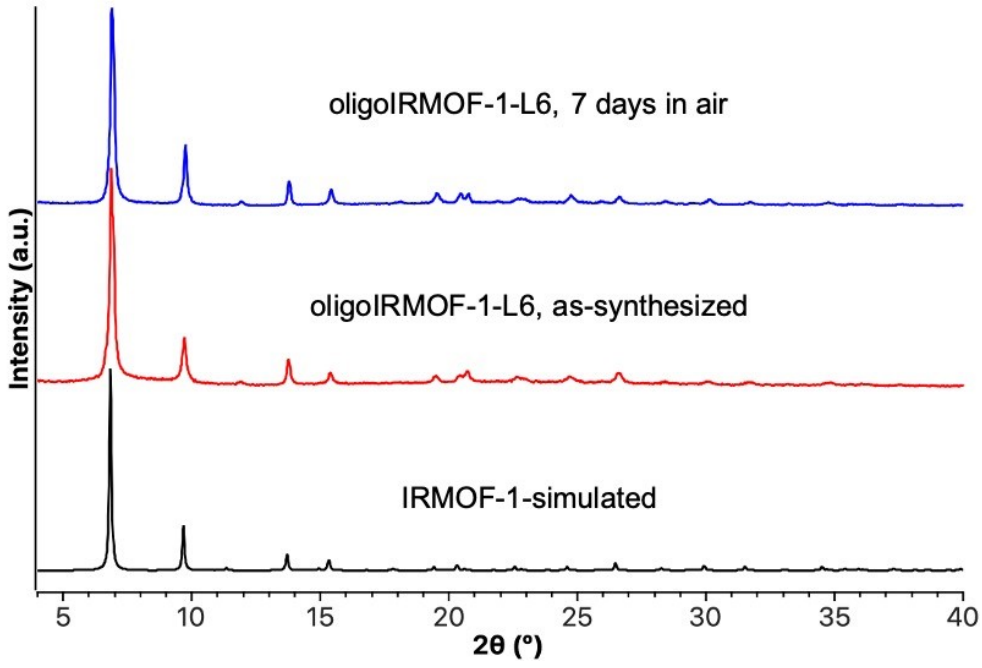

Figure S42. PXRD patterns of simulated IRMOF-1 (black), as-synthesized oligoIRMOF-1-alkyne-L6 (red), and oligoIRMOF-1-alkyne-L6 exposed to air for 7 days.

TGA thermograms of oligoIRMOF with functionalized tethers

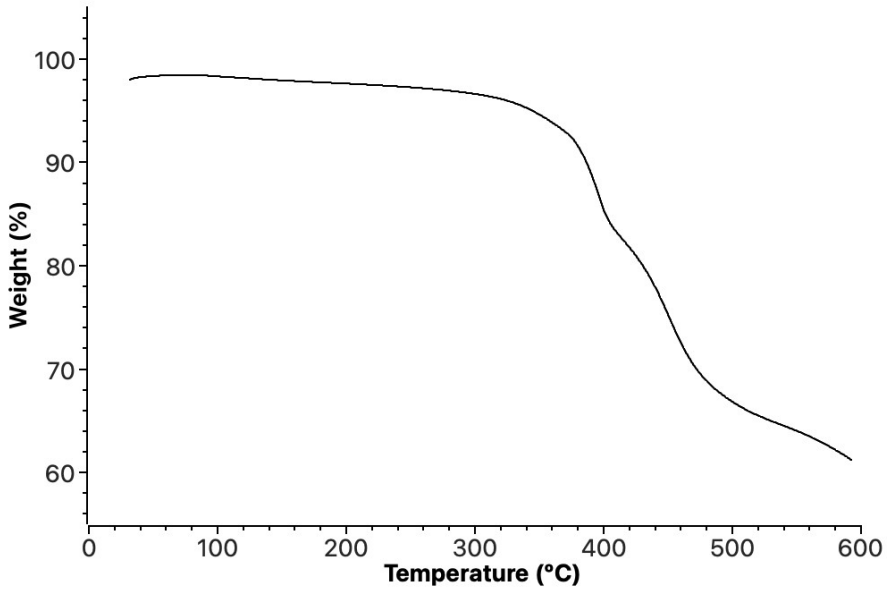

Figure S43. TGA trace of oligoIRMOF-1-L1. Decomposition temperature ~378 ºC.

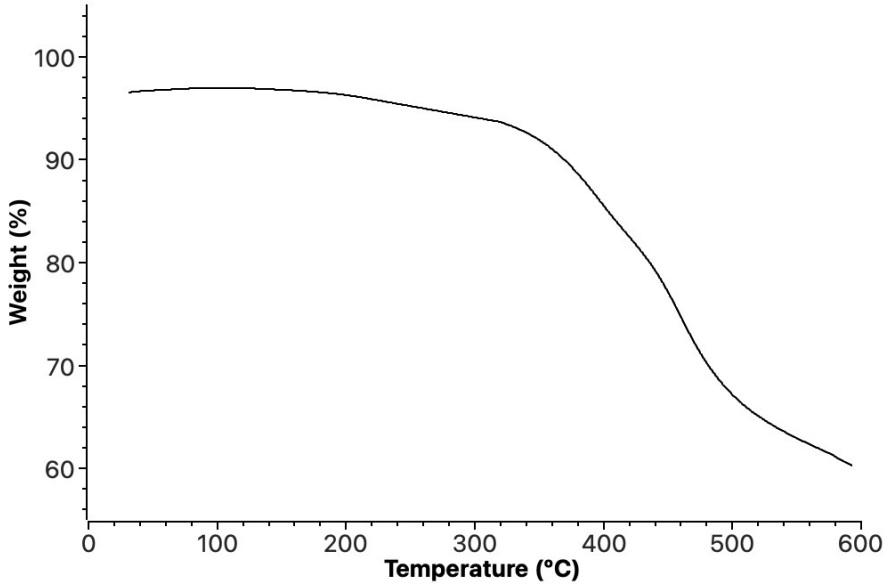

Figure S44. TGA trace of oligoIRMOF-1-L3. Decomposition temperature ~357 ºC.

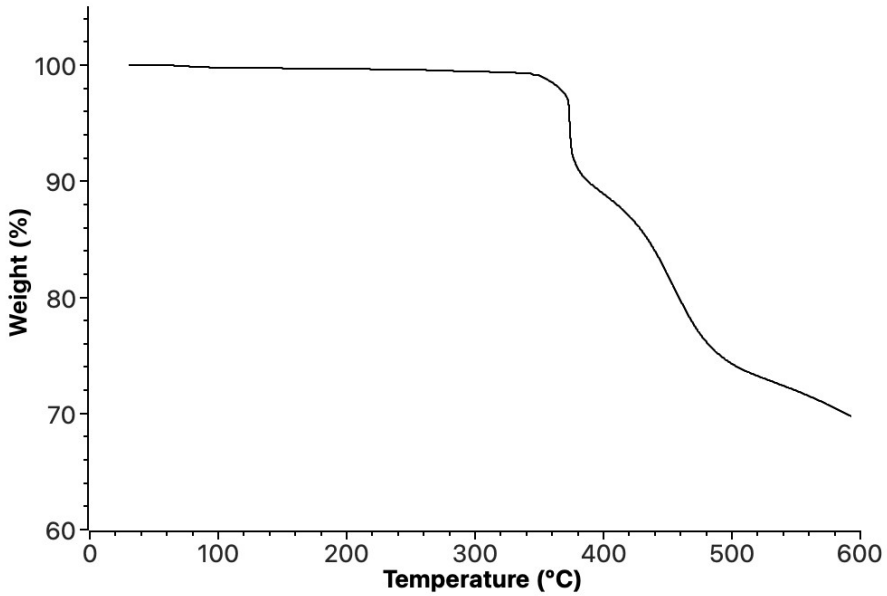

Figure S45. TGA trace of oligoIRMOF-1-L6. Decomposition temperature ~364 ºC.

E. Summary of BET surface area values

Table S2. Values of BET surface area of oligoMOFs

MOF	BET surface area
oligoIRMOF-1-L1	1819 ± 64 m^2/g
oligoIRMOF-1-L3	1410 ± 52 m^2/g
oligoIRMOF-1-L6	1852 ± 72 m^2/g
oligoIRMOF-1-benzyltriazole	1467 ± 53 m^2/g
oligoIRMOF-1-pyridinetriazole	1333 ± 42 m^2/g
oligoIRMOF-1-biphenyltriazole	1263 ± 62 m^2/g
oligoIRMOF-1-triazole$_2$-*o*-xylyl	1291 ± 30 m^2/g
oligoIRMOF-1-triazole$_2$-*m*-xylyl	1314 ± 31 m^2/g
oligoIRMOF-1-triazole$_2$-*p*-xylyl	1361 ± 49 m^2/g

Rouquerol and BET plots of oligoMOFs

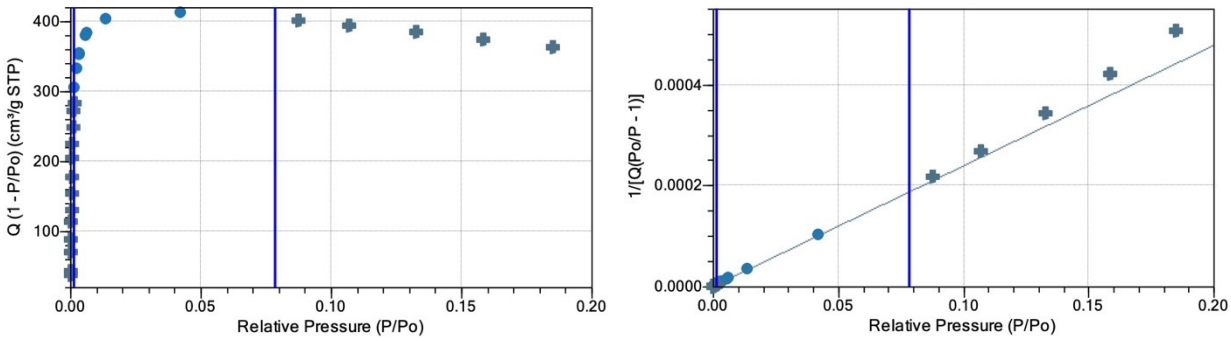

Figure S46. *Left*: Rouquerol plot of oligoIRMOF-1-L1. *Right*: BET plot of oligoIRMOF-1-L1. Selected P/P_0 range for BET fit: 0.0013 to 0.0786 (highlighted in blue lines). BET surface area: 1824 ± 2.0 m²/g. Slope: 0.002385 ± 0.000003 g/cm³. Y-intercept: 0.000001 ± 0.000000 g/cm³. C-constant: 1694.955450. Q_m: 418.9915 cm³/g. Correlation coefficient: 0.9999964.

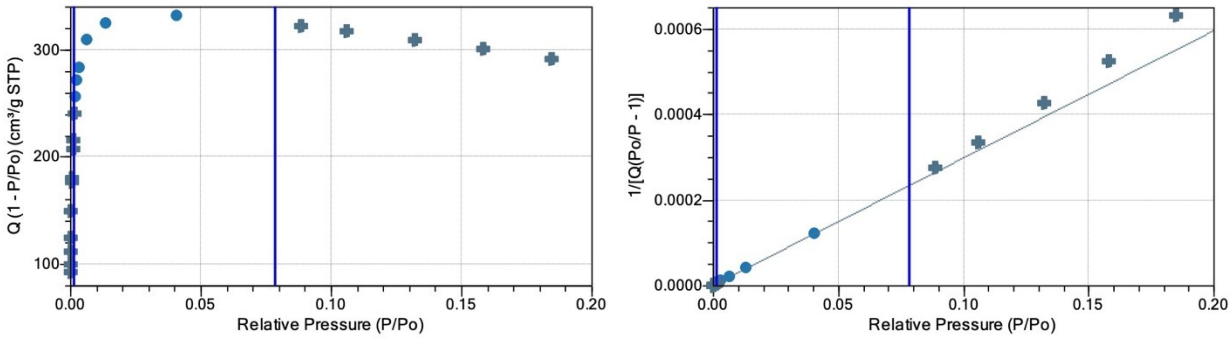

Figure S47. *Left*: Rouquerol plot of oligoIRMOF-1-L3. *Right*: BET plot of oligoIRMOF-1-L3. Selected P/P_0 range for BET fit: 0.0013 to 0.0786 (highlighted in blue lines). BET surface area: 1462 ± 2.1 m²/g. Slope: 0.002975 ± 0.000004 g/cm³. Y-intercept: 0.000002 ± 0.000000 g/cm³ STP. C-constant: 1783.694361. Q_m: 335.9295 cm³/g. Correlation coefficient: 0.9999958.

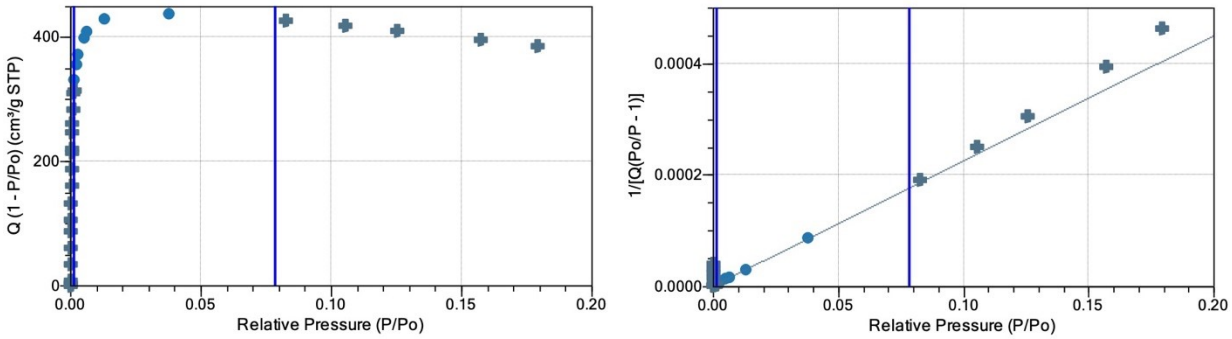

Figure S48. *Left*: Rouquerol plot of oligoIRMOF-1-L6. *Right*: BET plot of oligoIRMOF-1-L6. Selected P/P_0 range for BET fit: 0.0013 to 0.0786 (highlighted in blue lines). BET surface area: 1936 ± 3.0 m²/g. Slope: 0.002247 ± 0.000003 g/cm³. Y-intercept: 0.000001 ± 0.000000 g/cm³. C-constant: 1748.598233. Q_m: 444.7218 cm³/g. Correlation coefficient: 0.9999943.

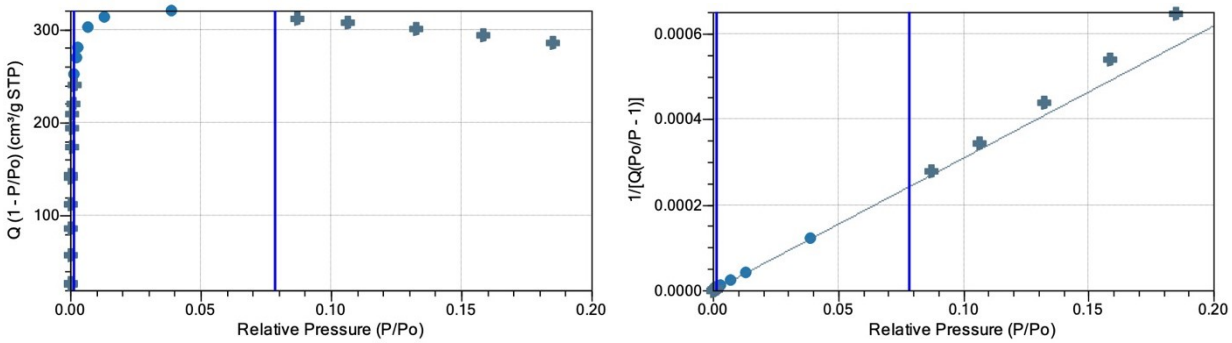

Figure S49. *Left*: Rouquerol plot of oligoMOF-1-benzyltriazole. *Right*: BET plot of oligoIRMOF-1-benzyltriazole. Selected P/P_0 range for BET fit: 0.0013 to 0.0786 (highlighted in blue lines). BET surface area: 1408 ± 1.0 m²/g. Slope: 0.003088 ± 0.000002 g/cm³. Y-intercept: 0.000001 ± 0.000000 g/cm³. C-constant: 2116.589287. Q_m: 323.6793 cm³/g. Correlation coefficient: 0.9999991.

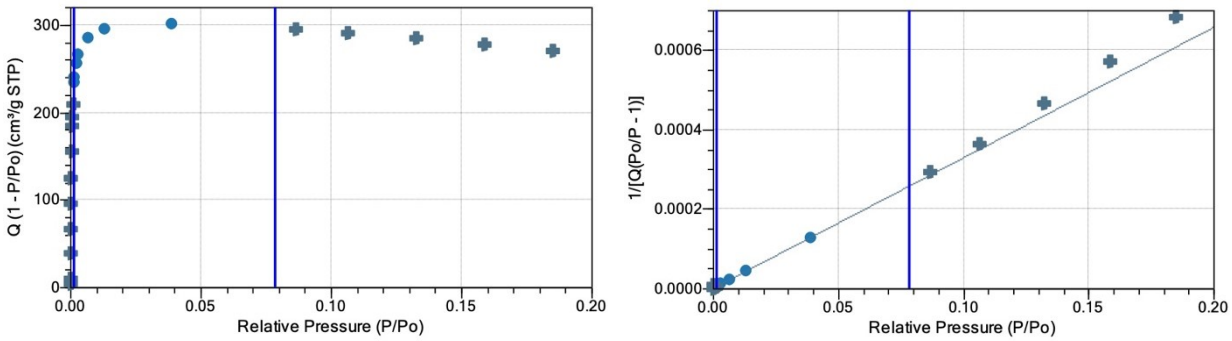

Figure S50. *Left*: Rouquerol plot of oligoIRMOF-1-pyridinetriazole. *Right*: BET plot of oligoIRMOF-1-pyridinetriazole. Selected P/P_0 range for BET fit: 0.0013 to 0.0786 (highlighted in blue lines). BET surface area: 1324 ± 1.0 m²/g. Slope: 0.003286 ± 0.000002 g/cm³. Y-intercept: 0.000001 ± 0.000000 g/cm³. C-constant: 2289.758369. Q_m: 304.1853 cm³/g. Correlation coefficient: 0.9999991.

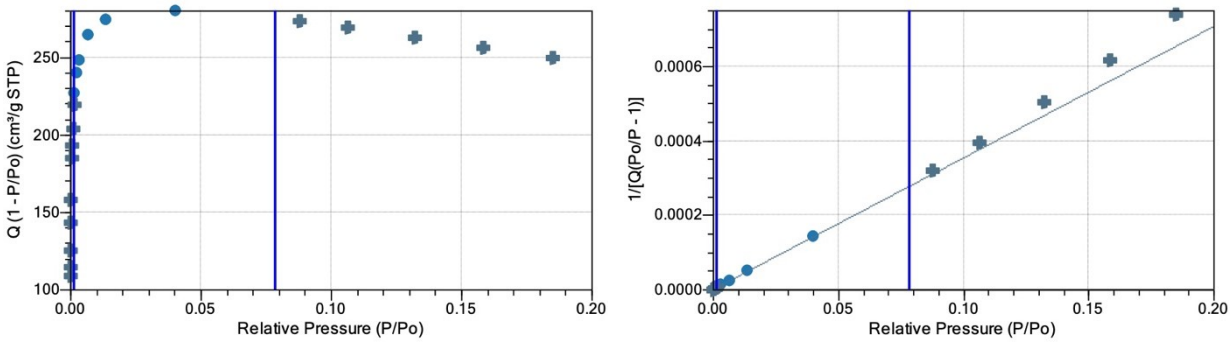

Figure S51. *Left*: Rouquerol plot of oligoIRMOF-1-biphenyltriazole. *Right*: BET plot of oligoIRMOF-1-biphenyltriazole. Selected P/P_0 range for BET fit: 0.0013 to 0.0786 (highlighted in blue lines). BET surface area: 1231 ± 1.0 m²/g. Slope: 0.003534 ± 0.000003 g/cm³. Y-intercept: 0.000002 ± 0.000000 g/cm³. C-constant: 2299.032374. Q_m: 282.8642 cm³/g. Correlation coefficient: 0.9999987.

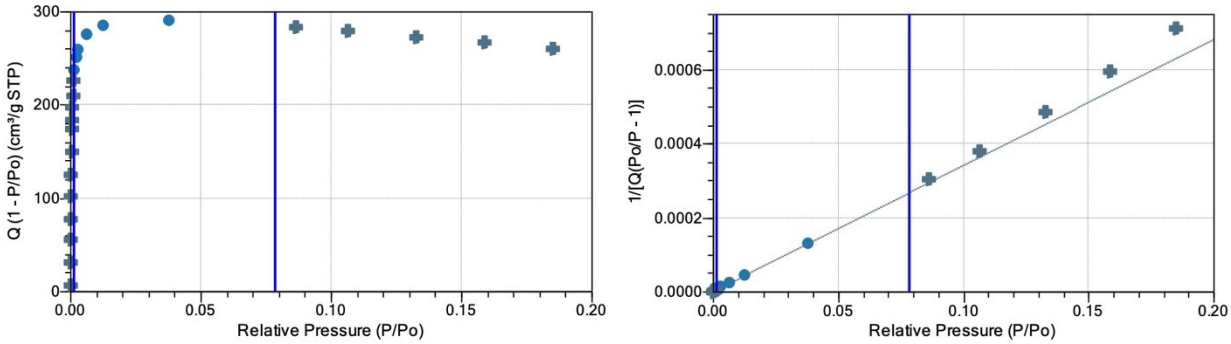

Figure S52. *Left*: Rouquerol plot of oligoIRMOF-1-triazole$_2$-*o*-xylyl. *Right*: BET plot of oligoIRMOF-1-triazole$_2$-*o*-xylyl. Selected P/P_0 range for BET fit: 0.0013 to 0.0786 (highlighted in blue lines). BET surface area: 1277 ± 1.0 m²/g. Slope: 0.003408 ± 0.000002 g/cm³. Y-intercept: 0.000001 ± 0.000000 g/cm³. C-constant: 2497.494277. Q_m: 293.3255 cm³/g. Correlation coefficient: 0.9999992.

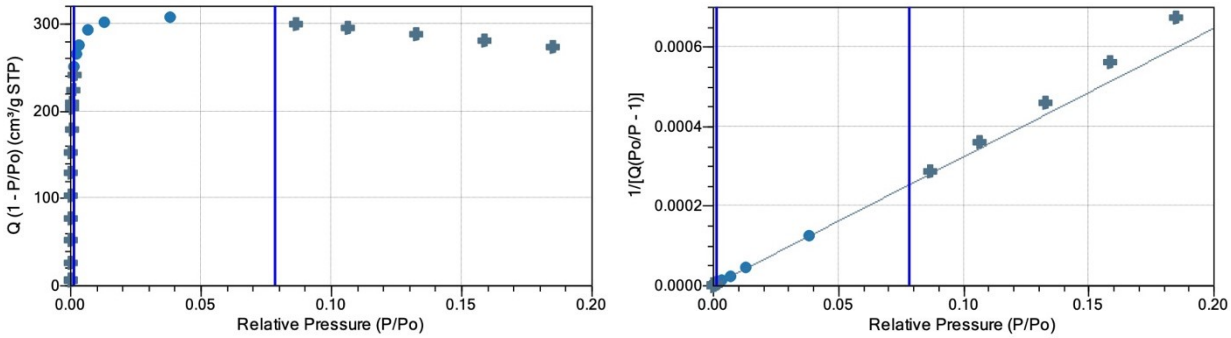

Figure S53. *Left*: Rouquerol plot of oligoIRMOF-1-triazole$_2$-*m*-xylyl. *Right*: BET plot of oligoIRMOF-1-triazole$_2$-*m*-xylyl. Selected P/P_0 range for BET fit: 0.0013 to 0.0786 (highlighted in blue lines). BET surface area: 1346 ± 1.0 m²/g. Slope: 0.003232 ± 0.000002 g/cm³. Y-intercept: 0.000001 ± 0.000000 g/cm³. C-constant: 2506.359237. Q_m: 309.2855 cm³/g. Correlation coefficient: 0.9999992.

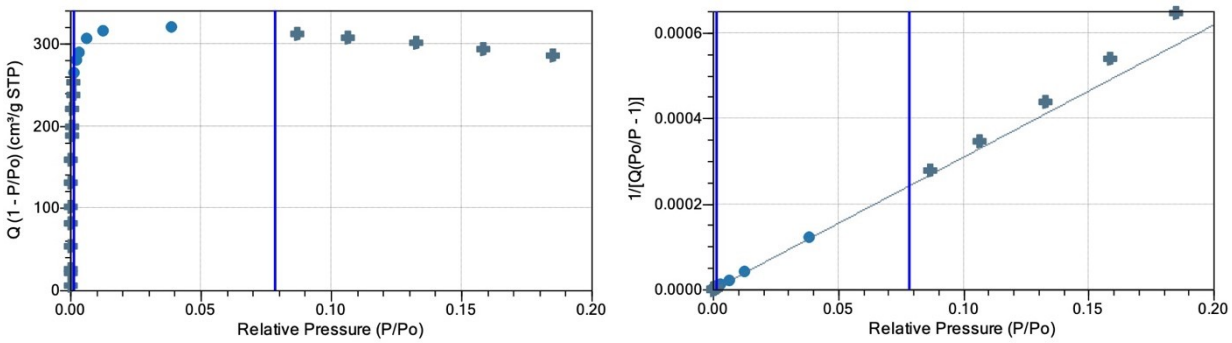

Figure S54. *Left*: Rouquerol plot of oligoIRMOF-1-triazole$_2$-*p*-xylyl. *Right*: BET plot of oligoIRMOF-1-triazole$_2$-*p*-xylyl. Selected P/P_0 range for BET fit: 0.0013 to 0.0786 (highlighted in blue lines). BET surface area: 1407 ± 1.0 m²/g. Slope: 0.003091 ± 0.000002 g/cm³. Y-intercept: 0.000001 ± 0.000000 g/cm³. C-constant: 2682.093304. Q_m: 323.3608 cm³/g. Correlation coefficient: 0.9999990.

F. ^{1}H and ^{13}C NMR spectrum of oligomeric ligands

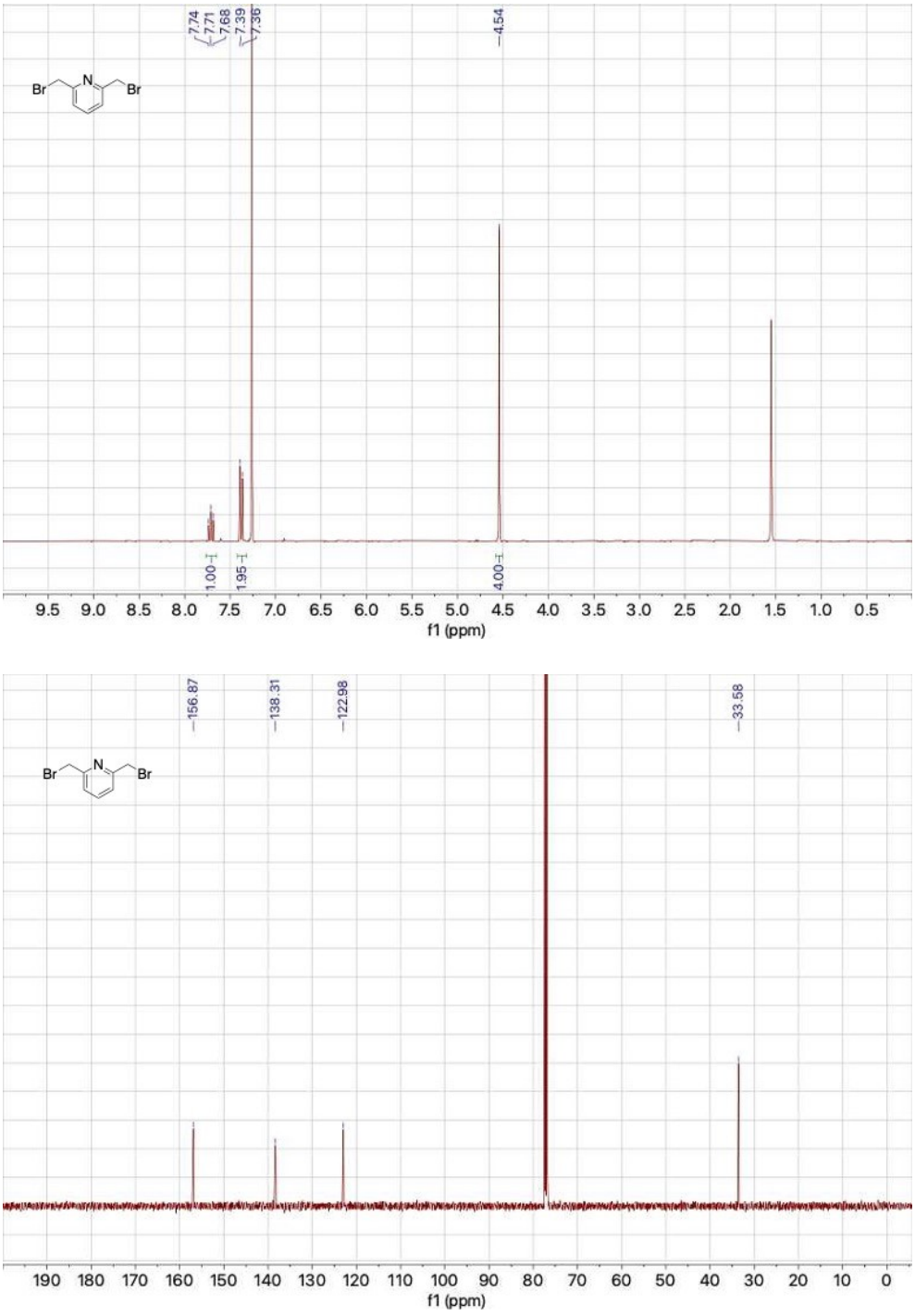

Figure S55. ^{1}H (*top*) and ^{13}C (*bottom*) NMR spectrum of 2,6-bis(bromomethyl)pyridine (**2**).

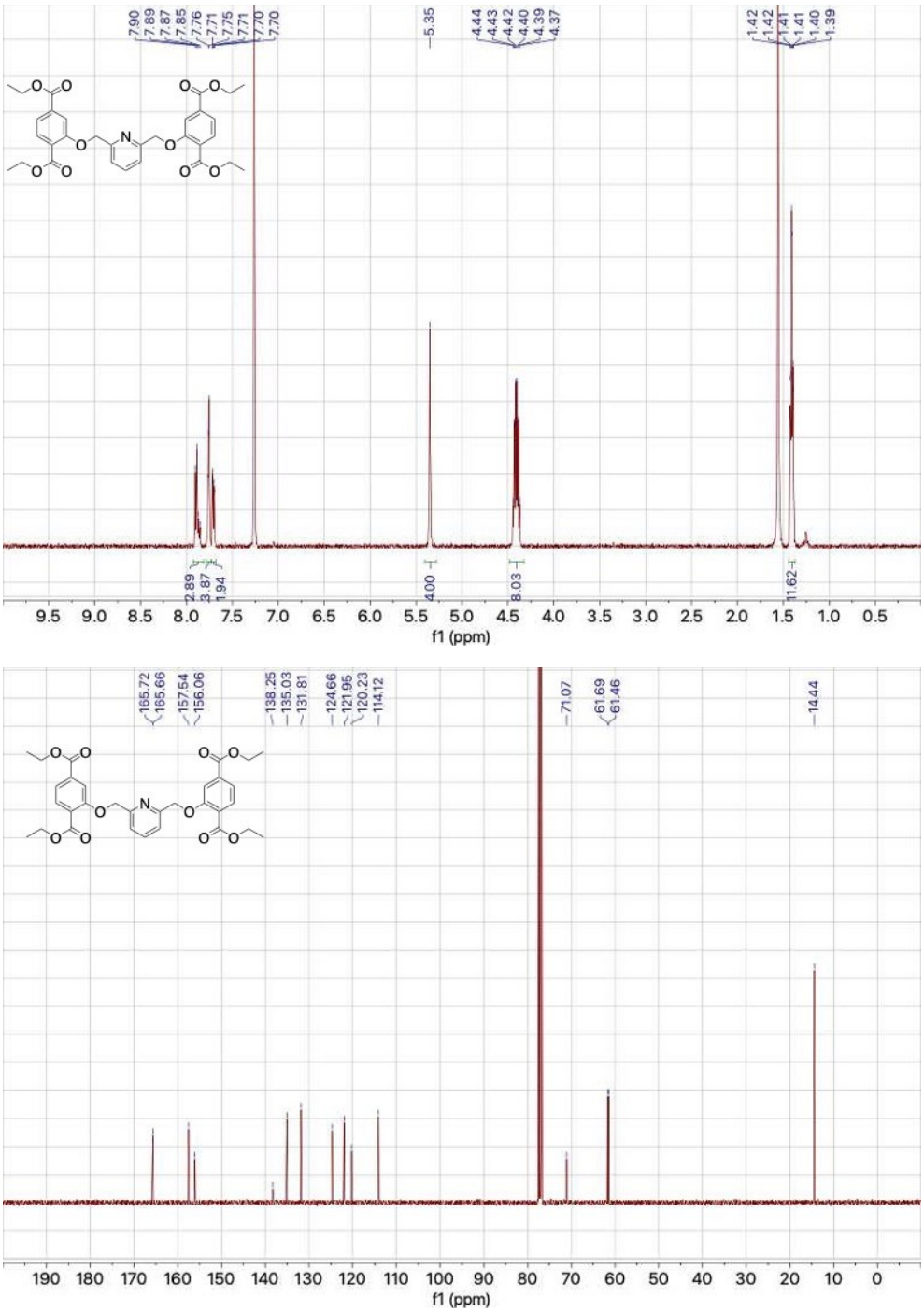

Figure S56. ^{1}H (*top*) and ^{13}C (*bottom*) NMR spectrum of tetraethyl 2,2'-((pyridine-2,6-diylbis(methylene))bis(oxy))diterephthalate (**4**).

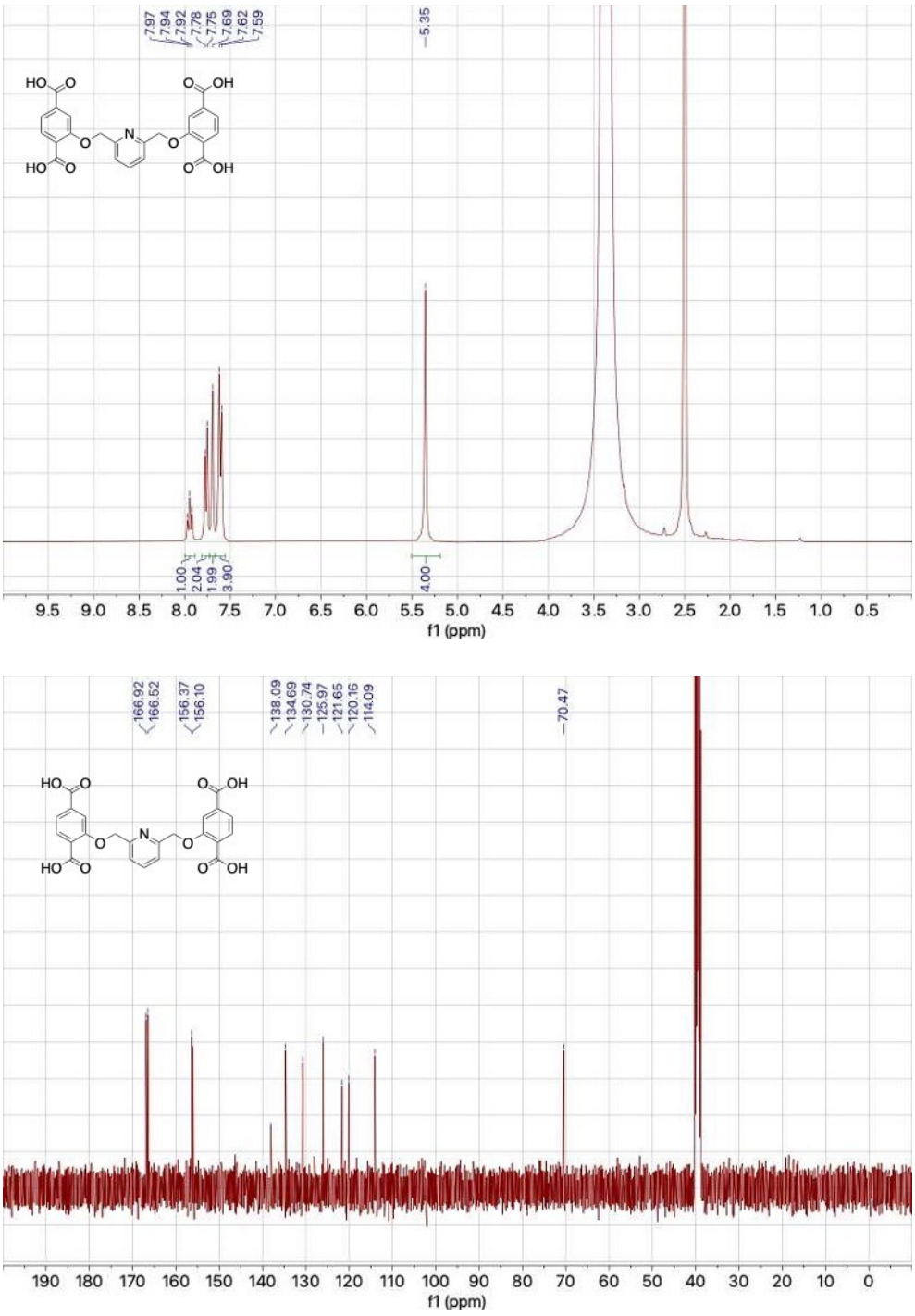

Figure S57. ^{1}H (*top*) and ^{13}C (*bottom*) NMR spectrum of 2,2'-((pyridine-2,6-diylbis(methylene))bis(oxy))diterephthalic acid (**L1**).

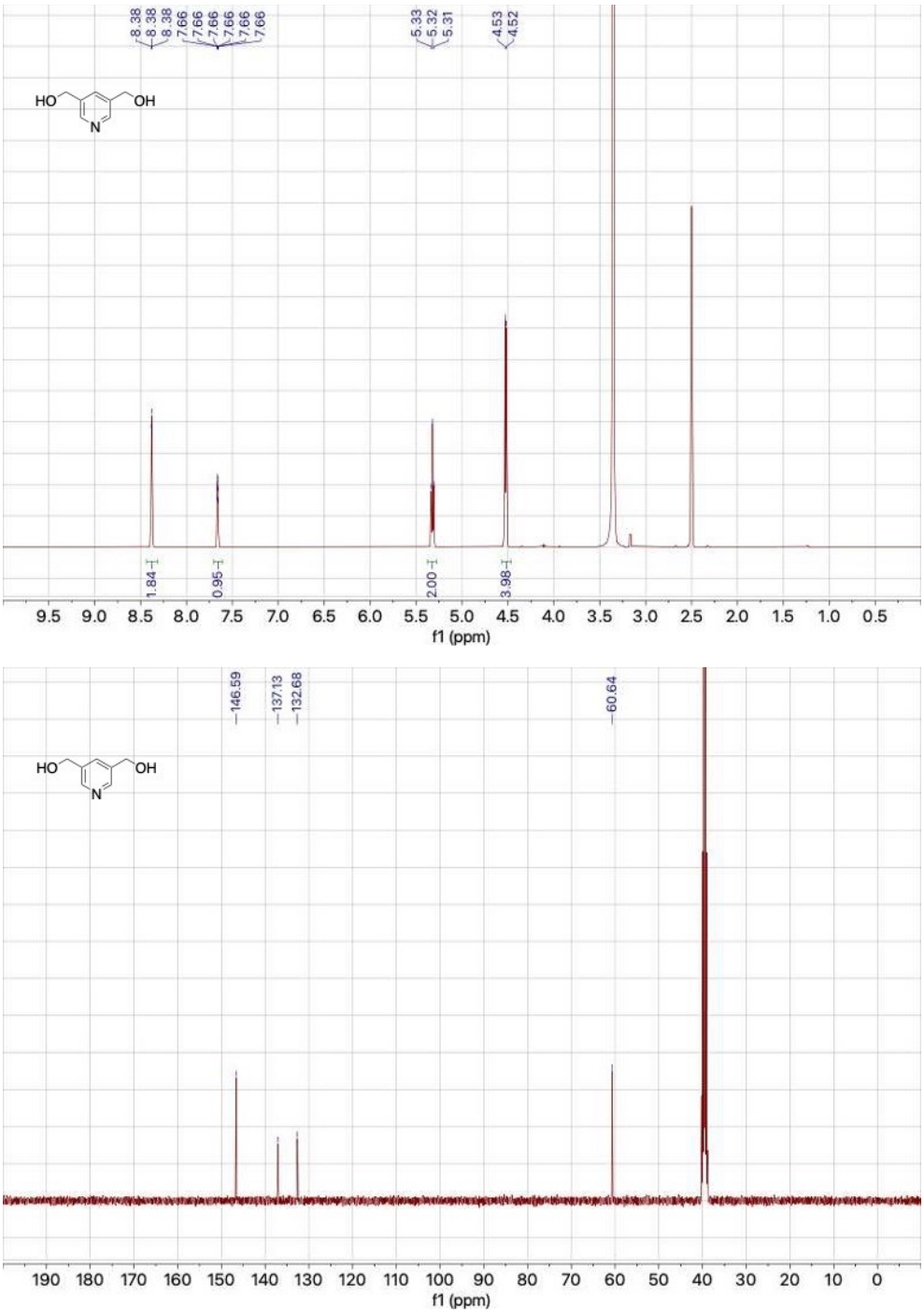

Figure S58. ^{1}H (*top*) and ^{13}C (*bottom*) NMR spectrum of pyridine-3,5-diyldimethanol (**6**).

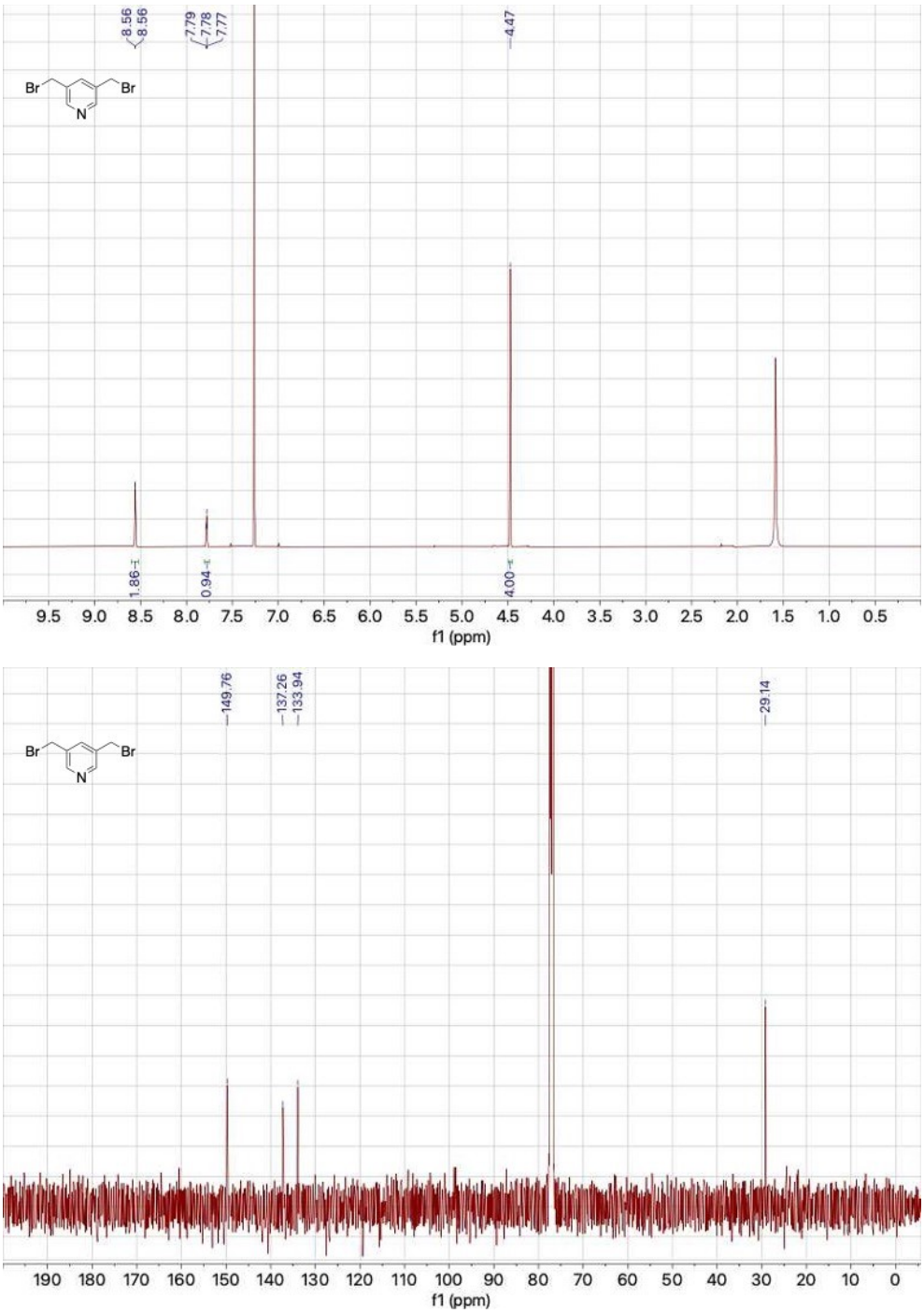

Figure S59. ^{1}H (*top*) and ^{13}C (*bottom*) NMR spectrum of 3,5-bis(bromomethyl)pyridine (**7**).

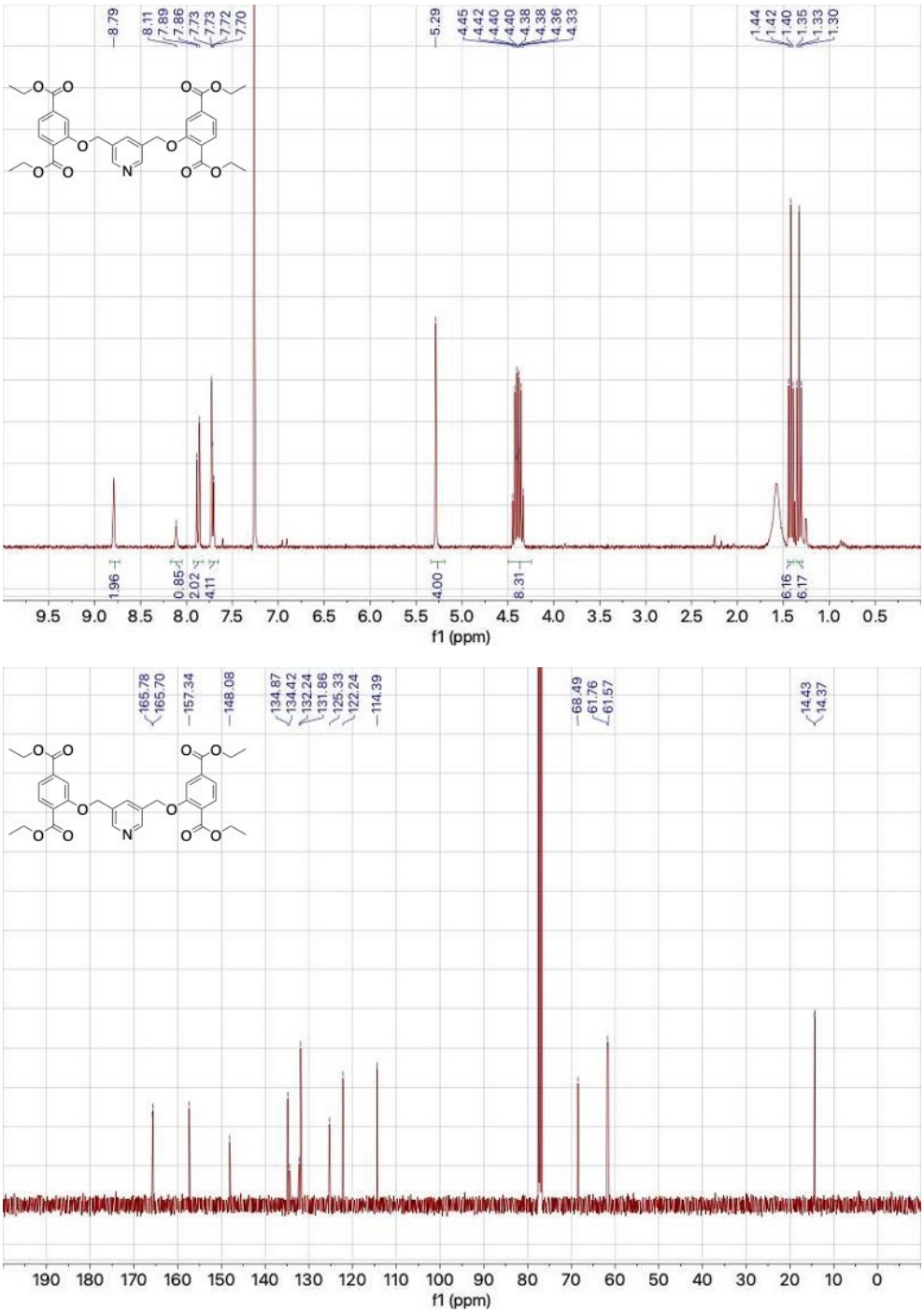

Figure S60. ^{1}H (*top*) and ^{13}C (*bottom*) NMR spectrum of tetraethyl 2,2'-((pyridine-3,5-diylbis(methylene))bis(oxy))diterephthalate (**8**).

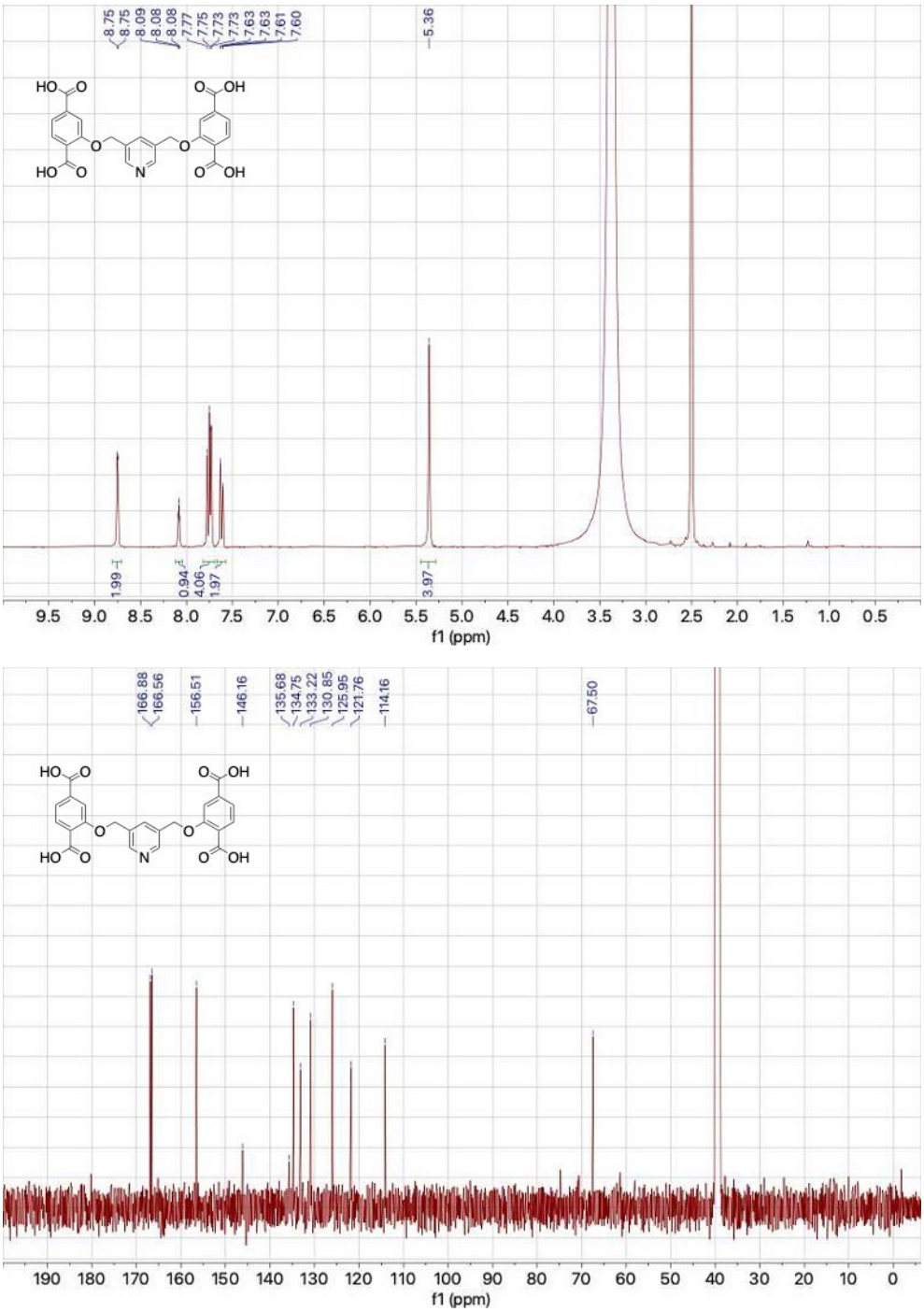

Figure S61. ^{1}H (*top*) and ^{13}C (*bottom*) NMR spectrum of 2,2'-((pyridine-3,5-diylbis(methylene))bis(oxy))diterephthalic acid (**L2**).

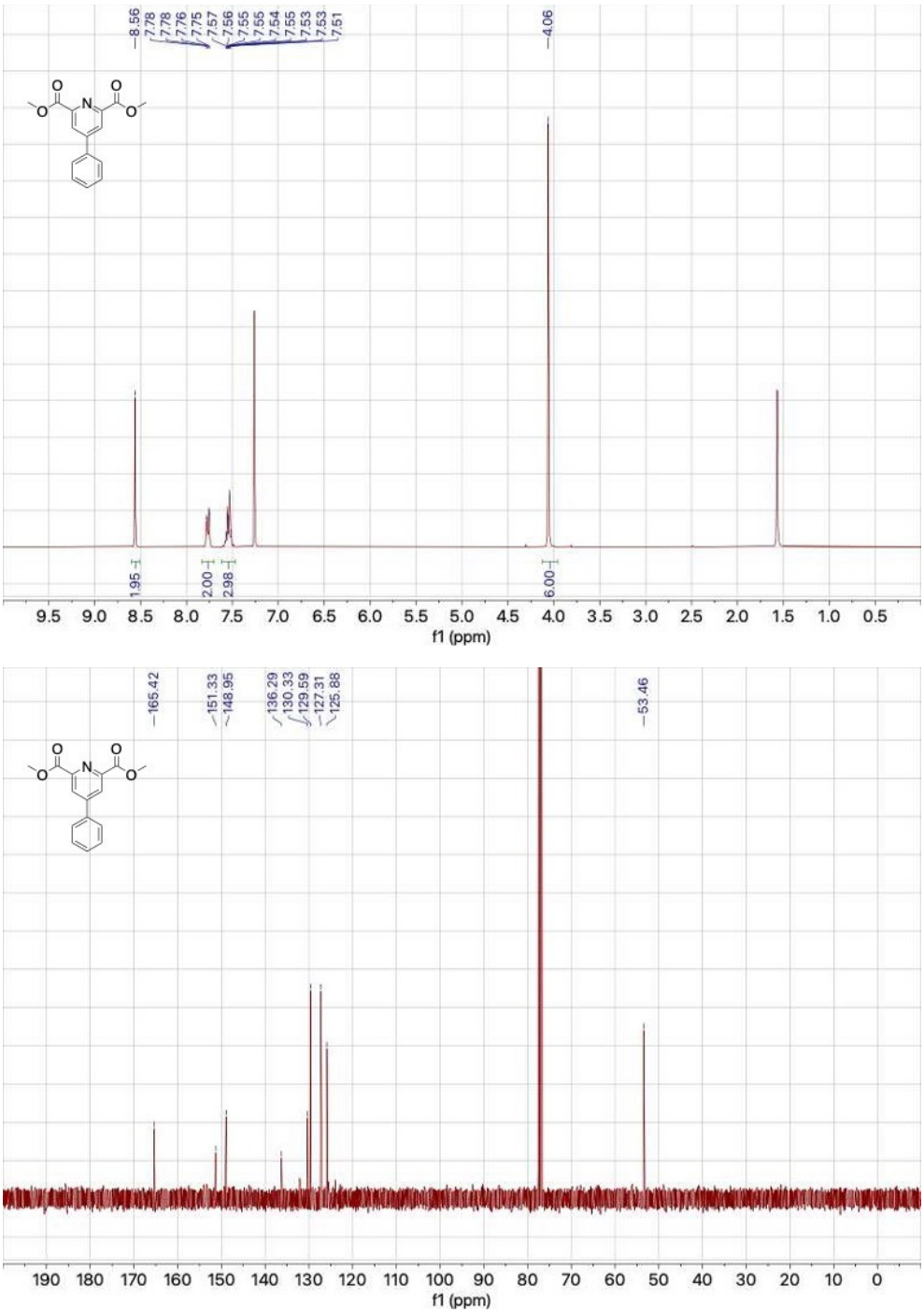

Figure S62. ^{1}H (*top*) and ^{13}C (*bottom*) NMR spectrum of dimethyl 4-phenylpyridine-2,6-dicarboxylate (**11**).

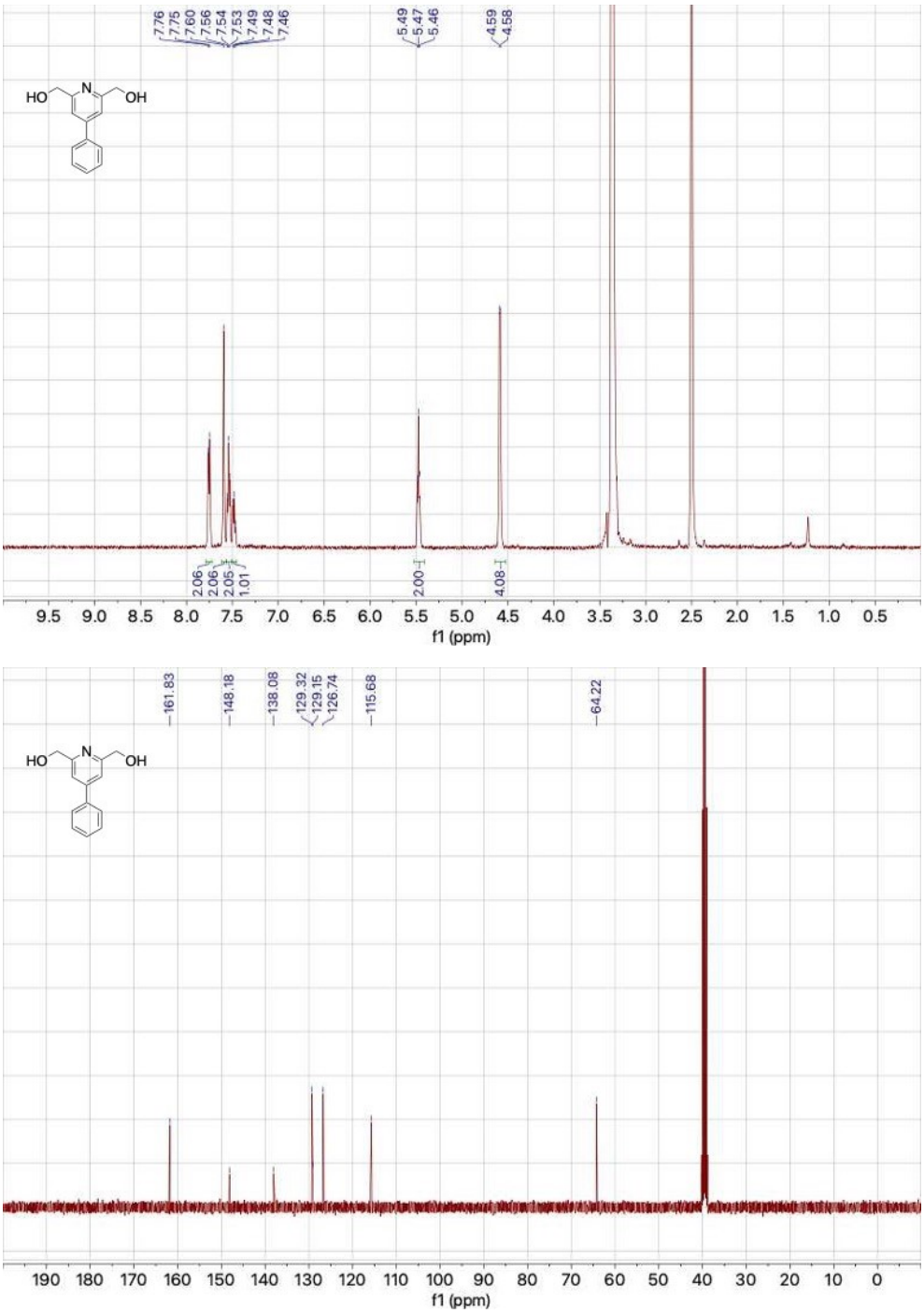

Figure S63. ^{1}H (*top*) and ^{13}C (*bottom*) NMR spectrum of (4-phenylpyridine-2,6-diyl)dimethanol (**12**).

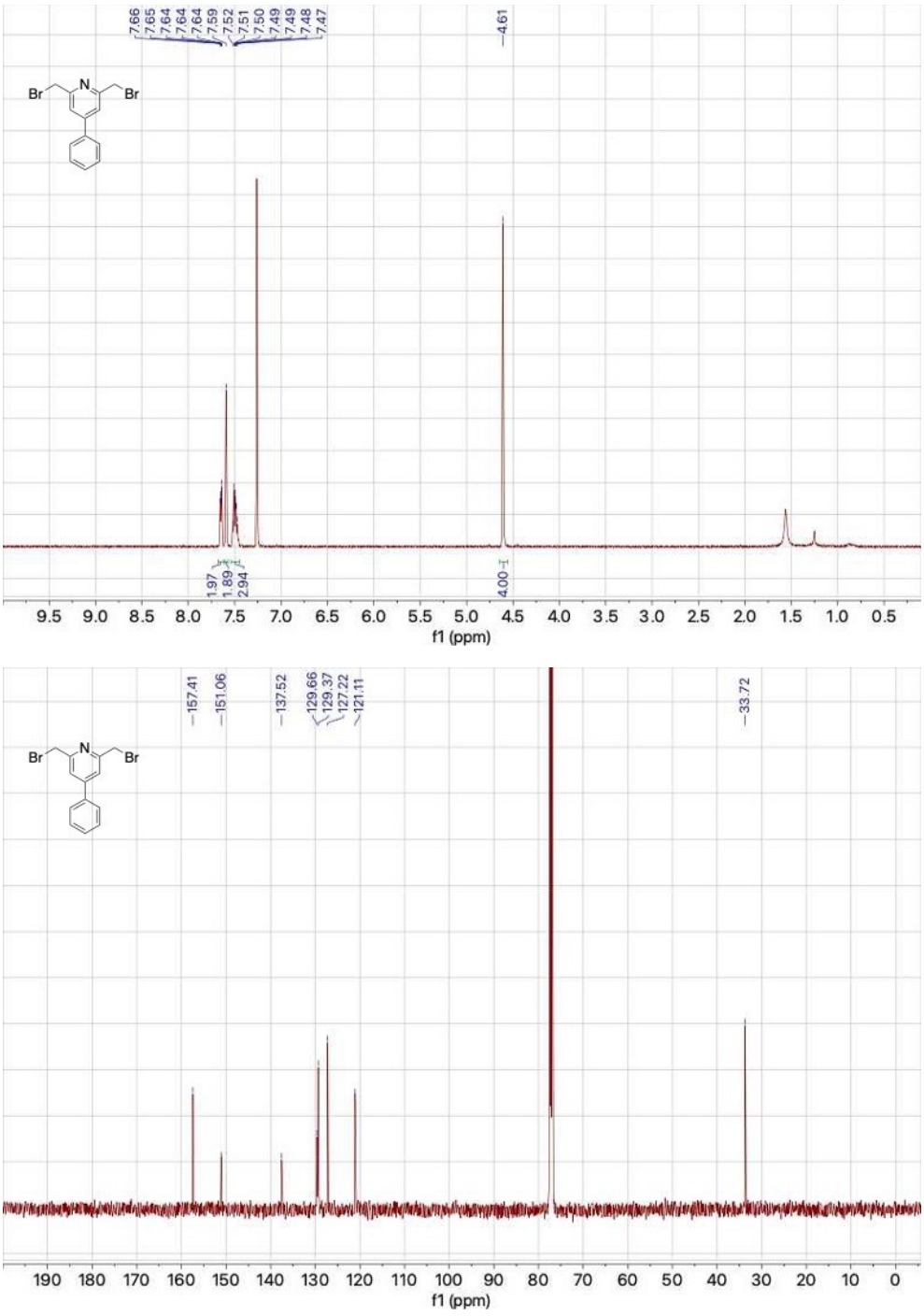

Figure S64. ^{1}H (*top*) and ^{13}C (*bottom*) NMR spectrum of 2,6-bis(bromomethyl)-4-phenylpyridine (**13**).

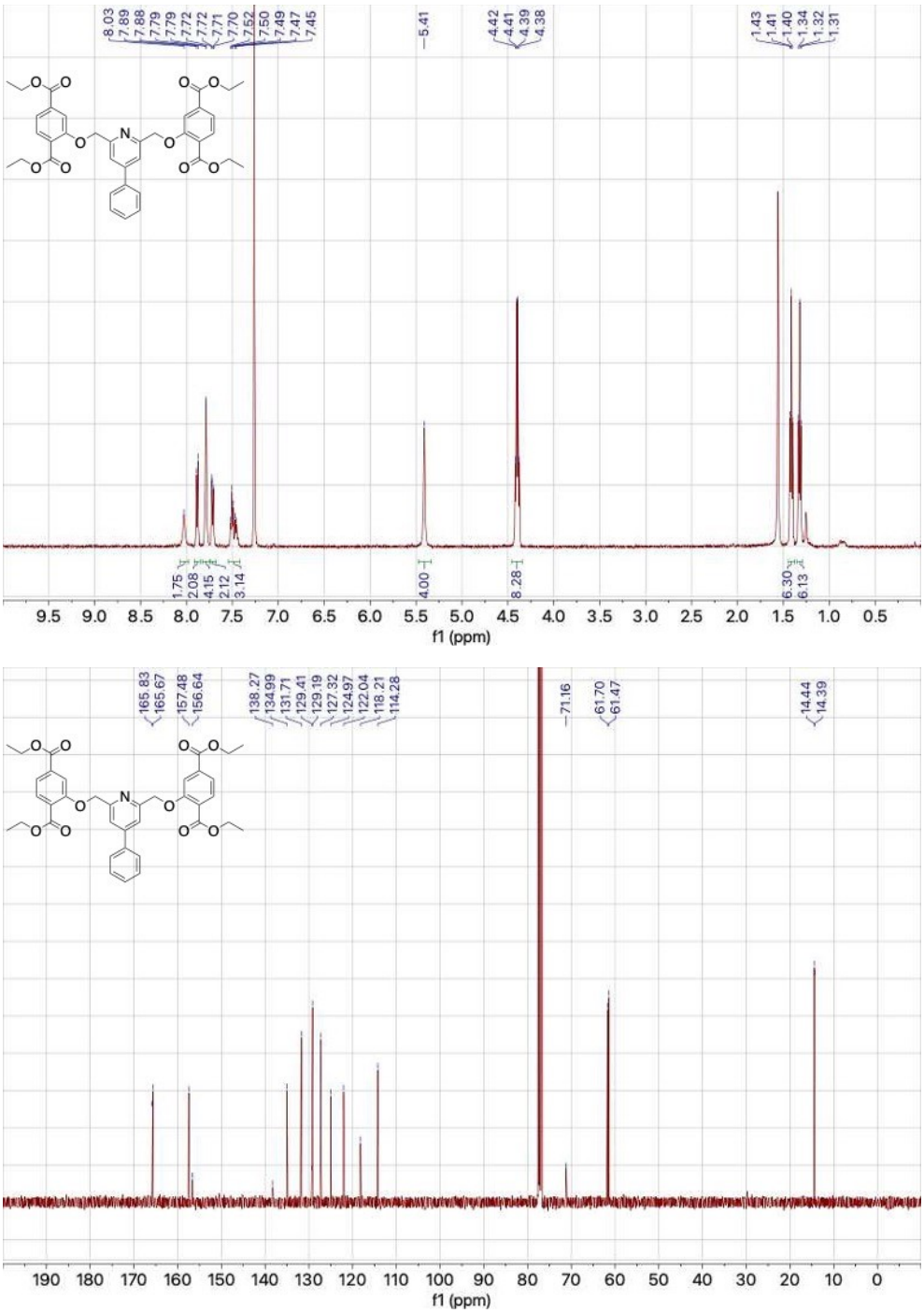

Figure S65. ^{1}H (*top*) and ^{13}C (*bottom*) NMR spectrum of tetraethyl 2,2'-(((4-phenylpyridine-2,6-diyl)bis(methylene))bis(oxy))diterephthalate (**14**).

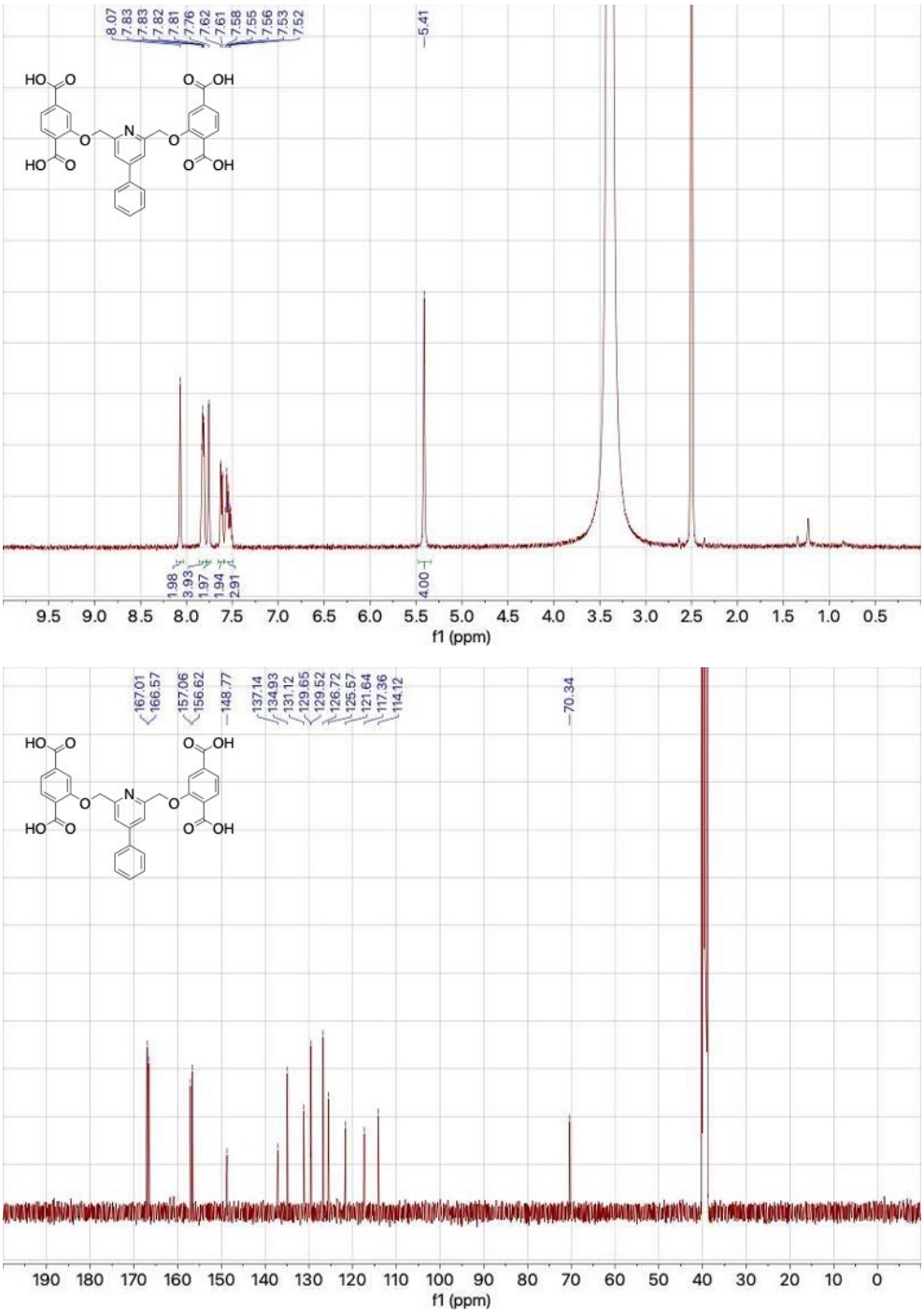

Figure S66. ^{1}H (*top*) and ^{13}C (*bottom*) NMR spectrum of 2,2'-(((4-phenylpyridine-2,6-diyl)bis(methylene))bis(oxy))diterephthalic acid (**L3**).

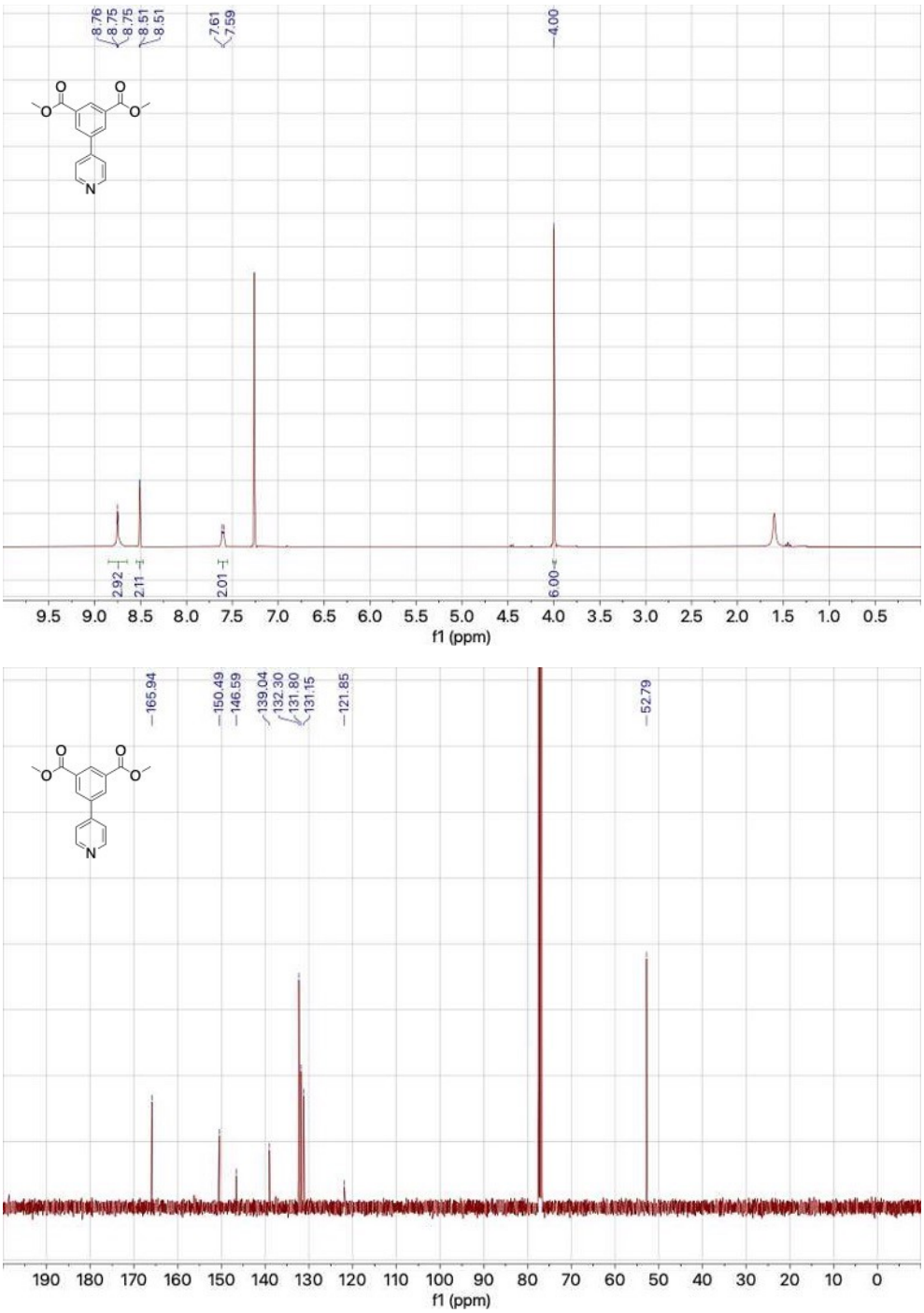

Figure S67. ^{1}H (*top*) and ^{13}C (*bottom*) NMR spectrum of dimethyl 5-(pyridin-4-yl)isophthalate (**17**).

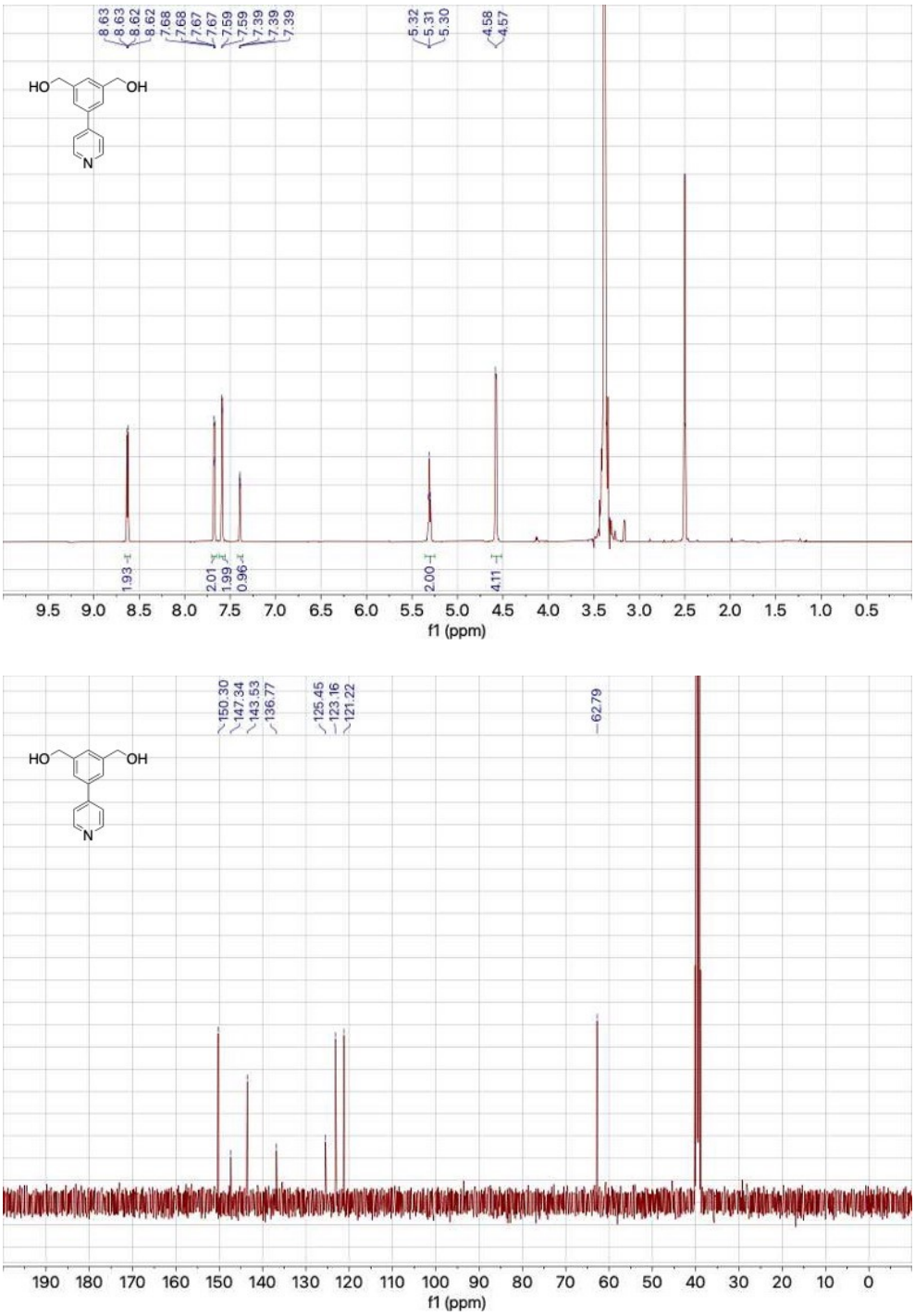

Figure S68. ^{1}H (*top*) and ^{13}C (*bottom*) NMR spectrum of **(**5-(pyridin-4-yl)-1,3-phenylene)dimethanol (**18**).

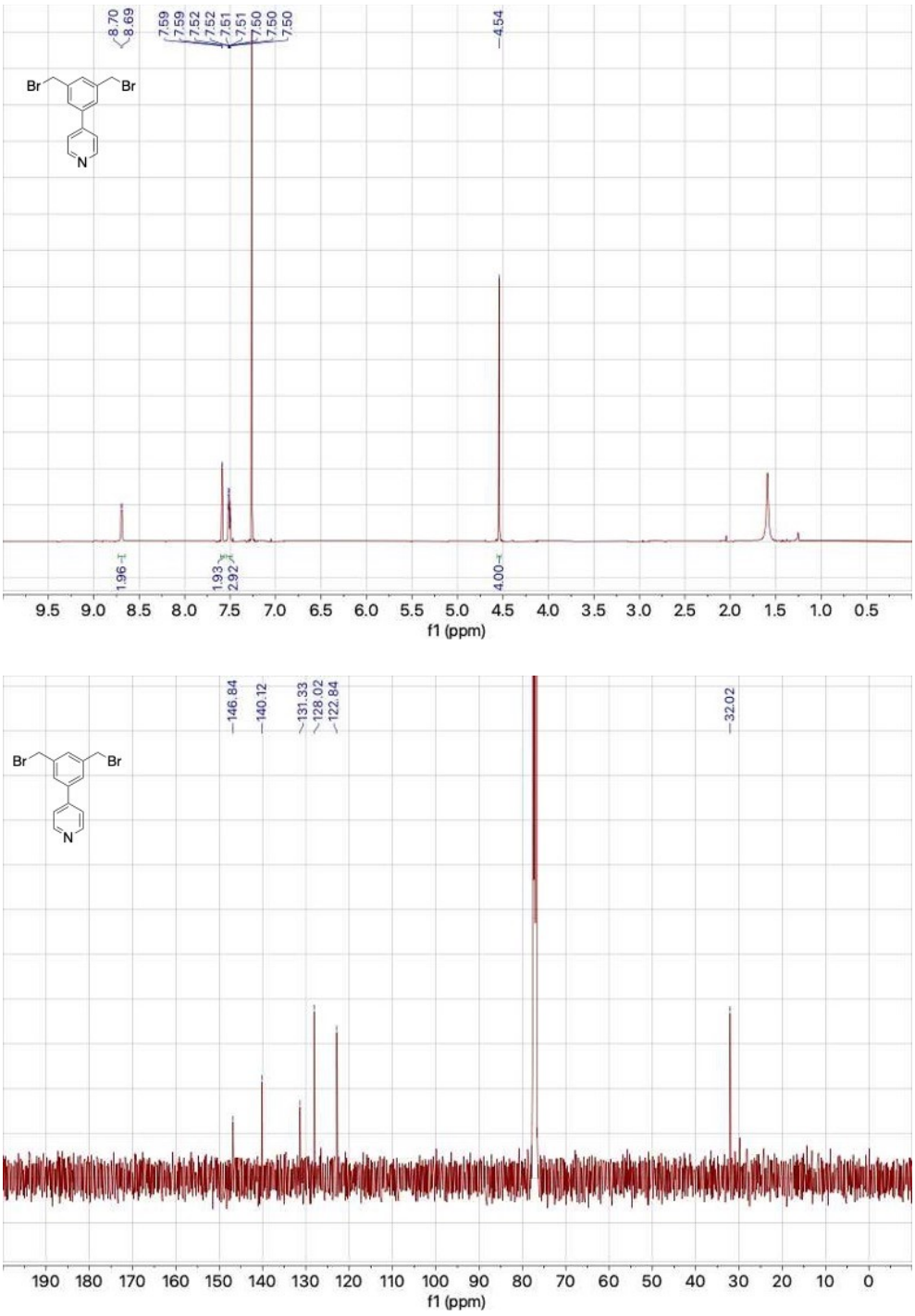

Figure S69. ^{1}H (*top*) and ^{13}C (*bottom*) NMR spectrum of 4-(3,5-bis(bromomethyl)phenyl)pyridine (**19**).

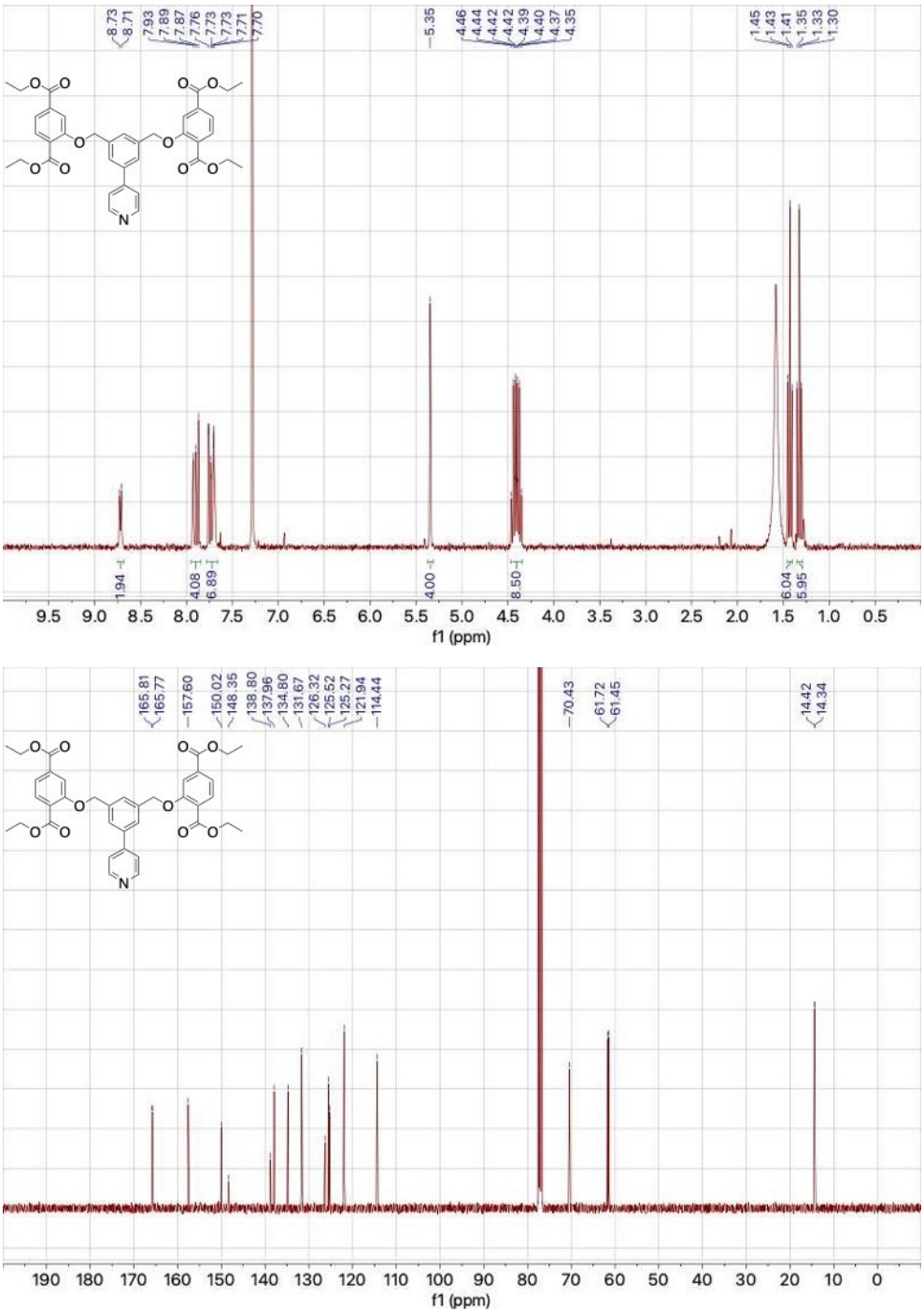

Figure S70. ^{1}H (*top*) and ^{13}C (*bottom*) NMR spectrum of tetraethyl 2,2'-(((5-(pyridin-4-yl)-1,3-phenylene)bis(methylene))bis(oxy))diterephthalate (**20**).

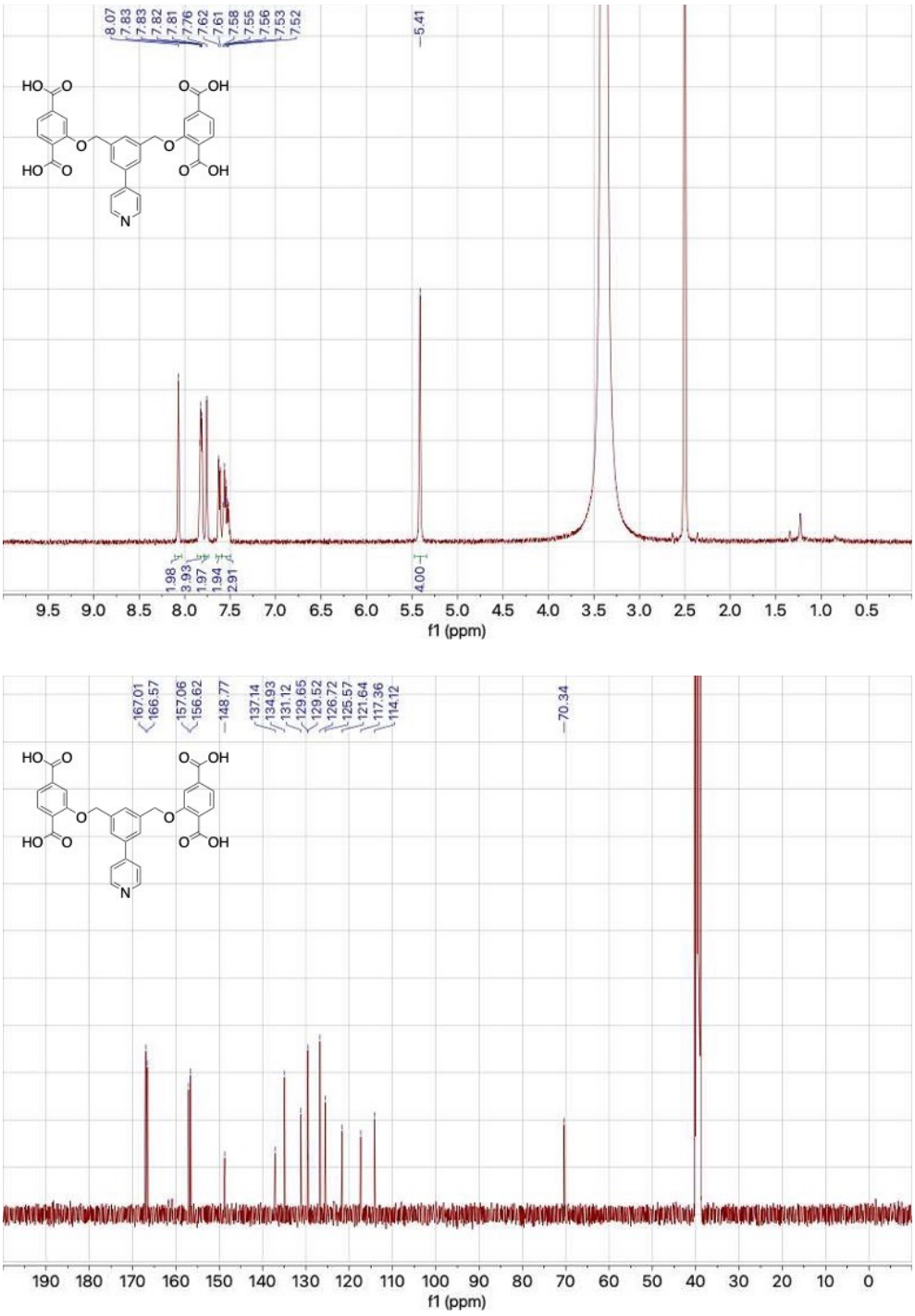

Figure S71. ^{1}H (*top*) and ^{13}C (*bottom*) NMR spectrum of 2,2'-(((5-(pyridin-4-yl)-1,3-phenylene)bis(methylene))bis(oxy))diterephthalic acid (**L4**).

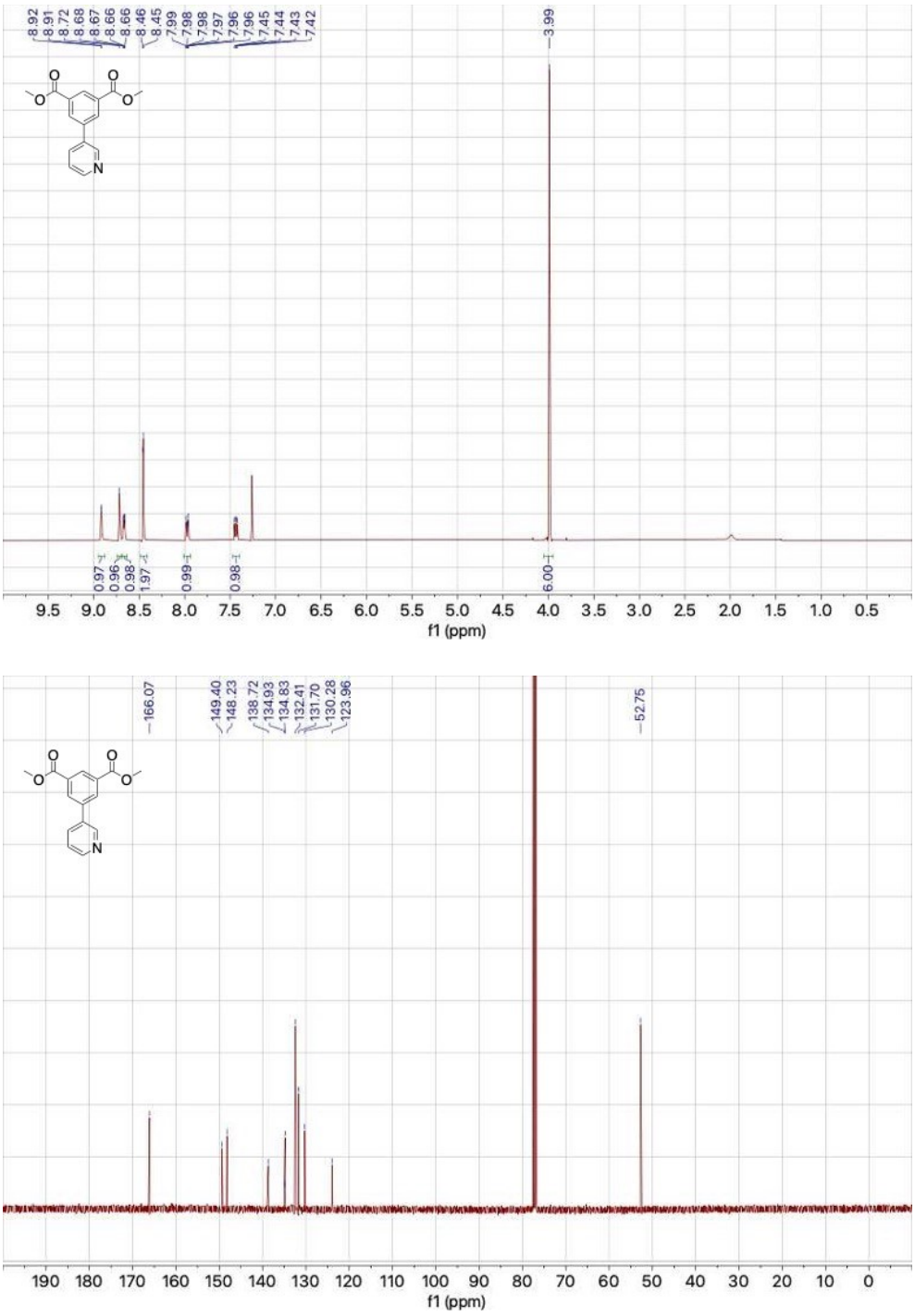

Figure S72. ^{1}H (*top*) and ^{13}C (*bottom*) NMR spectrum of dimethyl 5-(pyridin-3-yl)isophthalate (**22**).

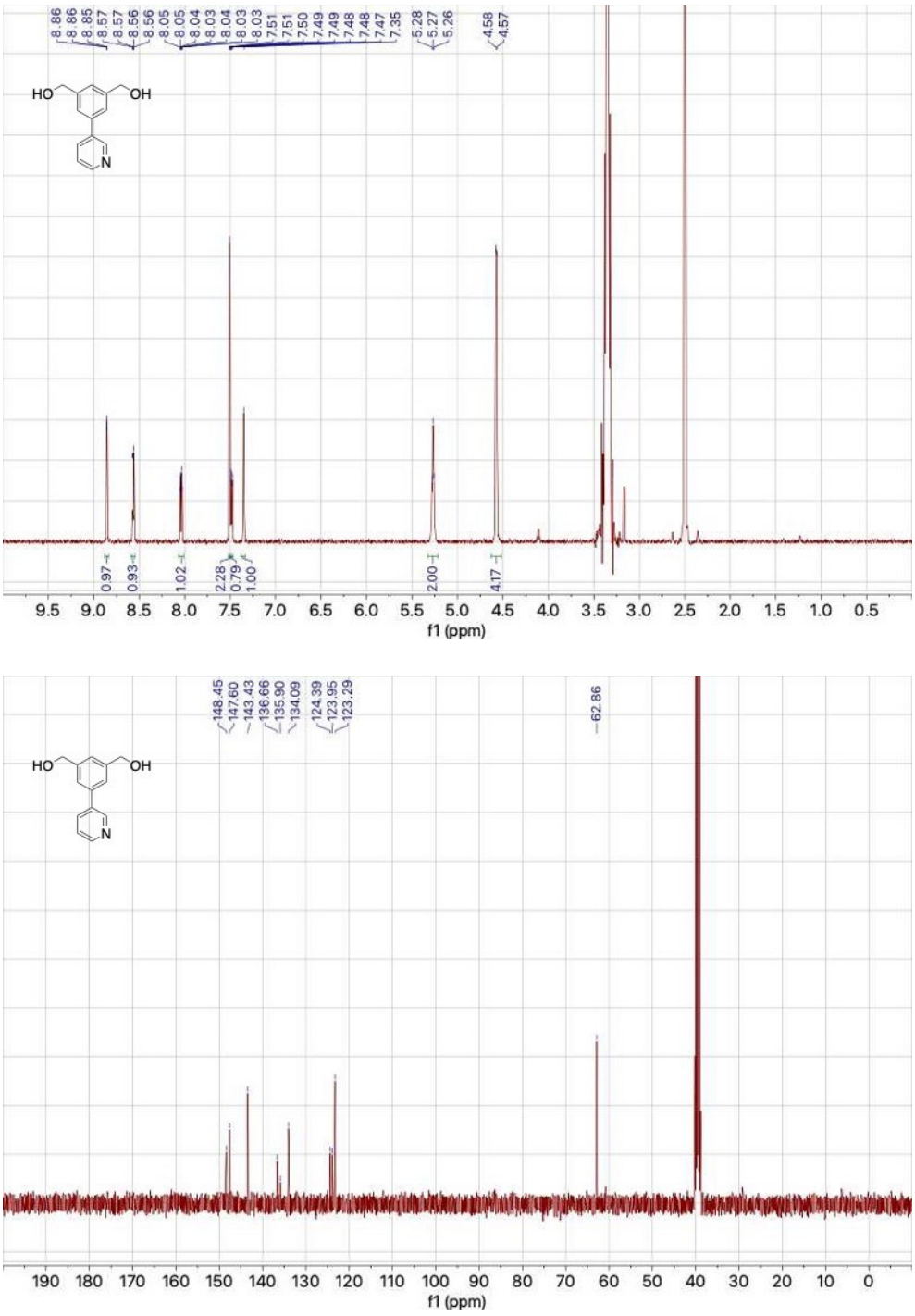

Figure S73. ^{1}H (*top*) and ^{13}C (*bottom*) NMR spectrum of **(**5-(pyridin-3-yl)-1,3-phenylene)dimethanol (**23**).

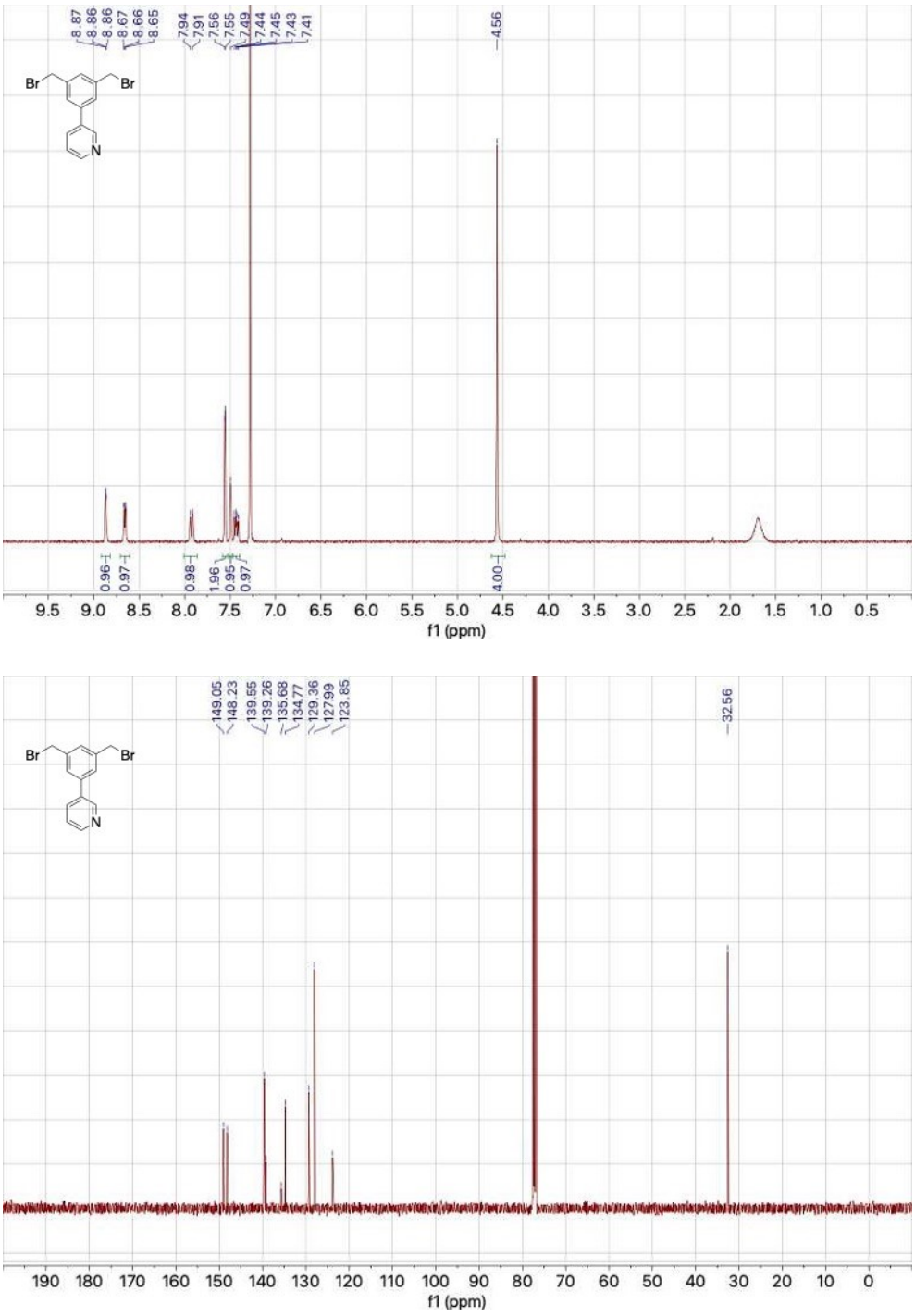

Figure S74. ^{1}H (*top*) and ^{13}C (*bottom*) NMR spectrum of 3-(3,5-bis(bromomethyl)phenyl)pyridine (**24**).

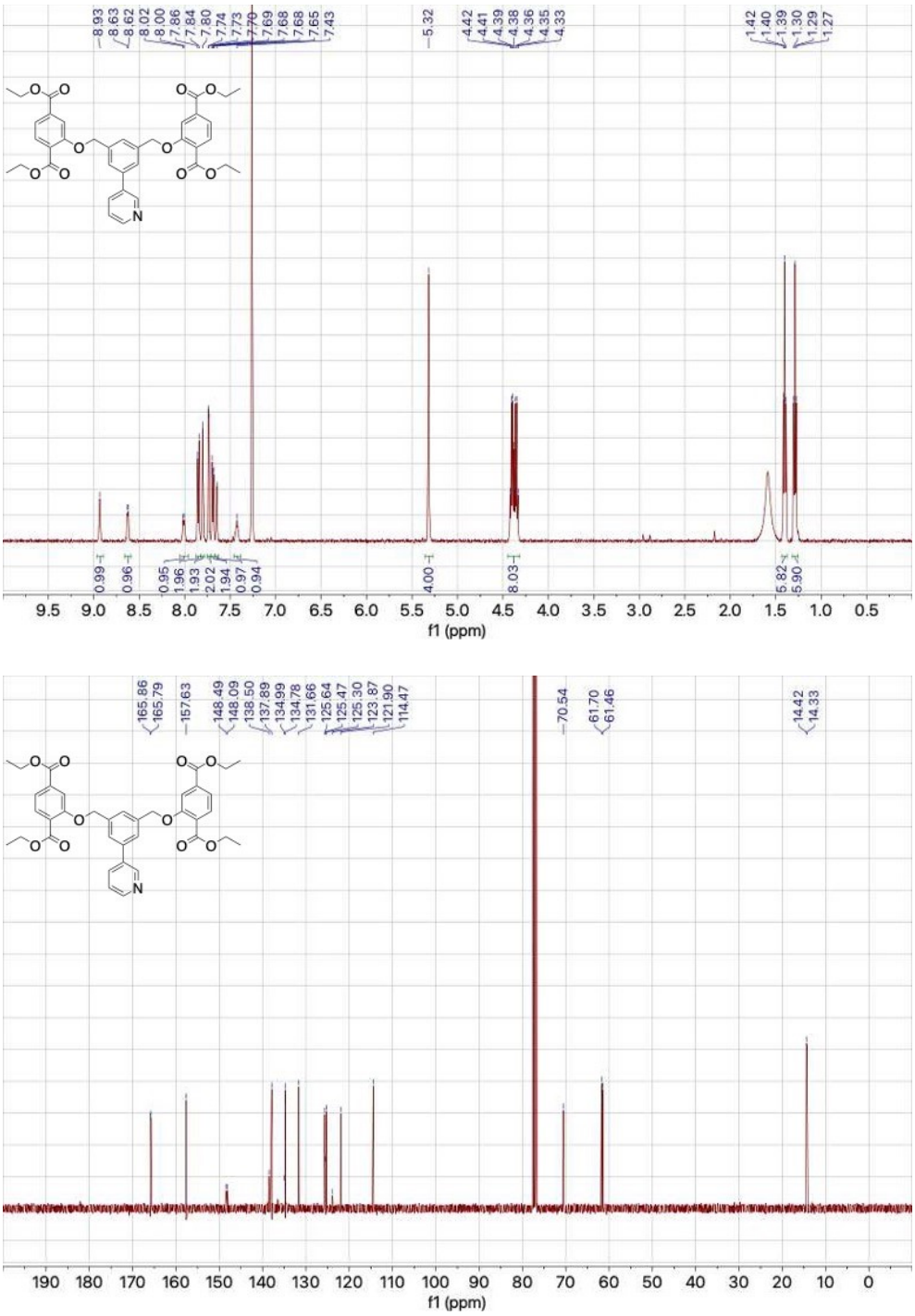

Figure S75. ^{1}H (*top*) and ^{13}C (*bottom*) NMR spectrum of tetraethyl 2,2'-(((5-(pyridin-3-yl)-1,3-phenylene)bis(methylene))bis(oxy))diterephthalate (**25**).

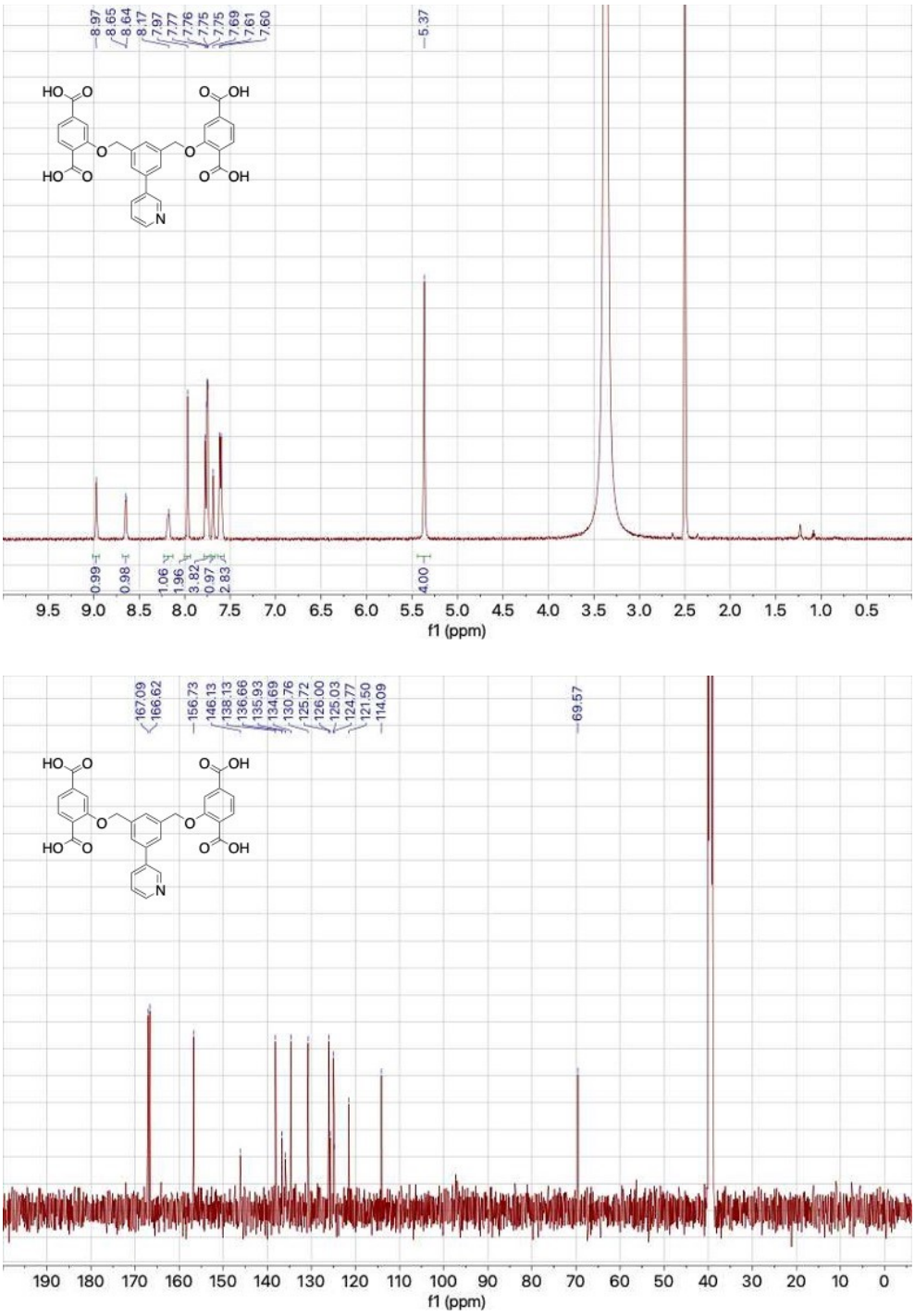

Figure S76. ^{1}H (*top*) and ^{13}C (*bottom*) NMR spectrum of 2,2'-(((5-(pyridin-3-yl)-1,3-phenylene)bis(methylene))bis(oxy))diterephthalic acid (**L5**).

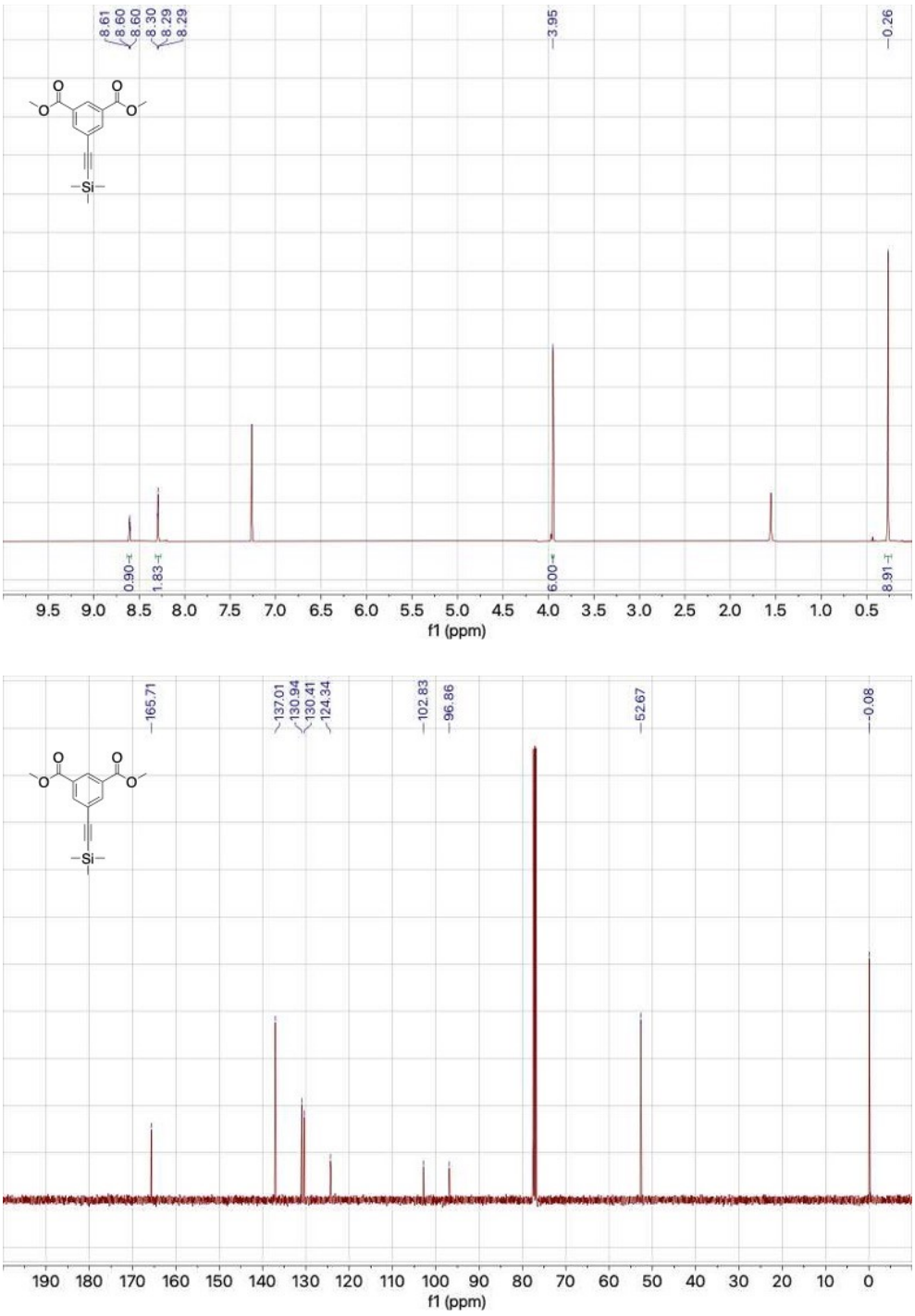

Figure S77. ^{1}H (*top*) and ^{13}C (*bottom*) NMR spectrum of dimethyl 5-((trimethylsilyl)ethynyl)isophthalate (**27**).

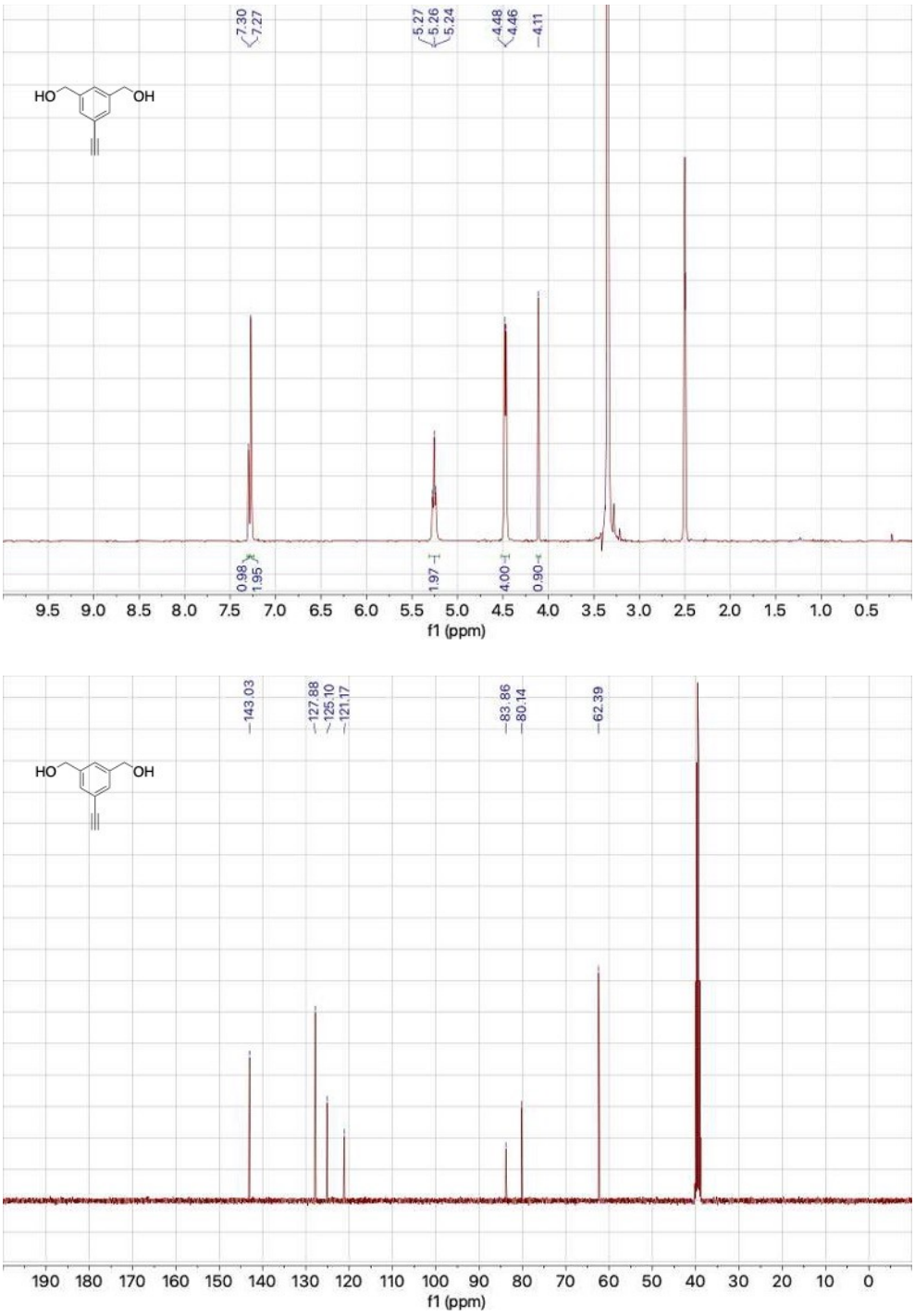

Figure S78. ^{1}H (*top*) and ^{13}C (*bottom*) NMR spectrum of (5-ethynyl-1,3-phenylene)dimethanol (**28**).

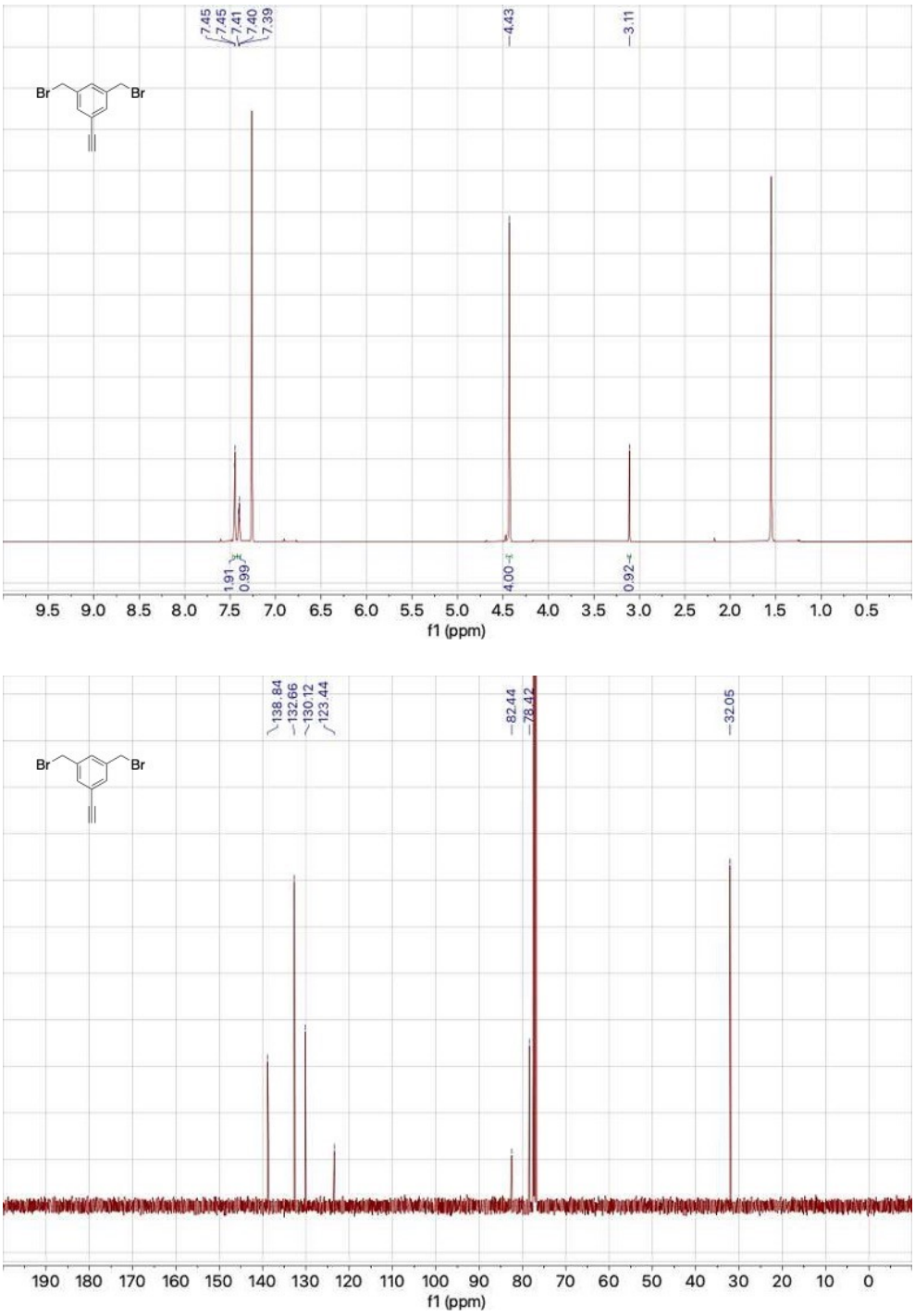

Figure S79. ^{1}H (*top*) and ^{13}C (*bottom*) NMR spectrum of 1,3-bis(bromomethyl)-5-ethynylbenzene (**29**).

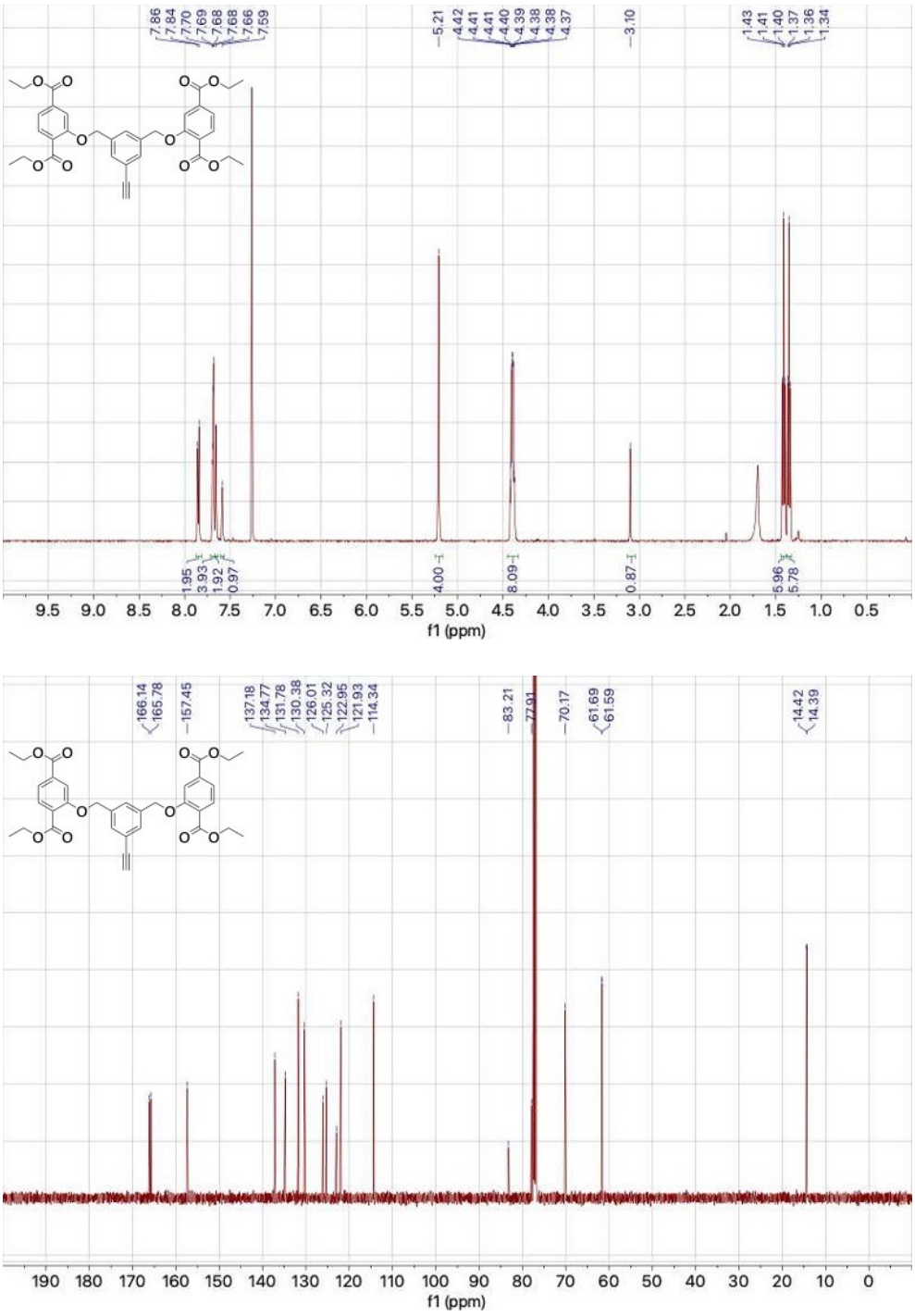

Figure S80. ^{1}H (*top*) and ^{13}C (*bottom*) NMR spectrum of tetraethyl 2,2'-(((5-ethynyl-1,3-phenylene)bis(methylene))bis(oxy))diterephthalate (**30**).

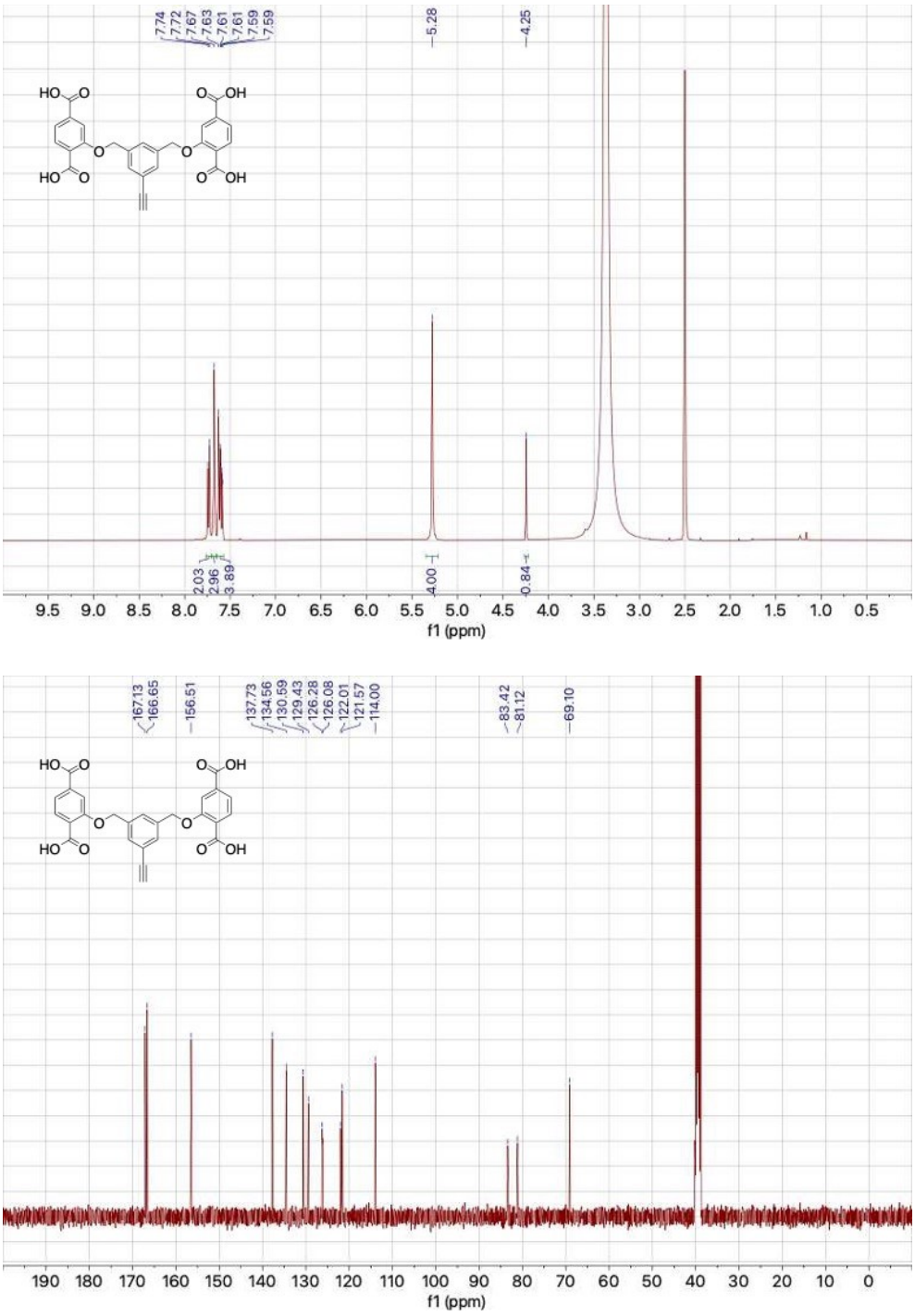

Figure S81. ^{1}H (*top*) and ^{13}C (*bottom*) NMR spectrum of 2,2'-(((5-ethynyl-1,3-phenylene)bis(methylene))bis(oxy))diterephthalic acid (**L6**).

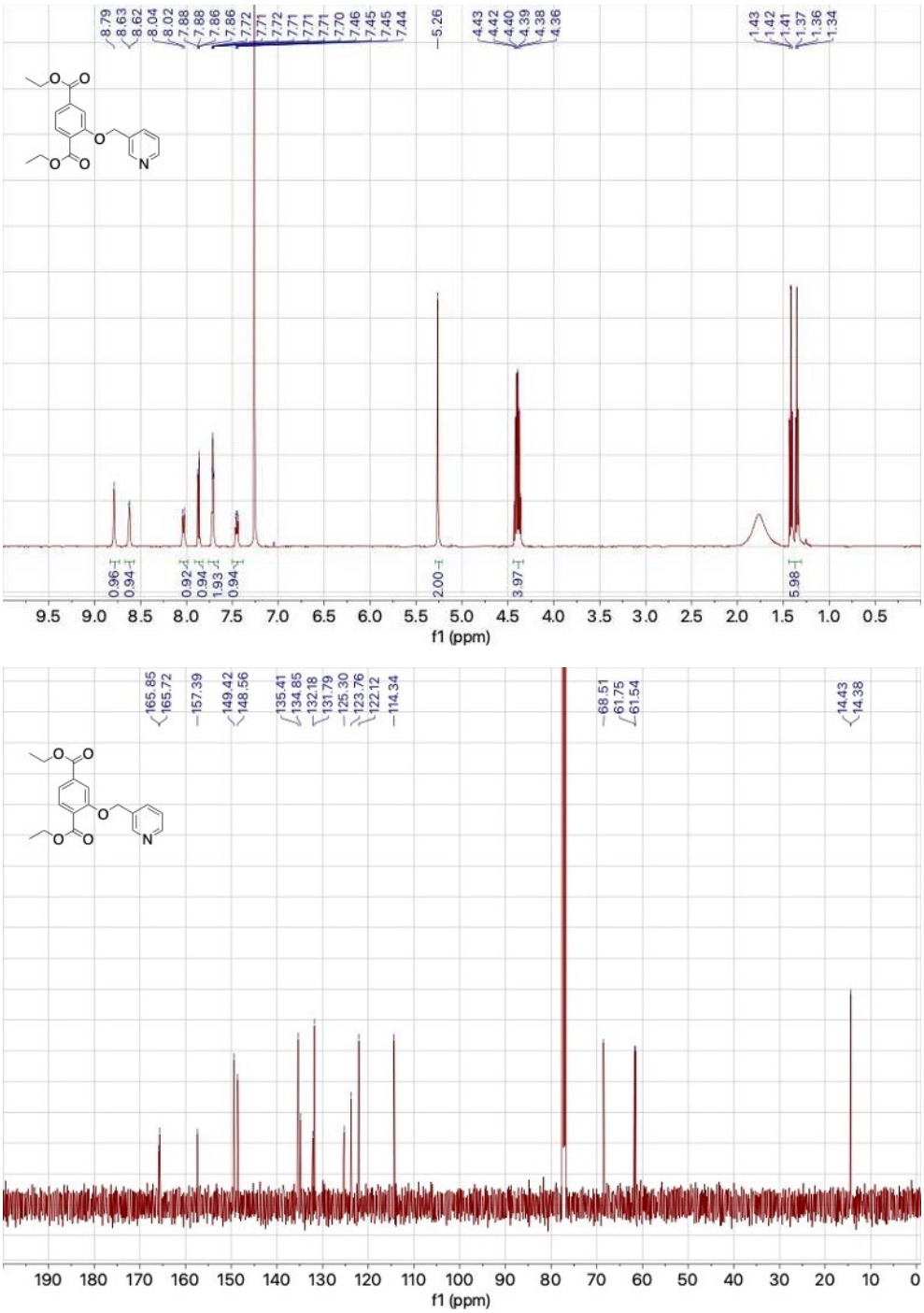

Figure S82. ^{1}H (*top*) and ^{13}C (*bottom*) NMR spectrum of diethyl 2-(pyridin-3-ylmethoxy)terephthalate (**32**).

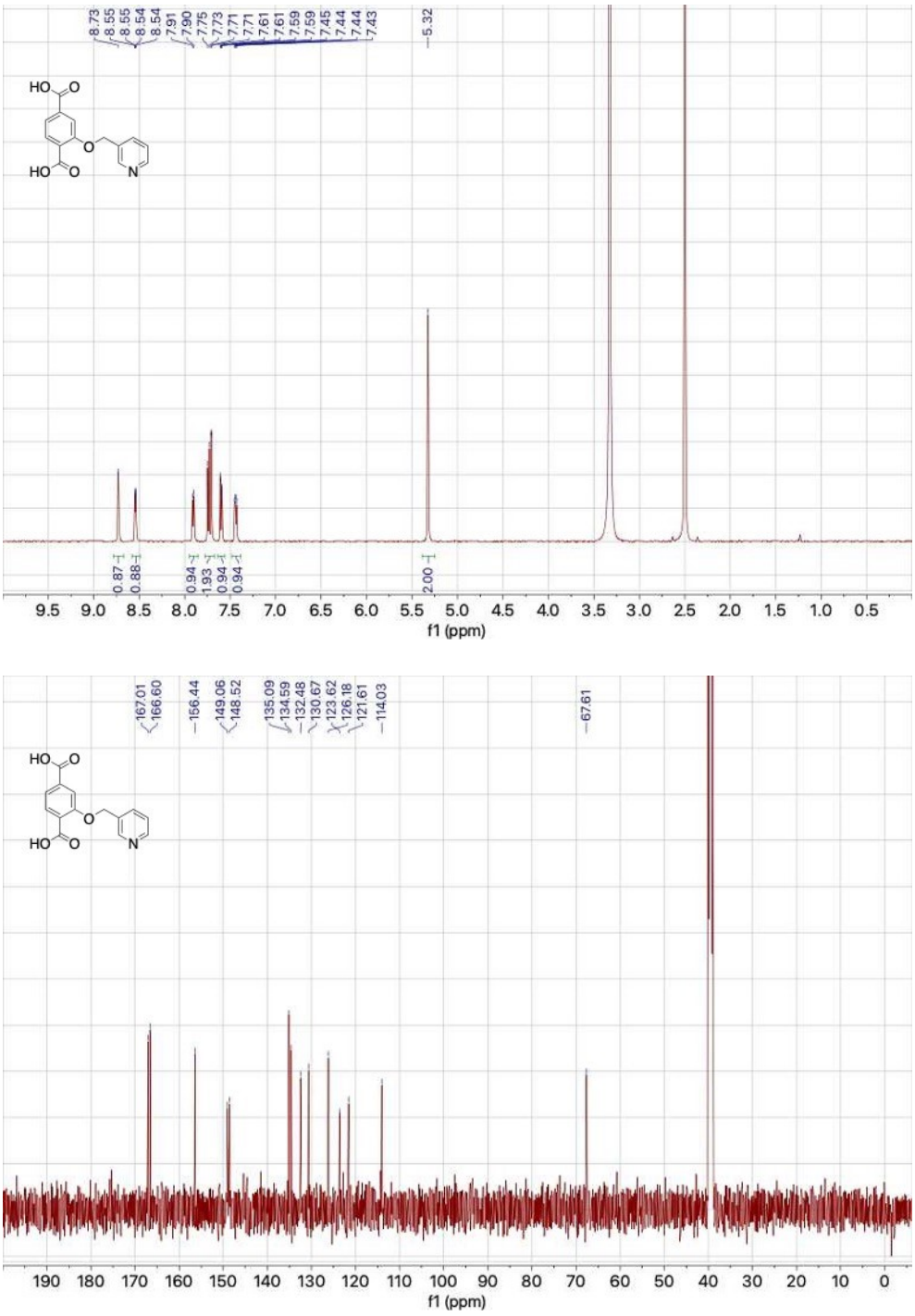

Figure S83. ^{1}H (*top*) and ^{13}C (*bottom*) NMR spectrum of 2-(pyridin-3-ylmethoxy)terephthalic acid (**H_2bdc-3-py**).

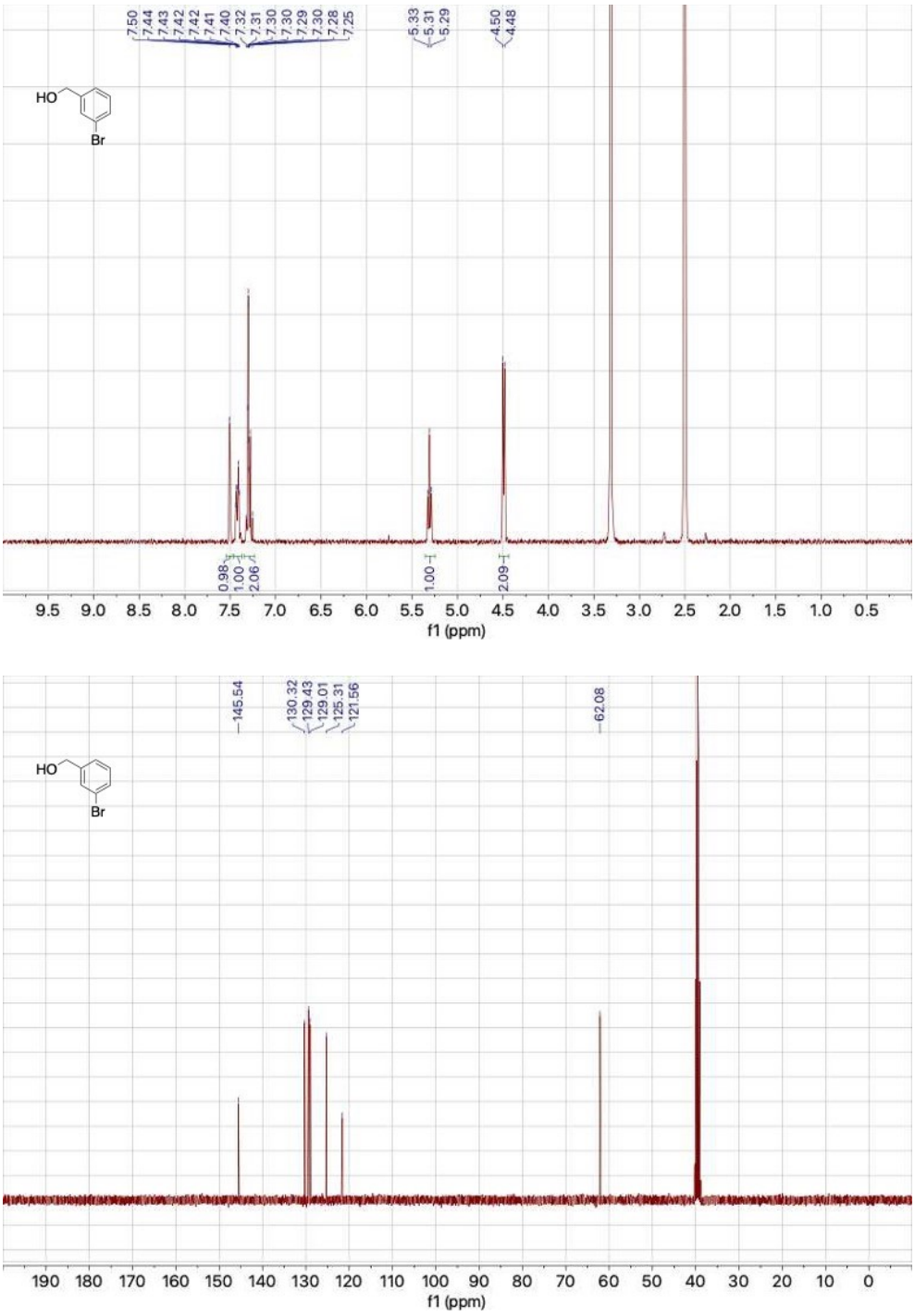

Figure S84. ^{1}H (*top*) and ^{13}C (*bottom*) NMR spectrum of 3-bromobenzyl alcohol (**34**).

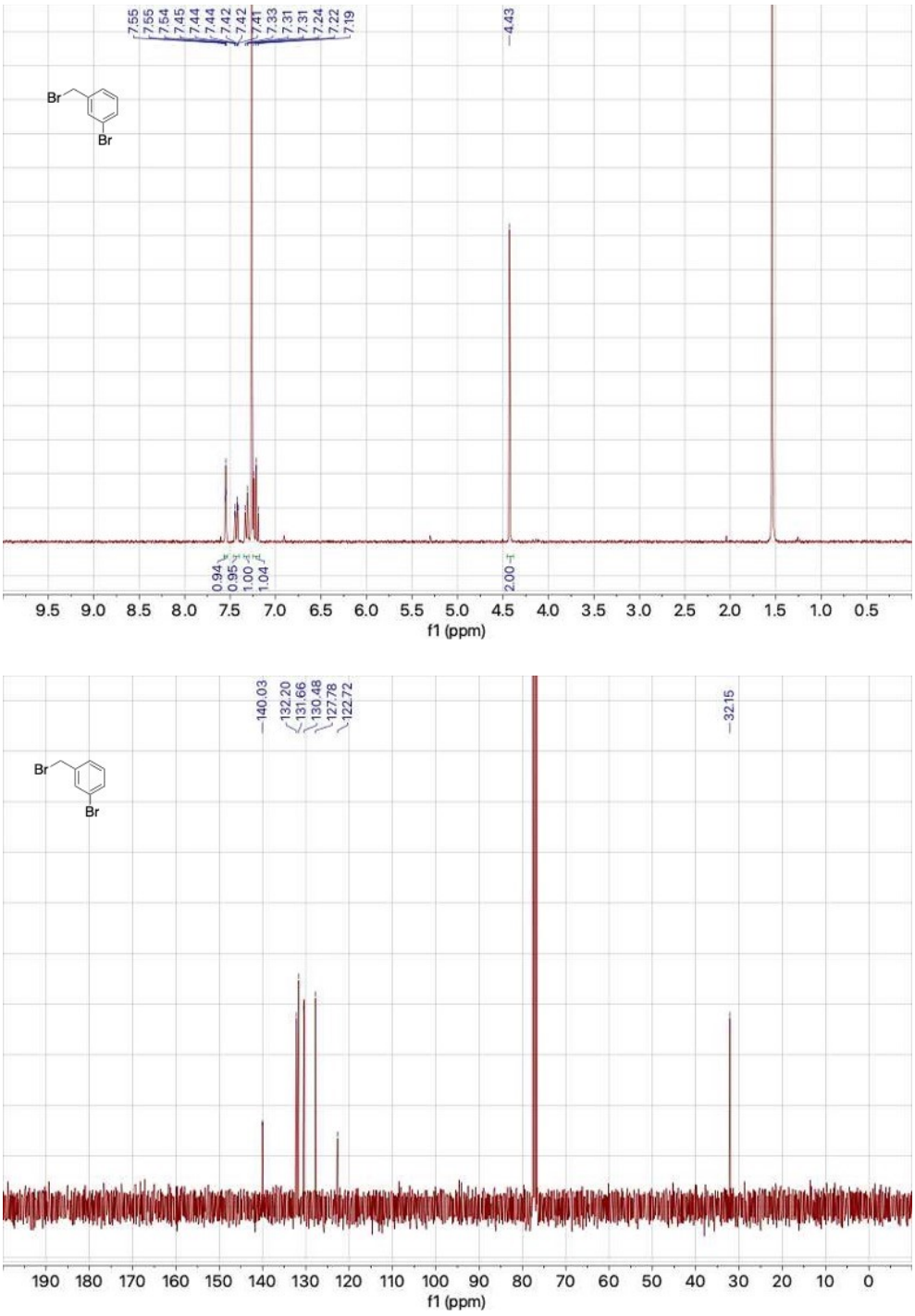

Figure S85. ^{1}H (*top*) and ^{13}C (*bottom*) NMR spectrum of 1-bromo-3-(bromomethyl)benzene (**35**).

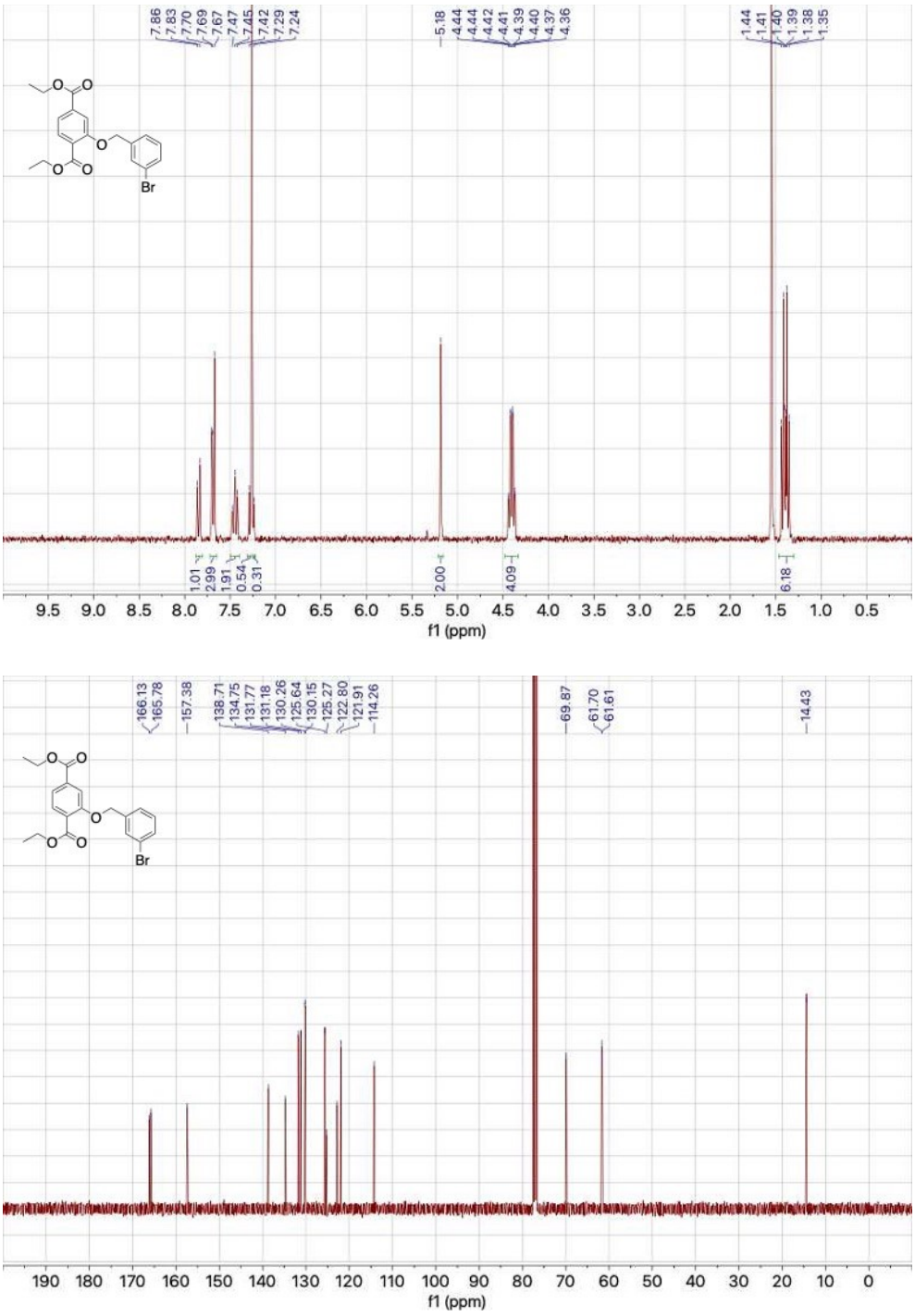

Figure S86. ^{1}H (*top*) and ^{13}C (*bottom*) NMR spectrum of diethyl 2-((3-bromobenzyl)oxy)terephthalate (**36**).

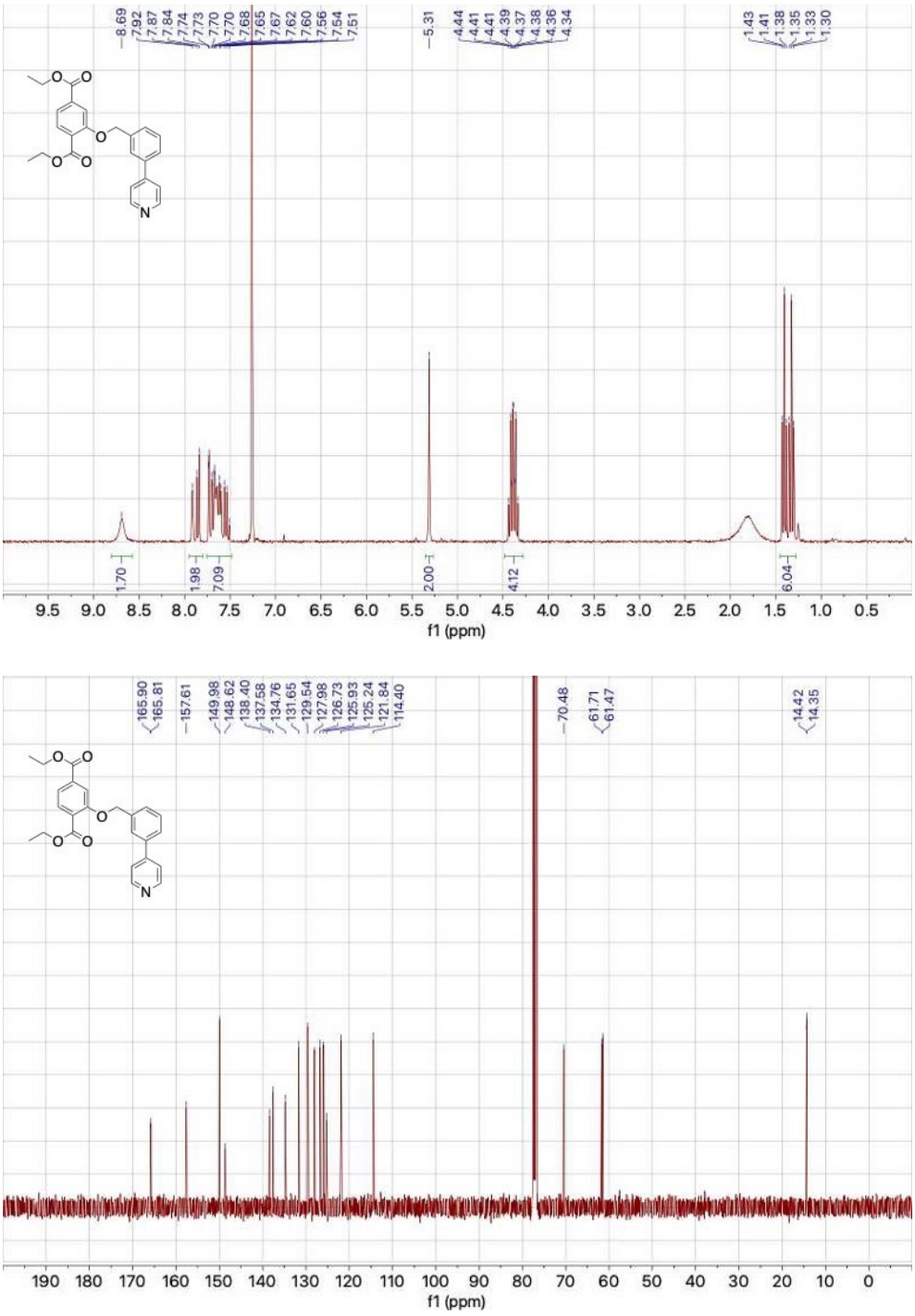

Figure S87. ^{1}H (*top*) and ^{13}C (*bottom*) NMR spectrum of diethyl 2-((3-(pyridin-4-yl)benzyl)oxy)terephthalate (**37**).

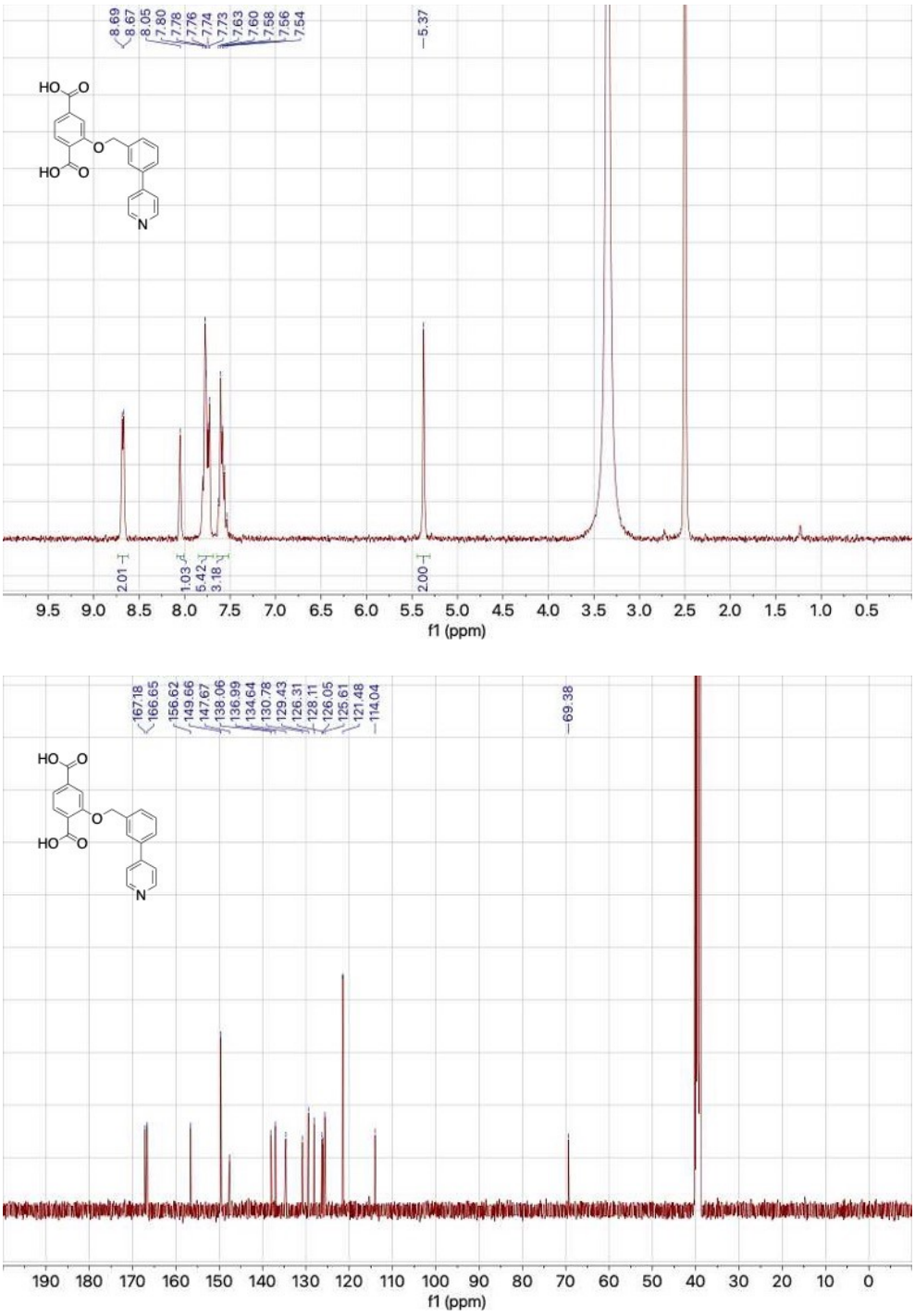

Figure S88. ^{1}H (*top*) and ^{13}C (*bottom*) NMR spectrum of 2-(pyridin-3-ylmethoxy)terephthalic acid (**H_2bdc-3-ph-4-py**).

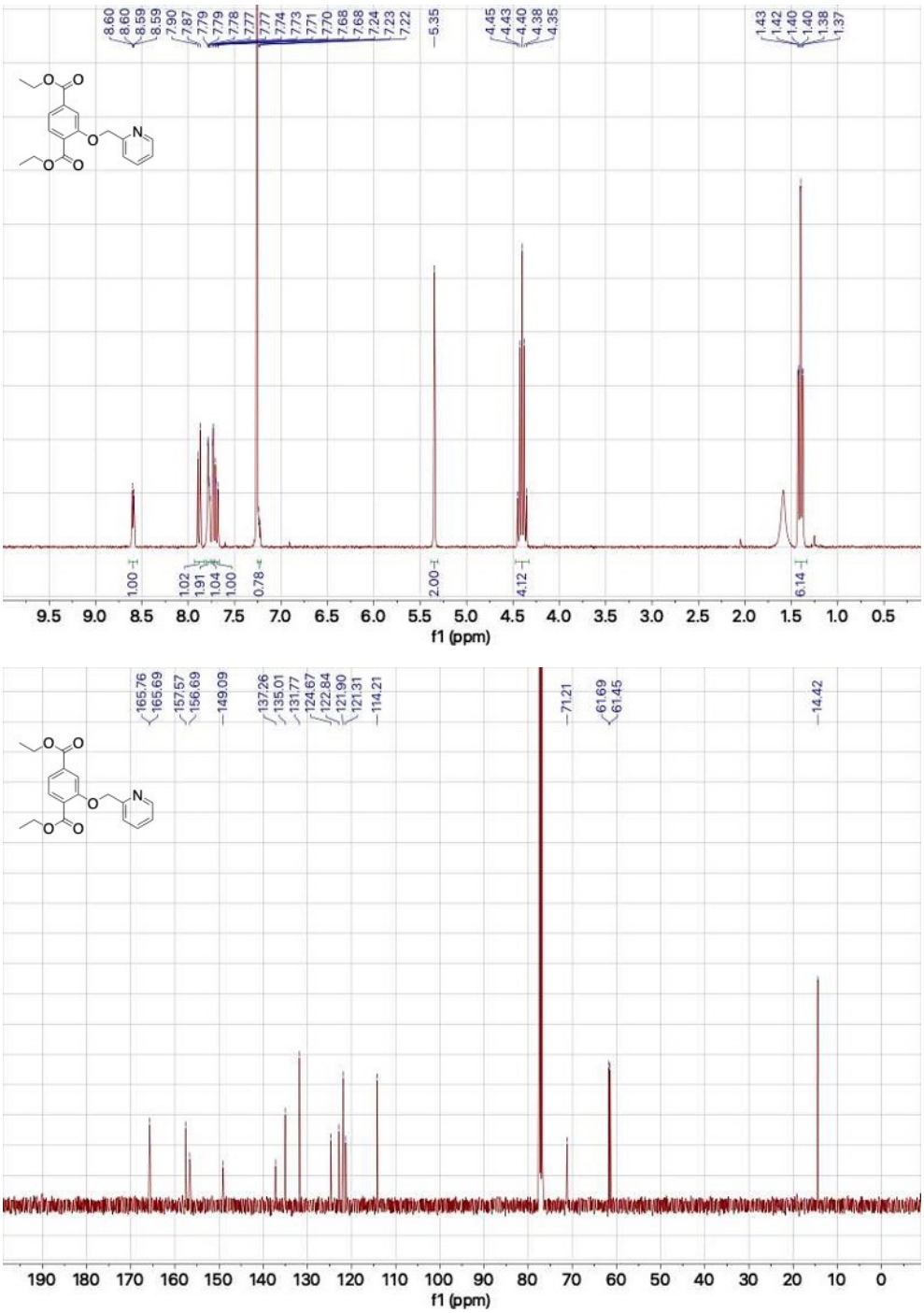

Figure S89. ^{1}H (*top*) and ^{13}C (*bottom*) NMR spectrum of diethyl 2-(pyridin-2-ylmethoxy)terephthalate (**39**).

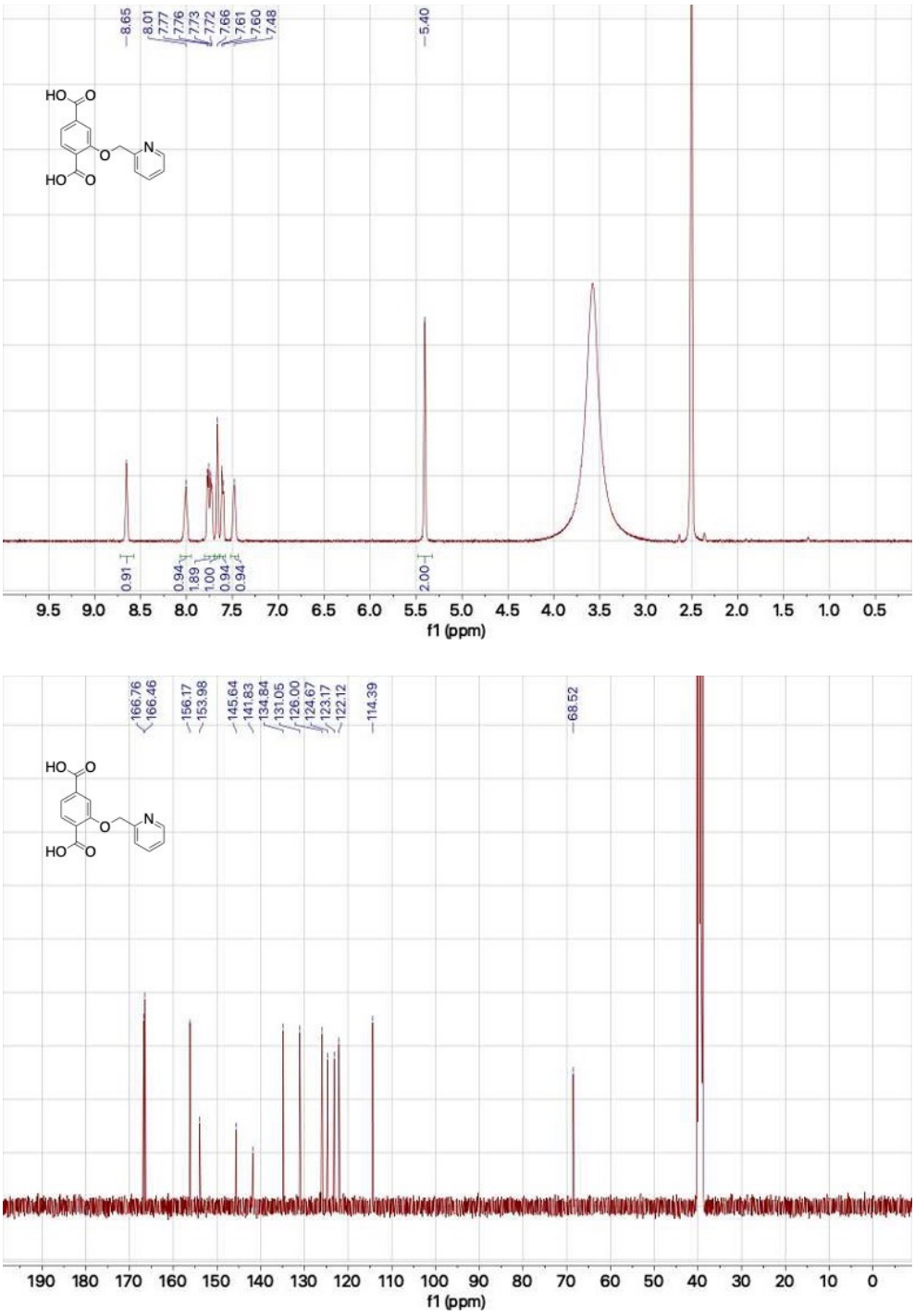

Figure S90. ^{1}H (*top*) and ^{13}C (*bottom*) NMR spectrum of 2-(pyridin-2-ylmethoxy)terephthalic acid (**H_2bdc-2-py**).

F. Single crystal X-ray structure determination

Single-crystal X-ray diffraction data (SCXRD) were collected at 100 K on a Bruker D8 Venture diffractometer equipped with a microfocus rotating anode (Mo Kα radiation, λ = 0.71073 Å) and a Photon 3 detector. Frame integration was carried out using SAINT (SAINT ver. 8.40B (Bruker, 2019)). The raw data was scaled and absorption corrected using a multiscan averaging of symmetry equivalent data using SADABS (SADABS ver. 2016/2). Contributions from the disordered solvent molecules and tether units were removed by the SQUEEZE program (PLATON, Spek, A. L. *Acta Crystallogr., Sect. A* **1990**, *46*, C34) and the outputs from the SQUEEZE calculations were attached to CIF files. The structure was solved by the direct method (SHELXT 2018/2) and refined by the full-matrix least-squares method based on F^2 utilizing SHELXL 2018/3 (Sheldrick, G. M. *Acta Crystallogr., Sect. A: Found. Crystallogr*. **2008**, *64*, 112–122).

Table S3. Crystal data and refinement parameters for oligoIRMOF-1-L1.

CCDC number	2387819	
Empirical formula	$C_{24}\ O_{13}\ Zn_4$	
Formula weight	757.72	
Temperature	100(2) K	
Wavelength	0.71073 Å	
Crystal system	Cubic	
Space group	$Fm\bar{3}m$	
Unit cell dimensions	a = 25.4150(9) Å	α = 90°
	b = 25.4150(9) Å	β = 90°
	c = 25.4150(9) Å	γ = 90°
Volume	16416.1(17) $Å^3$	
Z	8	
Density (calculated)	0.613 Mg/m^3	
Absorption coefficient	1.176 mm^{-1}	
F(000)	2944	
Crystal size	0.150 x 0.100 x 0.100 mm^3	
Theta range for data collection	1.602° to 26.299°	
Index ranges	$-27 \le h \le 25, -31 \le k \le 24, -31 \le l \le 26$	
Reflections collected	11556	
Independent reflections	901 [R(int) = 0.0492]	
Completeness to theta = 25.242°	99.9 %	
Absorption correction	Semi-empirical from equivalents	
Max. and min. transmission	0.891 and 0.781	
Refinement method	Full-matrix least-squares on F^2	
Data / restraints / parameters	901 / 8 / 31	
Goodness-of-fit on F^2	1.142	
Final R indices [I>2sigma(I)]	$R_1 = 0.0913$, $wR_2 = 0.2925$	
R indices (all data)	$R_1 = 0.1213$, $wR_2 = 0.3170$	
Largest diff. peak and hole	0.795 and -0.552 $e.Å^{-3}$	

Table S4. Crystal data and refinement parameters for oligoIRMOF-1-L3.

CCDC number	2387820	
Empirical formula	$C_{24}\ O_{13}\ Zn_4$	
Formula weight	757.72	
Temperature	100(2) K	
Wavelength	0.71073 Å	
Crystal system	Cubic	
Space group	$Pm\bar{3}m$	
Unit cell dimensions	a = 12.8235(12) Å	α = 90°
	b = 12.8235(12) Å	β = 90°
	c = 12.8235(12) Å	γ = 90°
Volume	2108.7(6) $Å^3$	
Z	1	
Density (calculated)	0.597 Mg/m^3	
Absorption coefficient	1.145 mm^{-1}	
F(000)	368	
Crystal size	0.150 x 0.100 x 0.100 mm^3	
Theta range for data collection	1.588° to 24.678°	
Index ranges	$-6 \le h \le 15, -11 \le k \le 7, -9 \le l \le 14$	
Reflections collected	2883	
Independent reflections	418 [R(int) = 0.0737]	
Completeness to theta = 24.678°	100.0 %	
Absorption correction	Semi-empirical from equivalents	
Max. and min. transmission	0.894 and 0.722	
Refinement method	Full-matrix least-squares on F^2	
Data / restraints / parameters	418 / 1 / 23	
Goodness-of-fit on F^2	1.082	
Final R indices [I>2sigma(I)]	$R_1 = 0.0707$, $wR_2 = 0.2126$	
R indices (all data)	$R_1 = 0.1106$, $wR_2 = 0.2534$	
Largest diff. peak and hole	0.470 and -0.294 e.$Å^{-3}$	

Table S5. Crystal data and refinement parameters for Zn(H_2bdc-3-py).

CCDC number	2387821	
Empirical formula	C_{14} N O_5 Zn	
Formula weight	327.52	
Temperature	100(2) K	
Wavelength	0.71073 Å	
Crystal system	Monoclinic	
Space group	*C2/c*	
Unit cell dimensions	a = 13.6279(13) Å	α = 90°
	b = 16.9199(17) Å	β = 91.635(3)°
	c = 19.7799(19) Å	γ = 90°
Volume	4559.0(8) $Å^3$	
Z	8	
Density (calculated)	0.954 Mg/m^3	
Absorption coefficient	1.088 mm^{-1}	
F(000)	1288	
Crystal size	0.100 x 0.100 x 0.050 mm^3	
Theta range for data collection	2.619° to 26.456°	
Index ranges	$-17 \le h \le 17$, $-21 \le k \le 21$, $-24 \le l \le 24$	
Reflections collected	33806	
Independent reflections	4686 [R(int) = 0.0875]	
Completeness to theta = 25.242°	99.8 %	
Absorption correction	Semi-empirical from equivalents	
Max. and min. transmission	0.948 and 0.776	
Refinement method	Full-matrix least-squares on F^2	
Data / restraints / parameters	4686 / 0 / 190	
Goodness-of-fit on F^2	1.087	
Final R indices [I>2sigma(I)]	R_1 = 0.0680, wR_2 = 0.1837	
R indices (all data)	R_1 = 0.0838, wR_2 = 0.1907	
Largest diff. peak and hole	0.966 and -0.562 e.$Å^{-3}$	

Table S6. Crystal data and refinement parameters for oligoIRMOF-1-L6.

CCDC number	2387822	
Empirical formula	$C_{96}\ O_{64}\ Zn_{16}$	
Formula weight	3222.88	
Temperature	100(2) K	
Wavelength	0.71073 Å	
Crystal system	Cubic	
Space group	$Fm\bar{3}m$	
Unit cell dimensions	a = 25.6171(9) Å	α = 90°
	b = 25.6171(9) Å	β = 90°
	c = 25.6171(9) Å	γ = 90°
Volume	16810.9(18) $Å^3$	
Z	2	
Density (calculated)	0.637 Mg/m^3	
Absorption coefficient	1.153 mm^{-1}	
F(000)	3136	
Crystal size	0.200 x 0.100 x 0.100 mm^3	
Theta range for data collection	2.637° to 26.945°	
Index ranges	$-32 \le h \le 28, -32 \le k \le 32, -32 \le l \le 32$	
Reflections collected	26386	
Independent reflections	973 [R(int) = 0.0571]	
Completeness to theta = 25.242°	99.4 %	
Absorption correction	Semi-empirical from equivalents	
Max. and min. transmission	0.893 and 0.767	
Refinement method	Full-matrix least-squares on F^2	
Data / restraints / parameters	973 / 0 / 31	
Goodness-of-fit on F^2	1.125	
Final R indices [I>2sigma(I)]	$R_1 = 0.0589$, $wR_2 = 0.1925$	
R indices (all data)	$R_1 = 0.0835$, $wR_2 = 0.2234$	
Largest diff. peak and hole	0.473 and -0.247 $e.Å^{-3}$	

Table S7. Crystal data and refinement parameters for oligoIRMOF-1-benzyltriazole.

CCDC number	2387823	
Empirical formula	$C_{96}\ O_{64}\ Zn_{16}$	
Formula weight	3222.88	
Temperature	100(2) K	
Wavelength	0.71073 Å	
Crystal system	Cubic	
Space group	$Fm\bar{3}m$	
Unit cell dimensions	a = 25.6309(9) Å	α = 90°
	b = 25.6309(9) Å	β = 90°
	c = 25.6309(9) Å	γ = 90°
Volume	16838.0(18) $Å^3$	
Z	2	
Density (calculated)	0.636 Mg/m^3	
Absorption coefficient	1.151 mm^{-1}	
F(000)	3136	
Crystal size	0.150 x 0.100 x 0.100 mm^3	
Theta range for data collection	2.636° to 24.695°	
Index ranges	$-29 \le h \le 30, -30 \le k \le 30, -26 \le l \le 30$	
Reflections collected	38112	
Independent reflections	777 [R(int) = 0.0921]	
Completeness to theta = 24.695°	99.0 %	
Absorption correction	Semi-empirical from equivalents	
Max. and min. transmission	0.894 and 0.747	
Refinement method	Full-matrix least-squares on F^2	
Data / restraints / parameters	777 / 0 / 31	
Goodness-of-fit on F^2	1.224	
Final R indices [I>2sigma(I)]	$R_1 = 0.0519$, $wR_2 = 0.1701$	
R indices (all data)	$R_1 = 0.0858$, $wR_2 = 0.2188$	
Largest diff. peak and hole	0.427 and -0.319 $e.Å^{-3}$	

Table S8. Crystal data and refinement parameters for oligoIRMOF-1-pyridinetriazole.

CCDC number	2387824	
Empirical formula	$C_{96}\ O_{64}\ Zn_{16}$	
Formula weight	3222.88	
Temperature	100(2) K	
Wavelength	0.71073 Å	
Crystal system	Cubic	
Space group	$Fm\bar{3}m$	
Unit cell dimensions	a = 25.6731(8) Å	α = 90°
	b = 25.6731(8) Å	β = 90°
	c = 25.6731(8) Å	γ = 90°
Volume	16921.3(16) $Å^3$	
Z	2	
Density (calculated)	0.633 Mg/m^3	
Absorption coefficient	1.146 mm^{-1}	
F(000)	3136	
Crystal size	0.150 x 0.100 x 0.100 mm^3	
Theta range for data collection	2.631° to 24.709°	
Index ranges	$-29 \le h \le 30, -28 \le k \le 30, -26 \le l \le 30$	
Reflections collected	37095	
Independent reflections	773 [R(int) = 0.0749]	
Completeness to theta = 24.709°	98.2 %	
Absorption correction	Semi-empirical from equivalents	
Max. and min. transmission	0.894 and 0.737	
Refinement method	Full-matrix least-squares on F^2	
Data / restraints / parameters	773 / 0 / 31	
Goodness-of-fit on F^2	1.226	
Final R indices [I>2sigma(I)]	$R_1 = 0.0550$, $wR_2 = 0.1717$	
R indices (all data)	$R_1 = 0.0903$, $wR_2 = 0.2272$	
Largest diff. peak and hole	0.433 and -0.292 $e.Å^{-3}$	

Table S9. Crystal data and refinement parameters for oligoIRMOF-1-biphenyltriazole.

CCDC number	2387825	
Empirical formula	$C_{96}\ O_{64}\ Zn_{16}$	
Formula weight	3222.88	
Temperature	100(2) K	
Wavelength	0.71073 Å	
Crystal system	Cubic	
Space group	$Fm\bar{3}m$	
Unit cell dimensions	a = 25.6846(8) Å	α = 90°
	b = 25.6846(8) Å	β = 90°
	c = 25.6846(8) Å	γ = 90°
Volume	16944.1(16) $Å^3$	
Z	2	
Density (calculated)	0.632 Mg/m^3	
Absorption coefficient	1.144 mm^{-1}	
F(000)	3136	
Crystal size	0.200 x 0.150 x 0.100 mm^3	
Theta range for data collection	2.630° to 24.698°	
Index ranges	$-30 \le h \le 30, -30 \le k \le 29, -30 \le l \le 29$	
Reflections collected	44614	
Independent reflections	775 [R(int) = 0.0784]	
Completeness to theta = 24.698°	98.5 %	
Absorption correction	Semi-empirical from equivalents	
Max. and min. transmission	0.894 and 0.739	
Refinement method	Full-matrix least-squares on F^2	
Data / restraints / parameters	775 / 47 / 31	
Goodness-of-fit on F^2	1.249	
Final R indices [I>2sigma(I)]	$R_1 = 0.0663$, $wR_2 = 0.2059$	
R indices (all data)	$R_1 = 0.0970$, $wR_2 = 0.2786$	
Largest diff. peak and hole	0.738 and -0.537 $e.Å^{-3}$	

Table S10. Crystal data and refinement parameters for oligoIRMOF-1-triazole$_2$-*o*-xylyl.

CCDC number	2387826	
Empirical formula	$C_{96}\ O_{64}\ Zn_{16}$	
Formula weight	3222.88	
Temperature	100(2) K	
Wavelength	0.71073 Å	
Crystal system	Cubic	
Space group	$Fm\bar{3}m$	
Unit cell dimensions	a = 25.6483(6) Å	α = 90°
	b = 25.6483(6) Å	β = 90°
	c = 25.6483(6) Å	γ = 90°
Volume	16872.4(12) Å^3	
Z	2	
Density (calculated)	0.634 Mg/m^3	
Absorption coefficient	1.149 mm^{-1}	
F(000)	3136	
Crystal size	0.250 x 0.200 x 0.200 mm^3	
Theta range for data collection	2.634° to 26.361°	
Index ranges	$-32 \le h \le 32, -29 \le k \le 32, -30 \le l \le 32$	
Reflections collected	68819	
Independent reflections	921 [R(int) = 0.0791]	
Completeness to theta = 25.242°	99.6 %	
Absorption correction	Semi-empirical from equivalents	
Max. and min. transmission	0.803 and 0.689	
Refinement method	Full-matrix least-squares on F^2	
Data / restraints / parameters	921 / 47 / 31	
Goodness-of-fit on F^2	1.171	
Final R indices [I>2sigma(I)]	R_1 = 0.0649, wR_2 = 0.2080	
R indices (all data)	R_1 = 0.0897, wR_2 = 0.2512	
Largest diff. peak and hole	0.452 and -0.574 e.Å^{-3}	

Table S11. Crystal data and refinement parameters for oligoIRMOF-1-triazole$_2$-*m*-xylyl.

CCDC number	2387827	
Empirical formula	$C_{96}\ O_{64}\ Zn_{16}$	
Formula weight	3222.88	
Temperature	100(2) K	
Wavelength	0.71073 Å	
Crystal system	Cubic	
Space group	$Fm\bar{3}m$	
Unit cell dimensions	a = 25.6455(7) Å	α = 90°
	b = 25.6455(7) Å	β = 90°
	c = 25.6455(7) Å	γ = 90°
Volume	16866.8(14) Å^3	
Z	2	
Density (calculated)	0.635 Mg/m^3	
Absorption coefficient	1.150 mm^{-1}	
F(000)	3136	
Crystal size	0.250 x 0.250 x 0.200 mm^3	
Theta range for data collection	2.634° to 24.680°	
Index ranges	-30 ≤ h ≤ 30, -30 ≤ k ≤ 30, -30 ≤ l ≤ 30	
Reflections collected	59257	
Independent reflections	782 [R(int) = 0.0820]	
Completeness to theta = 24.680°	99.6 %	
Absorption correction	Semi-empirical from equivalents	
Max. and min. transmission	0.803 and 0.693	
Refinement method	Full-matrix least-squares on F^2	
Data / restraints / parameters	782 / 47 / 31	
Goodness-of-fit on F^2	1.161	
Final R indices [I>2sigma(I)]	R_1 = 0.0559, wR_2 = 0.1774	
R indices (all data)	R_1 = 0.0735, wR_2 = 0.2042	
Largest diff. peak and hole	0.441 and -0.327 e.Å^{-3}	

Table S12. Crystal data and refinement parameters for oligoIRMOF-1-triazole$_2$-*p*-xylyl.

CCDC number	2387828	
Empirical formula	$C_{96}\ O_{64}\ Zn_{16}$	
Formula weight	3222.88	
Temperature	100(2) K	
Wavelength	0.71073 Å	
Crystal system	Cubic	
Space group	$Fm\bar{3}m$	
Unit cell dimensions	a = 25.6396(7) Å	α = 90°
	b = 25.6396(7) Å	β = 90°
	c = 25.6396(7) Å	γ = 90°
Volume	16855.2(14) Å^3	
Z	2	
Density (calculated)	0.635 Mg/m^3	
Absorption coefficient	1.150 mm^{-1}	
F(000)	3136	
Crystal size	0.250 x 0.200 x 0.200 mm^3	
Theta range for data collection	2.635° to 24.686°	
Index ranges	-30 ≤ h ≤ 30, -30 ≤ k ≤ 30, -30 ≤ l ≤ 30	
Reflections collected	44496	
Independent reflections	773 [R(int) = 0.0761]	
Completeness to theta = 24.686°	98.5 %	
Absorption correction	Semi-empirical from equivalents	
Max. and min. transmission	0.803 and 0.691	
Refinement method	Full-matrix least-squares on F^2	
Data / restraints / parameters	773 / 47 / 31	
Goodness-of-fit on F^2	1.237	
Final R indices [I>2sigma(I)]	R_1 = 0.0687, wR_2 = 0.2118	
R indices (all data)	R_1 = 0.1000, wR_2 = 0.2867	
Largest diff. peak and hole	0.877 and -0.589 e.Å^{-3}	

H. Topology determination of Zn(H_2bdc-3-py)

The topology of Zn(H_2bdc-3-py) was determined using the ToposPro software (Blatov, V. A.; Shevchenko, A. P.; Proserpio, D. M. *Cryst. Growth Des*. **2014**, *14*, 3576-3586). Details of the topological reduction are given below.

Structure consists of 3D framework with ZB2ZA

ZA is the 6-connected Zn SBU, and ZB is the 3-connected ligand.

Coordination sequences

ZA1:	1	2	3	4	5	6	7	8	9	10
Num	6	8	32	28	84	60	162	106	266	164
Cum	7	15	47	75	159	219	381	487	753	917

ZB1:	1	2	3	4	5	6	7	8	9	10
Num	3	13	16	54	42	119	81	210	133	327
Cum	4	17	33	87	129	248	329	539	672	999

TD10=972

Vertex symbols for selected sublattice

ZA1 Point symbol: {4^4.6^2.8^8.10}

Extended point symbol: [4.4.4.4.6.6.8(4).8(4).8(4).8(4).8(5).8(5).8(5).8(5).10(32)]

ZB1 Point symbol: {4^2.6}

Extended point symbol: [4.4.6]

Point symbol for net: {4^2.6}2{4^4.6^2.8^8.10}

3,6-c net with stoichiometry (3-c)2(6-c); 2-nodal net

Topological type: ant (topos&RCSR.ttd) {4^2.6}2{4^4.6^2.8^8.10} - VS [4.4.8(10)] [4.4.4.4.8(4).8(4).8(4).8(4).8(5).8(5).8(5).8(5).*.*.*]"